

Tesis defendida por  
**Guillermo Galaviz Yáñez**  
y aprobada por el siguiente comité

---

Dr. David Hilario Covarrubias Rosales  
Codirector del Comité

---

Dr. Ángel Gabriel Andrade Reátiga  
Codirector del Comité

---

Dr. Salvador Villarreal Reyes  
Miembro del Comité

---

Dr. José Martín Luna Rivera  
Miembro del Comité

---

Dr. Carlos Brizuela Rodríguez  
Miembro del Comité

---

Dr. César Cruz Hernández  
Coordinador del programa de posgrado  
en Electrónica y Telecomunicaciones

---

Dr. David H. Covarrubias Rosales  
Director de Estudios de Posgrado

1 de noviembre de 2012

**CENTRO DE INVESTIGACIÓN CIENTÍFICA Y DE  
EDUCACIÓN SUPERIOR DE ENSENADA**



---

**Programa de Posgrado en Ciencias  
en Electrónica y Telecomunicaciones**

---

Diseño de Algoritmos de Despacho de Recursos Espectrales para Sistemas  
LTE-Avanzados con Acumulación de Portadoras

Tesis

para cubrir parcialmente los requisitos necesarios para obtener el grado de  
Doctor en Ciencias

Presenta:

**Guillermo Galaviz Yáñez**

Ensenada, Baja California, México  
2012

Abstract of the thesis presented by Guillermo Galaviz Yáñez, in partial fulfillment of the requirements for the degree of Doctor of Science in Electronics and Telecommunications with orientation in TELECOMMUNICATIONS. Ensenada, Baja California, 2012.

## **Design of Spectrum Resource Scheduling Algorithms for LTE-Advanced Systems with Carrier Aggregation**

Abstract approved by

---

Dr. David Hilario Covarrubias Rosales

Codirector de Tesis

---

Dr. Ángel Gabriel Andrade Reátiga

Codirector de Tesis

In 2008 the International Telecommunication Union defined the requirements for the next generation of wireless cellular communication systems. These requirements were included in the International Mobile Telecommunications Advanced (IMT-Advanced) project, and are aimed at providing wireless broadband data services to fixed and mobile users. One of the requirements specifies a data rate of up to 1 Gbps for fixed users.

In order to achieve such data rate, key technologies such as Orthogonal Frequency Division Multiple Access (OFDMA), Multiple Input Multiple Output (MIMO), Cooperative Multi-point Transmission and Reception (CoMP), and the use of repeaters are specified in order to increase spectral efficiency and improve the channel conditions observed by a user. However, even with the use of these technologies there is a large requirement of spectrum bandwidth of up to 100 MHz.

Carrier Aggregation (CA) has been defined as a solution for the lack of spectrum in the frequency bands specified for the operation of IMT-Advanced standards. CA allows for the use of fragmented spectrum and provides a mechanism for backward compatibility with non IMT-Advanced standards. This thesis is focused on the design of schedulers for CA in macrocellular environments. Particularly, we develop a novel scheduling method that reduces delay in resource assignment by forming sets of spectrum resources prior to their assignment. Our proposal allows to control throughput, fairness, and user capacity based on the maximum number of spectrum resources in a set.

Keywords: Carrier Aggregation, Schedulers, Resource Blocks, Spatial Channel Models, IMT-Advanced, LTE-Advanced Systems.

Resumen de la tesis de Guillermo Galaviz Yáñez, presentada como requisito parcial para la obtención del grado de Doctor en Ciencias en Electrónica y Telecomunicaciones con orientación en TELECOMUNICACIONES. Ensenada, Baja California, 2012.

## **Diseño de Algoritmos de Despacho de Recursos Espectrales para Sistemas LTE-Avanzados con Acumulación de Portadoras**

En el 2008 la Unión Internacional de Telecomunicaciones definió los requerimientos para la próxima generación de sistemas de comunicaciones inalámbricas celulares. Estos requerimientos se incluyeron en el proyecto denominado International Mobile Telecommunications Advanced (IMT-Advanced) o IMT-Avanzadas, y se enfocan en proporcionar servicios de banda ancha inalámbrica a usuarios fijos y móviles. Uno de los requerimientos establece una tasa de transmisión de hasta 1 Gbps para usuarios fijos.

Para lograr la tasa de transmisión objetivo, se define el uso de diversas plataformas tecnológicas tales como Acceso Múltiple por División de Frecuencias Ortogonales (OFDMA), esquemas de Entrada Múltiple Salida Múltiple (MIMO), Transmisión y Recepción Multi-punto Coordinada (CoMP) así como el uso de repetidores. Todo esto con el propósito de incrementar la eficiencia espectral y mejorar las condiciones de canal observadas por el usuario. Sin embargo, aún con el uso de estas plataformas tecnológicas existe un requerimiento de espectro radioeléctrico de hasta 100 MHz.

Acumulación de Portadoras (CA) se definió como la solución para la falta de espectro en las bandas de frecuencia especificadas para la operación de estándares IMT-Avanzados. CA permite el uso de espectro fragmentado y proporciona un mecanismo para la compatibilidad con usuarios de sistemas de estándares previos. Esta tesis se enfoca en el diseño de despachadores para CA en entornos macrocelulares. En lo particular, se desarrolló un método novedoso de despacho que reduce el retardo en el proceso de asignación de recursos. Para esto, los recursos disponibles son agrupados en conjuntos previo a la asignación de los mismos por parte del despachador. Nuestra propuesta permite el control del caudal eficaz, equidad y capacidad de usuarios controlando el número máximo de recursos espectrales por conjunto.

Palabras Clave: Acumulación de Portadoras, Despachadores, Bloques de Recursos, Modelos Espaciales de Canal Radio, IMT-Avanzadas, Sistemas LTE-Avanzados.

*To Ariadna, my beloved wife,  
and my daughters Natalia and Isabel*

# Acknowledgments

This work was possible thanks to the support of the National Council of Science and Technology (CONACYT), Mexico, through scholarship number 92845. I would also like to thank the Research and Higher Education Center of Ensenada (CICESE), the Department of Electronics and Telecommunications, and the Autonomous University of Baja California for the support they provided during the development of this research.

I would personally like to thank the guidance from my advisors, Dr. David H. Covarrubias and Dr. Angel G. Andrade. Their advice was essential for the successful completion of this work and has provided the basis for a long term professional and personal relationship. To them, my greatest respect and gratitude.

The feedback obtained from the members of my thesis committee was also critical to properly direct the work efforts of this research. I thank Dr. Salvador Villarreal, Dr. Carlos Brizuela and Dr. José Martín Luna for their time and critical advice.

Special thanks to the friends I made during the four years spent in the development of this work, Armando Arce, Alejandro Galaviz, Edwin Martínez, Pedro Valenzuela, Christian Soto, Liliana Castorena, Leonardo Yepes, Fernando Ortega, Leopoldo Garza, Dr. Miguel Alonso and so many others to list.

Thanks to my wife and daughters for their support and comprehension during my studies. Also to my parents for their constant help with my family needs during our stay in Ensenada.

# Contents

	Page
<b>Abstract</b>	<b>i</b>
<b>Resumen</b>	<b>ii</b>
<b>Dedication</b>	<b>iii</b>
<b>Acknowledgments</b>	<b>iv</b>
<b>List of Figures</b>	<b>viii</b>
<b>List of Tables</b>	<b>xi</b>
<b>1. Introduction</b>	<b>1</b>
1.1 Problem Statement . . . . .	3
1.1.1 Spectrum Availability. . . . .	3
1.1.2 Spectrum Management in Wireless Cellular Communication Systems. . . . .	6
1.2 Aim of Thesis . . . . .	9
1.3 Thesis Outline . . . . .	10
1.4 Outcomes . . . . .	12
<b>2. Technological Aspects of Carrier Aggregation and Scheduler Design</b>	<b>14</b>
2.1 Carrier Aggregation . . . . .	14
2.1.1 Carrier Aggregation Deployment Scenarios . . . . .	16
2.1.2 Carrier Aggregation Implementation Issues. . . . .	19
2.2 Scheduler Design for Carrier Aggregation . . . . .	20
2.2.1 Radio Resource Management in Circuit Switched Cellular Net- works. . . . .	21
2.2.2 Radio Resource Management in 3G Cellular Systems. . . . .	22
2.2.3 Radio Resource Management in LTE-Advanced Systems . . . . .	26
2.2.4 Schedulers for Carrier Aggregation . . . . .	30
2.2.5 Chapter Summary . . . . .	32
<b>3. Channel Models for the Evaluation of LTE-Advanced Systems</b>	<b>33</b>
3.1 The Multi Cluster Gaussian Scatterer Distribution Channel Model . . . . .	34
3.1.1 Related work . . . . .	36
3.1.2 Multi Cluster Gaussian Scatterer Distribution Model . . . . .	38
3.1.3 Uplink modeling and analysis . . . . .	40

# Contents

	Page
3.1.4	Downlink modeling and analysis . . . . . 46
3.1.5	Second order moment analysis of the MC-GSDM . . . . . 49
3.2	The use of the MC-GSDM in the design of future generation wireless systems . . . . . 55
3.2.1	Cost 259 Directional Channel Modeling . . . . . 55
3.2.2	WINNER II Channel Modeling . . . . . 56
3.3	Channel Quality Indicator Estimation. . . . . 56
3.4	Chapter Summary . . . . . 58
<b>4.</b>	<b>Scheduling Algorithms for Carrier Aggregation. 60</b>
4.1	Introduction . . . . . 60
4.2	Evaluation Scenario and Simulation Parameters . . . . . 61
4.2.1	Evaluation Scenario . . . . . 61
4.2.2	Simulation Parameters . . . . . 65
4.3	Set Scheduling and resource block organization algorithm . . . . . 66
4.3.1	Set Scheduling . . . . . 66
4.3.2	Resource block organization algorithm . . . . . 67
4.3.3	Operation of Set Scheduling . . . . . 69
4.4	Evaluation results and analysis . . . . . 72
4.4.1	Delay analysis . . . . . 72
4.4.2	Complexity description . . . . . 76
4.4.3	User capacity analysis . . . . . 79
4.4.4	Throughput evaluation . . . . . 83
4.5	Chapter Summary . . . . . 85
<b>5.</b>	<b>Set Scheduling with Fairness Considerations 87</b>
5.1	Introduction . . . . . 87
5.2	Schedulers with Fairness . . . . . 89
5.3	Fairness under Heterogeneous Traffic Conditions . . . . . 94
5.4	Evaluation of Fairness with Set Scheduling . . . . . 97
5.5	Chapter Summary . . . . . 99
<b>6.</b>	<b>Conclusions and Future Work. 102</b>
6.1	Summary of Research Results. . . . . 102
6.1.1	Channel Modeling Results Summary. . . . . 102
6.1.2	Scheduler Design Results Summary. . . . . 105
6.2	Summary of Contributions . . . . . 107
6.3	Future Research and Recommendations. . . . . 108

# Contents

	Page
References	110

# List of Figures

Figure		Page
1	Spectrum available and spectrum to be released for IMT-Advanced services in Europe, adapted from Analysis Mason (2011), The momentum behind LTE worldwide, GSMA White Paper. . . . .	4
2	Traffic from voice and data sources in wireless cellular networks worldwide, adapted from Gilstrap, D., Traffic and Market Report, Ericsson Report, 2012. . . . .	5
3	Broadband wireless subscriber growth adapted from Gilstrap, D., Traffic and Market Report, Ericsson Report, 2012. . . . .	6
4	Thesis structure. . . . .	12
5	Structure of a Resource Block. . . . .	15
6	General operation of CA. . . . .	15
7	Classification of CA based on the frequency band and availability of CCs. . . . .	17
8	Scenario 1 for CA deployment considering overlapped coverage. . . . .	18
9	Scenario 2 for CA deployment considering different range. . . . .	18
10	Scenario 3 for CA deployment for increased cell edge coverage. . . . .	19
11	Scenario 4 for CA deployment considering Remote Radio Heads. . . . .	19
12	General structure of available spectrum and its use in pre-3G systems. . . . .	22
13	General structure of spectrum usage in 3G systems . . . . .	23
14	General structure of spectrum usage in LTE Release 8. . . . .	25
15	General structure of spectrum usage in LTE Advanced. . . . .	27
16	Two stage scheduler structure (Disjoint Queue). . . . .	29
17	Single stage scheduler structure (Joint Queue). . . . .	29
18	Evaluation Geometry for the MC-GSDM model . . . . .	40
19	Joint ToA-AoA pdf for a three cluster MC-GSDM channel model. . . . .	42
20	Simulation scenario used for validation. . . . .	43

# List of Figures

Figure		Page
21	Scatterplot of simulated data showing ToA-AoA pairs for a three cluster MC-GSDM channel model . . . . .	44
22	Marginal AoA pdf for the example three cluster MC-GSDM. . . . .	44
23	Marginal ToA pdf for a three cluster MC-GSDM. . . . .	46
24	Joint ToA-AoA pdf for the downlink in a three cluster MC-GSDM. . .	47
25	Scatterplot of the ToA-AoA pairs for the downlink of a three cluster MC-GSDM . . . . .	48
26	Marginal AoA pdf for the downlink in a three cluster MC-GSDM. . . .	49
27	Angle Spread behavior for different secondary cluster position in the example two cluster MC-GSDM. . . . .	51
28	Relative power delay using marginal ToA pdf without path loss consideration. . . . .	53
29	Power Delay Profile using Walfish Ikegami Path Loss Model and the relative power delay. . . . .	53
30	RMS-DS behavior using a two cluster MC-GSDM and parameters of Table 2. . . . .	54
31	Single cell evaluation scenario. . . . .	62
32	General Block by Block Scheduling. . . . .	66
33	Set Scheduling strategy. . . . .	67
34	Resource block organization algorithm—Algorithm 1 . . . . .	69
35	Resource block organization algorithm—Algorithm 2 . . . . .	70
36	Expected time required to execute the RB organization algorithm. . . .	75
37	Expected delay due to resource assignment. . . . .	77
38	PQ metric of the different scheduling strategies for a maximum file size $S_b \text{ max} = 2,000$ bits. . . . .	81
39	PQ metric of the different scheduling strategies for a maximum file size $S_b \text{ max} = 5,000$ bits. . . . .	82

# List of Figures

Figure		Page
40	PQ metric for the different maximum file size $S_b$ max of the best performing scheduling strategies. . . . .	83
41	Throughput percentage (assigned throughput/requested throughput) for Block by Block Scheduling and Set Scheduling. . . . .	84
42	Average assigned throughput per user for Block by Block Scheduling and Set Scheduling. . . . .	85
43	Representation of the MCPF problem. . . . .	91
44	Representation of the PF with Set Scheduling problem. . . . .	91
45	Throughput per user considering uniform set sizes and homogeneous traffic.	92
46	Throughput per user considering non-uniform set sizes and homogeneous traffic. . . . .	93
47	CDF plots for the reference data set and the evaluated data set. . . . .	96
48	CDF plots of Normalized Max Data Rate for $N_{\max} = 21$ and $R_{b\max} = 7000$ kbps. . . . .	98
49	Fairness Index $F_G$ for $N_{\max} = 21$ . . . . .	99
50	CDF plots of normalized Max Data Rate for $N_{\max} = 21$ and $S_{b\max} = 2000$ bits . . . . .	100
51	Fairness Index $F_G$ for $S_{b\max} = 5000$ bits . . . . .	101

# List of Tables

Table		Page
1	Evaluation channel parameters . . . . .	41
2	Channel parameters for AS and RMS Delay Spread evaluation . . . . .	51
3	CQI to S(CQI) and R(CQI) mapping. . . . .	64
4	Simulation parameters and values . . . . .	65
5	Comparison of the number of operations required per attended user considering Block by Block Scheduling and Set Scheduling . . . . .	80
6	Comparison of MCPF and RR schedulers with uniformly and non-uniformly sized spectrum resources. . . . .	92

# Chapter 1

## Introduction

Wireless cellular communication systems have been part of our everyday life for more than 30 years. During this time, cellular communication systems have evolved from voice oriented solutions into wireless broadband communication systems that provide a wide range of services. This evolution has been triggered by the increasing demand for digital services and the growing market (Analysys Mason, 2011).

Derived from the continuous development of wireless mobile telecommunication technologies and the increasing user demands for broadband services, in 2007 the International Telecommunications Union (ITU) proposed the International Mobile Telecommunications - Advanced project (IMT-Advanced) for Fourth Generation (4G) cellular communication systems. Among the requirements for a standard to be considered as a 4G candidate, IMT-Advanced establishes a 1 Gbps downlink data rate for low mobility users and 100 Mbps downlink data rate for high mobility users. In order to fulfill this requirement, the use of advanced key technologies is necessary (Parkvall et al., 2008),(Parkvall and Astely, 2009):

- Transmission using “wider” bandwidths and flexibility in spectrum usage by means of Carrier Aggregation (CA).
- Use of array antenna systems for Multiple Input Multiple Output (MIMO) schemes as well as beamforming.
- Coordinated Multi Point Transmission and Reception (CoMP)
- Use of repeaters to reduce the distance between transmitter and receiver.
- Backward compatibility with previous broadband standards

- Support for a wide range of services
- Increased user capacity
- Support for heterogeneous and Self Optimizing Networks (SON)

The Third Generation Partnership Project (3GPP) and the International Electrical and Electronics Engineers (IEEE) 802.16 work group have proposed the two main candidates of an IMT-Advanced compliant system. Namely, the 3GPP standard corresponds to the LTE Release 10 (LTE-Advanced) while the IEEE standard corresponds to the 802.16m (Wireless MAN Advanced). Both of these standards are an evolution of already available broadband wireless communication systems. In the case of the 3GPP, the evolution is taken from High Speed Packet Access, which then evolved to LTE Release 8, while in the case of the IEEE the Wireless MAN Advanced results from the evolution of WiMAX. LTE Release 8 is available commercially since 2010 and has been labeled as a 4G standard, although it does not meet the IMT-Advanced requirements (ITU, 2010). Both LTE Release 8 and WiMAX make use of flexible channel bandwidths of up to 20 MHz. Designers of LTE-Advanced and Wireless MAN Advanced systems decided to maintain backward compatibility with previous standards using component carriers of 20 MHz. In order to provide larger bandwidths to a single user, CA allows the system to aggregate up to five component carriers for a maximum bandwidth of 100 MHz. Using this strategy, non IMT-Advanced users will make use of 20 MHz channels, while IMT-Advanced users will be able to use up to 100 MHz of channel bandwidth (Yuan et al., 2010). The 100 MHz bandwidth will allow IMT-Advanced users to achieve a download data rate of up to 1 Gbps with low mobility, or up to 100 Mbps with high mobility or cell edge conditions.

In order to achieve the data rates required by IMT-Advanced, spectrum efficiency has become a physical layer design priority. Technology developments such as Multiple Input Multiple Output (MIMO) in combination with Orthogonal Frequency Division Multiplexing (OFDM), together with high order modulation schemes and efficient error correcting codes, allow for a peak spectrum efficiency of up to 15 bps/Hz (Döttling

et al., 2009). However, even with such high spectrum efficiency (achieved only under optimum conditions (Mehlführer et al., 2009)) there is a large requirement of spectrum bandwidth. For the 1 Gbps transfer rate and a spectrum efficiency of 15 bps/Hz, approximately 67 MHz of bandwidth would be required by one user during enough time to complete a data transfer.

## 1.1 Problem Statement

Current versions of broadband wireless systems make use of channel bandwidths of up to 20 MHz (Dahlman et al., 2011). Therefore, a different spectrum management scheme is required for next generation wireless systems within the IMT-Advanced project in order to provide the bandwidth required to achieve the data rate goals. Due to the fragmentation of the spectrum bands for next generation broadband wireless cellular systems, the expected growth of broadband wireless users, and the large bandwidths required to provide high data rate services, the spectrum available is considered to be scarce and fragmented (Lazarus, 2010).

### 1.1.1 Spectrum Availability.

In commercial wireless communication systems, spectrum is the most valuable resource due to the cost of the concession rights (Analysys Mason, 2011). Although there is spectrum available at different frequency bands worldwide, not all frequency bands are adequate for broadband wireless services (Lazarus, 2010). Also, one of the interests of the ITU is to standardize global spectrum usage in order to provide roaming capabilities to mobile users (Dahlman et al., 2011). Combining these two situations, the ITU with the help of the scientific community gathered at the 2007 World Radio Conference (ITU-R, 2008) identified spectrum bands available worldwide for IMT-Advanced (4G) broadband wireless services. The new identified spectrum, together with available spectrum for 3G and Beyond 3G services, yields a total bandwidth of 620 MHz in Eu-

rope. Other world regions have slight differences. Figure 1 shows a plot of the available spectrum and the frequency bands where it is located (Analysis Mason, 2011).

Considering the LTE-Advanced proposal, up to 100 MHz of bandwidth are to be provided to a single user for data transmission (Dahlman et al., 2011). From Fig. 1, it can be observed that only three bands have more than 100 MHz of contiguous bandwidth. These bands are at 1800 MHz, 2100 MHz with Time Division Duplexing (TDD) and the 2600 MHz band with Frequency Division Duplexing (FDD). This situation brings the problem that only three “typical”<sup>1</sup> radio channels of 100 MHz are available for IMT-Advanced services. This limits the number of operators able to operate with LTE-Advanced services in a given geographical area to only three. Also, the number of simultaneous transmissions (users) using 100 MHz would be limited to three. Considering that a total of 620 MHz are available, there is the possibility of forming at least six 100 MHz channels. In order to do so, a mechanism to utilize fragmented spectrum needs to be used.

Wireless broadband services available worldwide have changed the mobile market. With the availability of broadband services, traffic in mobile cellular networks has

<sup>1</sup>By typical we refer to contiguous spectrum, corresponding to a single wide band radio channel.

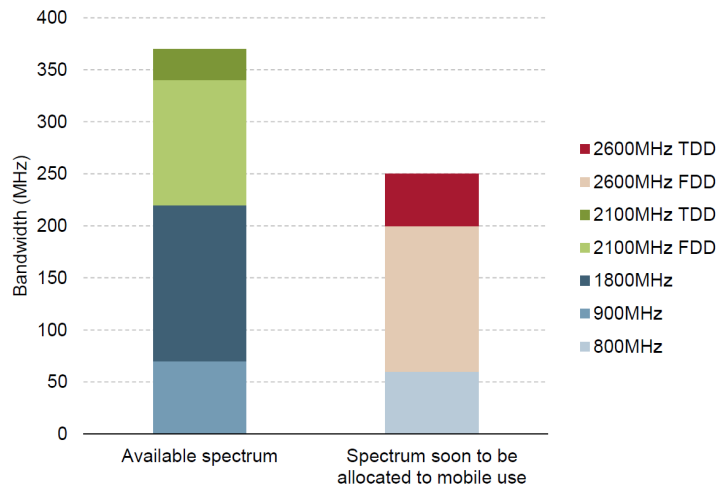


Figure 1. Spectrum available and spectrum to be released for IMT-Advanced services in Europe, adapted from Analysis Mason (2011), The momentum behind LTE worldwide, GSMA White Paper.

shifted. While cellular networks were mainly used for voice services, their main source of traffic is now data (Gilstrap, 2012). Figure 2 shows the measured behavior of traffic in cellular networks worldwide. The shift in traffic in the last five years can be observed, showing an exponential growth in data traffic while voice traffic has been stable for the last three years.

Together with the fragmentation and limited spectrum availability for IMT-Advanced services such as LTE-Advanced, the forecasted growth in broadband mobile users represents another challenge for spectrum management. Given the availability of broadband wireless services worldwide, the growth in mobile broadband subscribers has shown an exponential behavior. Figure 3 shows the measured market up to 2012 and the forecasted subscriber growth up to 2017 from (Gilstrap, 2012).

The predicted growth in mobile broadband subscribers responds to the expected market penetration of LTE-Advanced systems to compete with wired broadband services such as Direct Subscriber Lines (DSL) and Cable services. One of the aims of LTE-Advanced systems is to compete with wired services through the use of heterogeneous networks, supporting data rates of up to 1Gbps with international roaming

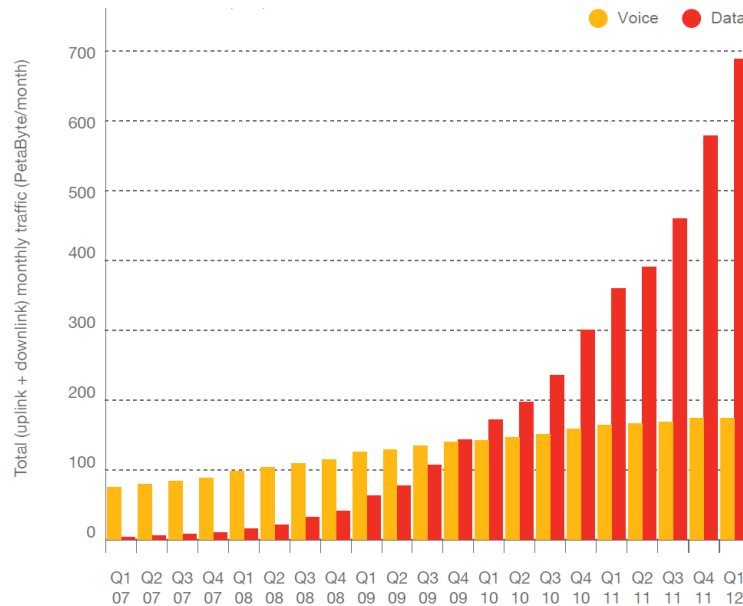


Figure 2. Traffic from voice and data sources in wireless cellular networks worldwide, adapted from Gilstrap, D., Traffic and Market Report, Ericsson Report, 2012.

and mobility capabilities (Gilstrap, 2012). The increased market growth is another challenge that has to be addressed by spectrum management strategies proposed for LTE-Advanced systems.

### 1.1.2 Spectrum Management in Wireless Cellular Communication Systems.

Spectrum management has been an important aspect of wireless cellular network design. As a matter of fact, the main reason for cellular sectoring was to efficiently use available spectrum with minimized interference (Rappaport, 2002). Different strategies of spectrum management have been proposed and used in wireless cellular networks. A review of the main aspects of the different types of spectrum management is provided in Chapter 2 of this document.

Namely, two types of connections (links) are used in cellular networks: Circuit Switched and Packet Switched. Fixed and dynamic channel assignment strategies are used to provide circuit switched connections. Circuit switched connections were the choice for voice oriented services. When data services began to be the focus of cellular networks, packet switched connections were implemented (Döttling et al., 2009). Packet switching provides an efficient way of sharing a channel (wired or wireless) between users of data traffic. Once packet switching is used, a scheduler is required to determine who and when will use the channel. The scheduler becomes the system component directly

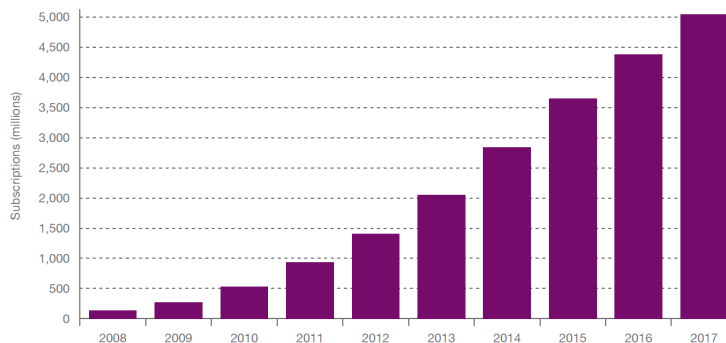


Figure 3. Broadband wireless subscriber growth adapted from Gilstrap, D., Traffic and Market Report, Ericsson Report, 2012.

responsible of channel usage, and is thus one of the most important components of every packet switched network (Porto Cavalcanti and Andersson, 2009).

Packet switching strategies in broadband wireless systems such as the High Speed Packet Access (HSPA) allow to share a channel between users using scheduling strategies in the time domain (Porto Cavalcanti and Andersson, 2009). Under this strategy, the scheduler determines who will use a specified radio channel and the time (moment) to do so. This considers the use of a single radio channel by each user at each time. Therefore, regardless of the service required, a user will make use of the “complete” radio channel for a given amount of time. In HSPA systems each channel corresponds to 5 MHz of bandwidth. Under heterogeneous traffic conditions where users have different types of Quality of Service (QoS) requirements, and thus different data rates, the aforementioned scheduling strategy can be improved to increase spectrum efficiency (Porto Cavalcanti and Andersson, 2009). In further evolutions of the HSPA systems, namely the Long Term Evolution (LTE) Release 8 (Dahlman et al., 2011), flexible spectrum bandwidths were incorporated in order to improve spectrum usage efficiency. An LTE Release 8 channel has a total of 20 MHz of bandwidth structured in Resource Blocks (RBs) of 180 kHz. A user can make use of flexible bandwidths from 1.5 MHz up to the complete 20 MHz available (Dahlman et al., 2011) depending on the number of RBs assigned. This brings several combinations of bandwidth assignments on a single channel. For example, the scheduler can divide the 20 MHz channel four different channels with bandwidths of 10, 5, 3.5 and 1.5 MHz, simultaneously serving four users with different QoS requirements.

The spectrum management strategies used in LTE Release 8 standards allow flexibility for bandwidths up to 20 MHz. This strategy could be maintained for channels of up to 100 MHz, but given the scarcity of available spectrum with such bandwidth, the fragmentation of the bands for IMT-Advanced services, the expected growth in the broadband mobile market and the competition among operators, a different spectrum management strategy is required.

Carrier aggregation (CA) has been defined as an enabling technology to overcome

the spectrum scarcity and fragmentation problem (Shen et al., 2012). CA allows a system to aggregate multiple spectrum resources (resource blocks or RBs) and assign them to a single user in order to provide the sufficient bandwidth for a given service. CA works by allowing the system to assign spectrum blocks that may or may not be contiguous within a frequency band. Also, the possibility that these spectrum blocks are in different frequency bands is considered. This derives in three different types of CA (Yuan et al., 2010):

- Contiguous CA: Aggregation of contiguous RBs within the same frequency band.
- Non-contiguous intra-band CA: Aggregation of non-contiguous RBs available within the same frequency band.
- Non-contiguous inter-band CA: Aggregation of non-contiguous RBs available in different frequency bands.

The successful implementation of CA is fundamental to achieve the data rate goals established by IMT-Advanced. An adequate implementation of CA guarantees the coexistence of IMT-Advanced systems with previous standards. It also determines the efficiency in the use of the spectrum in terms of user capacity and quality of service. An implementation of CA must meet the following requirements (Parkvall and Astely, 2009):

- Assign-release carriers in a dynamic fashion
- The spectrum resource assignment delay must be below 1 msec
- Spectrum assignment must be optimal, maximizing throughput and minimizing multiple access interference
- Spectrum assignment algorithms must be feasible to implement
- Computational complexity of the assignment algorithms must be low or distributed

The use of CA brings many challenges to system design. Among these challenges are physical layer implementation, link layer and medium access control (MAC) layer issues. In the physical layer, the main problem is to simultaneously receive signals in different frequency bands when inter-band CA is used. Signals on different frequency bands behave differently, and thus the effects of the radio channel have to be compensated accordingly. Problems of mutual coupling as well as amplifier design have been addressed in experimental implementations such as (Saito et al., 2012b), (Cattoni et al., 2012) and (Kakishima et al., 2011). In the link layer, methods for fragmentation and reconstruction of packets from data received at different RBs are required. In (Vivier et al., 2011) methods to achieve this have been studied and implemented. Both physical layer and link layer proposals are focused on the possibility of implementing CA. However, they are not responsible for how the spectrum is used. The elements of the MAC layer are responsible for the efficient usage of the available spectrum resources.

In the MAC layer, the research work from the scientific community has focused on scheduler design. A summary of the reviewed literature on scheduler design for CA is presented in Chapter 2. Since the efficient use of the available spectrum is directly related to the operation of the scheduler, the possibility of implement CA to solve the scarcity and fragmentation of the spectrum depends on an efficient scheduler design.

Proposals of scheduler design for CA are varied, and range from adaptations of well known wired scheduling strategies to sophisticated scheduling proposals that include multiple stage schedulers. The design of a scheduler can be aimed at improving a system metric, such as throughput or fairness. However, the criteria that has to be considered in scheduler design for CA in order to increase throughput, fairness and reduce latency in LTE-Advanced systems is not defined.

## 1.2 Aim of Thesis

Carrier Aggregation is proposed for LTE-Advanced and Wireless MAN Advanced standards. In this thesis we will focus on LTE-Advanced specifications. In order to im-

plement CA, a scheduler with multiple spectrum resource assignment capabilities is required by the system. Schedulers with CA capabilities provide the mean to aggregate carriers depending on a user demand (Lei and Zheng, 2009). As shown in (Yuan et al., 2010), CA involves changes in every layer of the system. For instance, the process of packet fragmentation and reconstruction has to be taken into account in the transport layer. In the case of Inter-Band CA, a transceiver architecture with simultaneous transmission and reception in different frequency bands has to be available. Given the experience and interests of the Wireless Communications Group at the CICESE Research Center, the objective of this thesis is aimed at scheduler design as follows:

**Design, analyze and evaluate a scheduler for Carrier Aggregation with delay reduction and fairness capabilities to improve spectrum usage under heterogeneous traffic in LTE-Advanced systems.**

Developments in CA propose the use of the LTE Release 8 spectrum organization as a basis for the design of scheduler structures. Proposals such as (Lei and Zheng, 2009) (Songsong et al., 2009) and (Chen et al., 2009) make use of individual Resource Blocks (RB) for assignment. Based on the need to reduce the delay in resource assignment as well as to improve efficiency of spectrum resource usage, in this thesis we propose a novel approach to scheduler design based on the assignment of pre-defined sets of RBs. The proposed scheduling structure allows to reduce de delay in resource assignment and provides a mechanism to improve spectrum usage in terms of user capacity and throughput. It also allows to adjust fairness in heterogeneous traffic conditions using a single parameter.

### 1.3 Thesis Outline

During the last four years the development of scheduling strategies for CA has been addressed in literature. Chapter 2 presents the details of CA in order to understand

the problems associated with its implementation. A review of scheduling algorithms for CA found in literature is also presented.

Although LTE-Advanced systems will operate in different environments such as outdoor to outdoor, outdoor to indoor, and indoor to indoor, for the evaluation of the proposed scheduling strategy we focus on the outdoor to outdoor macrocellular scenario. To take into account the use of Adaptive Modulation and Coding (AMC) schemes used in LTE and LTE-Advanced standards, a channel model is used to evaluate the performance of a scheduler. In Chapter 3 a channel model for a highly dispersive macrocellular urban environment is developed.

The mechanism to adapt the AMC scheme is based on a feedback of the channel conditions. Specifically, in the Downlink (DL) the User Equipment (UE) sends a report of the channel condition using a Channel State Indicator (CSI). The CSI corresponds to a message transmitted periodically by the UE to the Enhanced Node B (ENodeB). The CSI includes a Channel Quality Indicator (CQI) that informs the ENodeB of the Signal to Interference and Noise Ratio (SINR) observed by the UE in each of the available channels. The CQI reported determines the AMC scheme to be used by the ENodeB with the UE. Chapter 4 presents an analysis of the dependance between the CQI and the required amount of spectrum resources for a specific type of traffic and environment. This analysis provides a model of the statistical behavior of the CQI and the spectrum required by a user.

Chapter 4 also presents the proposal of a novel scheduling strategy for CA based on the organization of available resource blocks in sets. This strategy is referred to as Set Scheduling. The proposed scheduling strategy is evaluated in an urban macrocellular environment in order to determine its performance without service priorities. The resulting evaluation provides an insight of the potential of Set Scheduling for the reduction of resource assignment delay as well as to increase user capacity.

In order to further analyze the performance of the proposed scheduling strategy, an analysis of fairness in the presence of heterogeneous traffic is presented in Chapter 5. In order to analyze the fairness of Set Scheduling, a fairness metric for heterogeneous

traffic is proposed and compared to the well known Proportional Fairness (PF) (Han and Lu, 2011) criterion.

Chapter 6 presents a summary of the results, general conclusions and future work areas identified with the realization of this project.

A schematic diagram with the structure of this thesis is shown in Fig. 4.

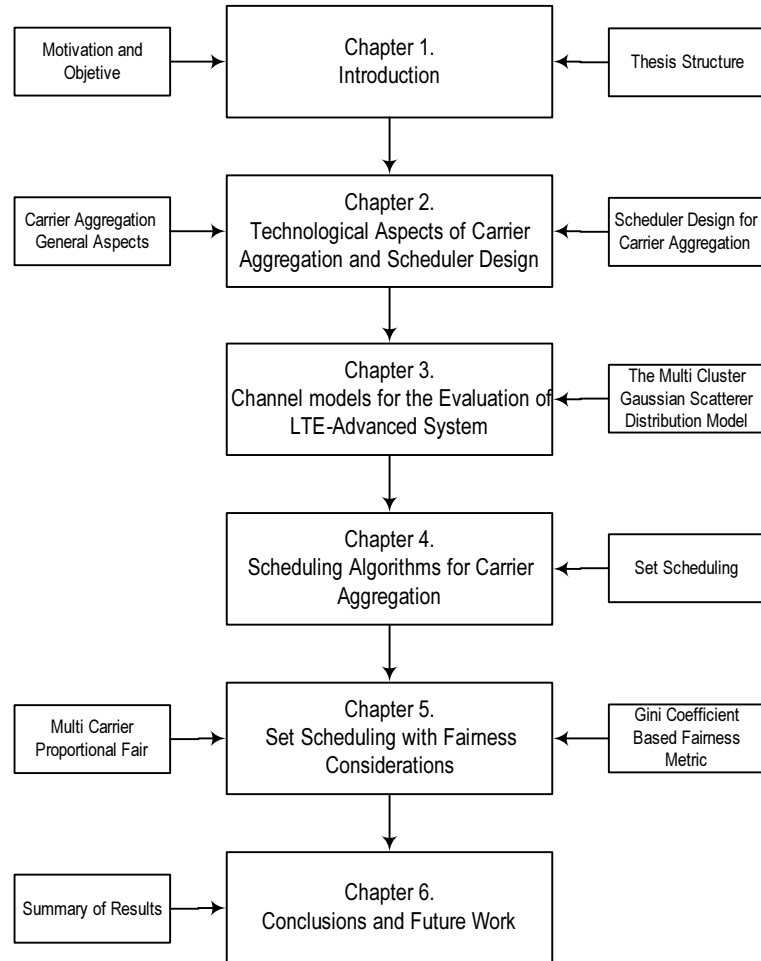


Figure 4. Thesis structure.

## 1.4 Outcomes

The work on the channel model proposed contributed to the following papers:

- Galaviz Yáñez, G. y D. H. Covarrubias Rosales. (2010) Characterization of second order moments of a multi-cluster Gaussian scatterer distribution channel model. 4th European Conference on Antennas and Propagation (EuCAP)2010, April 12-16. Barcelona, Spain.
- Galaviz Yáñez, G., D. H. Covarrubias Rosales y A. G. Andrade Reátiga. (2012) Evaluation of a multi cluster Gaussian Scatterer distribution channel model. IEEE Transactions on Communications. E95-B(1): 296-299 p.

The work on scheduler design contributed to following papers:

- Galaviz Yáñez, G., D. H. Covarrubias Rosales y A. G. Andrade Reátiga. (2011) On a spectrum resource organization strategy for scheduling time reduction in carrier aggregated systems. IEEE Communications Letters. 15(11): 1302-1304 p. doi:10.1109/LCOMM.2011.090611.111473
- Galaviz Yáñez, G., D. H. Covarrubias Rosales, A. G. Andrade Reátiga y S. Villarreal Reyes. (2012) A resource block organization strategy for scheduling in carrier aggregated systems. EURASIP Journal on Wireless Communications and Networking. doi:10.1186/1687-1499-2012-107

## Chapter 2

# Technological Aspects of Carrier Aggregation and Scheduler Design

In order to implement CA spectrum assignment to a single user, a scheduler with multiple RB assignment capabilities is required by the system. In general, the task of the scheduler will be to optimize resource usage in a feasible amount of time. In this chapter we present the general operation of CA and schedulers in the context of LTE-Advanced systems. An analysis of existing work in schedulers for CA implementation is also presented.

### 2.1 Carrier Aggregation

The use of CA allows to create a radio channel of certain bandwidth using narrower component channels. Specifically for LTE-Advanced, the narrow channels are identified as Component Carriers (CC) and correspond to LTE Release 8 channels that span a bandwidth of 20 MHz. Using carrier aggregation, up to five CCs can be aggregated in order to create a 100 MHz channel considered as needed to achieve data rates of up to 1 Gbps. To better understand the operation of CA, it is important to describe the spectrum resource organization in LTE Release 8 also used in LTE-Advanced.

The basic spectrum resource is defined as a Resource Block (RB) (Dahlman et al., 2011). A single RB is a frequency-time resource, and corresponds to a set of 12 OFDM subcarriers during 7 OFDM symbols. A single OFDM subcarrier during one symbol time is defined as a Resource Element (RE). Therefore, a single RB is a set of 84 REs. A time slot is defined as the duration of 7 OFDM symbols and takes 0.5 ms. The use of an Adaptive Modulation and Coding (AMC) scheme determines the bit rate and payload of a single RB. Given three different modulation schemes (QPSK, 16 QAM and

64 QAM), and a fixed duration of each time slot, the bit rate supported by a single RB can be calculated. Figure 5 shows the structure of a single RB and the corresponding bandwidths for a single OFDM subcarrier and a complete RB.

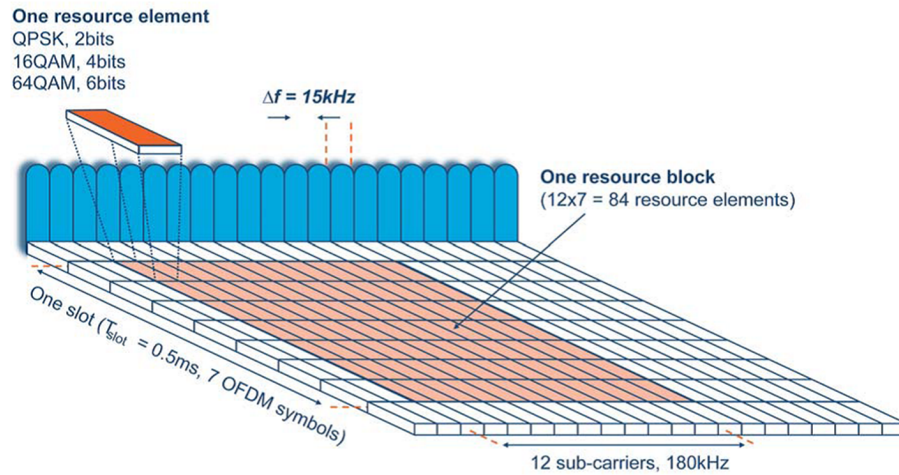


Figure 5. Structure of a Resource Block.

A set of 100 RBs spans a total of 20 MHz (considering guard bands) to form a CC. Figure 6 shows the general operation of CA describing the use of 20 MHz CCs. Considering the case of five CCs to span a bandwidth of 100 MHz, a total of 500 RBs would be used.

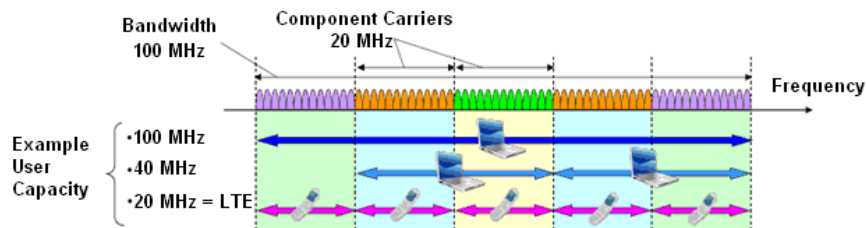


Figure 6. General operation of CA.

Depending on the frequency band in which CCs are located and their availability, CA can be classified as Contiguous, Non-contiguous Intra-band or Inter-band. Figure 7 shows this classification. Each type of CA presented in Fig. 7 has its own implications.

- Contiguous CA: Aggregation of contiguous RBs within the same frequency band involves the use of a scheduler capable of assigning from one up to five contiguous CCs. This operation is similar to that required for flexible bandwidth assignment

in LTE Release 8 systems (Porto Cavalcanti and Andersson, 2009). Contiguous CA requires an operator to own the rights of all the contiguous CCs to be used.

- **Non-contiguous intra-band CA:** Aggregation of non-contiguous RBs available within the same frequency band allows the use of CCs available within the same frequency band, but not needing for them to be contiguous. This type of operation of CA involves a scheduler capable of assigning fragmented CCs to a user. Although in general it is similar to Contiguous CA, the option of assigning fragmented spectrum allows for a more efficient use of available spectrum (Chen et al., 2009). Non-contiguous intra-band CA would allow an operator to own the rights of fragments of a frequency band rather than contiguous spectrum.
- **Non-contiguous inter-band CA:** Aggregation of non-contiguous RBs available in different frequency bands allows the use of CCs in one frequency band to be aggregated with CCs from a different frequency band. The different propagation characteristics of the frequency bands adds an extra level of complexity to this type of CA. A scheduler capable of selecting CCs from different frequency bands is required (Lei and Zheng, 2009). An operator would be able to aggregate CCs from different frequency bands in order to reach a desired bandwidth. This will allow an operator to own a limited amount of spectrum in two different frequency bands and aggregate it to achieve a larger bandwidth to serve its users.

### **2.1.1 Carrier Aggregation Deployment Scenarios**

From the different types of CA, Inter-Band CA involves the greatest challenges for implementation. The main problem lies in the different propagation characteristics of the frequency bands to be used, which will vary in Path Loss (PL), building penetration, coverage, doppler shift, etc. (Zhang et al., 2011). With regards to the rights ownership of the spectrum, there exists the option to allow operators to share spectrum bands. The possibility of using shared spectrum results in CA types that involve the use of

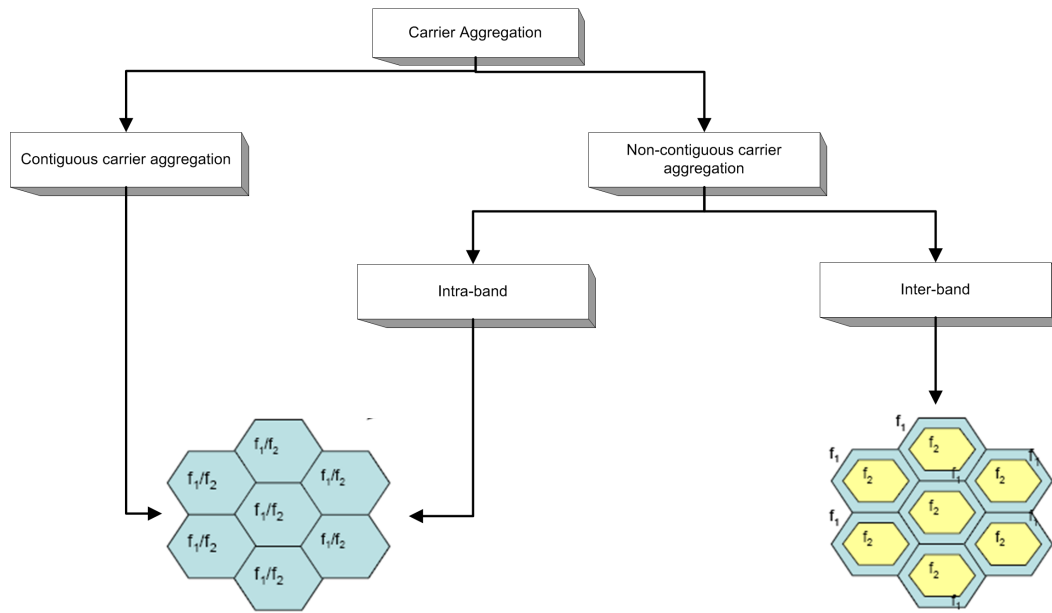


Figure 7. Classification of CA based on the frequency band and availability of CCs.

owned spectrum and shared spectrum. Although the use of shared spectrum may add additional complexity to the system, it would allow for a more efficient use of the available resources (Songsong et al., 2009).

Together with the different types of CA, the 3GPP has defined a set of deployment scenarios where two different frequency bands are used by a single base station. As defined in (3GPP, 2010), CA deployment scenarios consider two frequency bands F1 and F2.

Figure 8 shows scenario 1. F1 and F2 cells are co-located and overlaid, providing nearly the same coverage. Both layers provide sufficient coverage. Mobility can be supported on both layers. Likely scenario when F1 and F2 are in the same frequency band, e.g.,  $F1 = F2 = 2$  GHz. It is expected that aggregation is possible between overlaid F1 and F2 cells. Given the case of equal frequency bands for F1 and F2, in order to provide equal coverage the power transmitted in each band will be the same. Users can be assigned to either band or use intra-band CA for greater bandwidth.

Figure 9 shows scenario 2. F1 and F2 cells are co-located and overlaid, but F2 has smaller coverage due to larger path loss. Only F1 provides sufficient coverage and F2

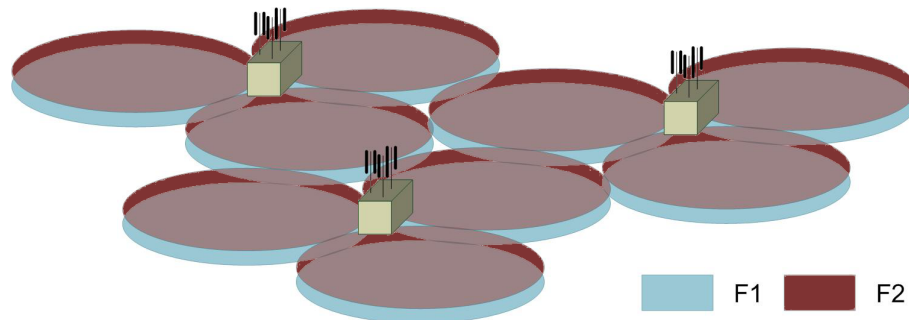


Figure 8. Scenario 1 for CA deployment considering overlapped coverage.

is used to provide throughput. Mobility is performed based on F1 coverage. Likely scenario when F1 and F2 are of different bands, e.g.,  $F1 = 2$  GHz and  $F2 = 3.5$  GHz. It is expected that aggregation is possible between overlaid F1 and F2 cells. This scenario considers the case of equal power transmission for the two bands, thus different coverage. Users within the range of F2 can be assigned to either band or use inter-band CA for increased bandwidth. Users at the cell edge can only be assigned to the F1 band.

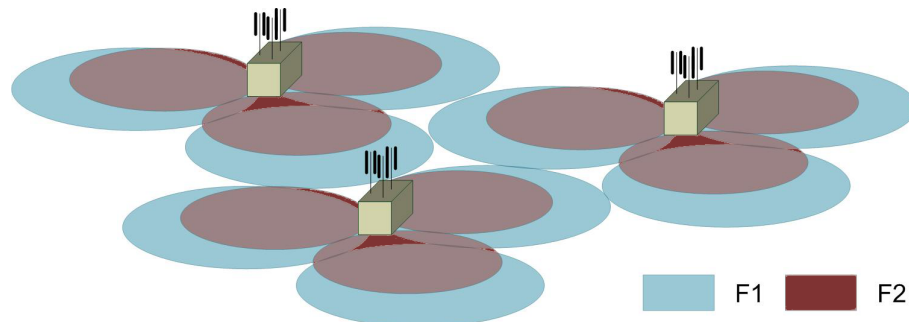


Figure 9. Scenario 2 for CA deployment considering different range.

Figure 10 shows scenario 3. F1 and F2 cells are co-located but F2 antennas are directed to the cell boundaries of F1 so that cell edge throughput is increased. F1 provides sufficient coverage but F2 potentially has holes, e.g., due to larger path loss. Mobility is based on F1 coverage. Likely scenario when F1 and F2 are of different bands, e.g.,  $F1 = 2$  GHz and  $F2 = 3.5$  GHz. It is expected that F1 and F2 cells of the same eNodeB can be aggregated where coverage overlap. This scenario is designed to provide extended coverage to cell edge users with the possibility of increased bandwidth with inter-band CA to users in overlapped regions.

Figure 11 shows scenario 4. F1 provides macro coverage and on F2 Remote Radio

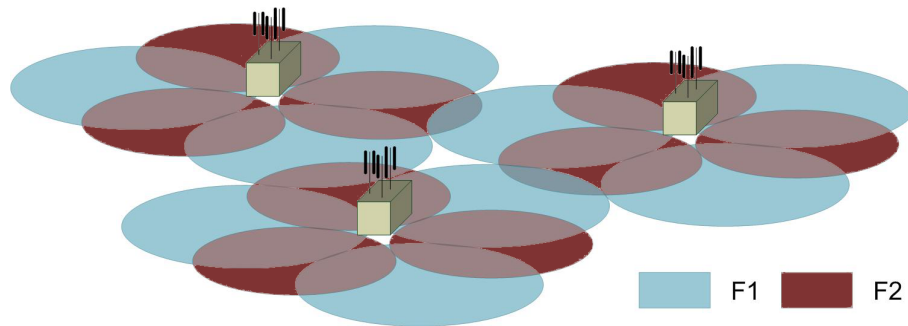


Figure 10. Scenario 3 for CA deployment for increased cell edge coverage.

Heads (RRHs) or repeaters are used to provide throughput at hot spots. Mobility is performed based on F1 coverage. Likely scenario when F1 and F2 are of different bands, e.g.,  $F1 = 2 \text{ GHz}$  and  $F2 = 3.5 \text{ GHz}$ . It is expected that F2 RRHs cells can be aggregated with the underlying F1 macro cells. This is considered to provide increased user capacity with the possibility of inter-band aggregation in hot spots to provide greater bandwidth to users.

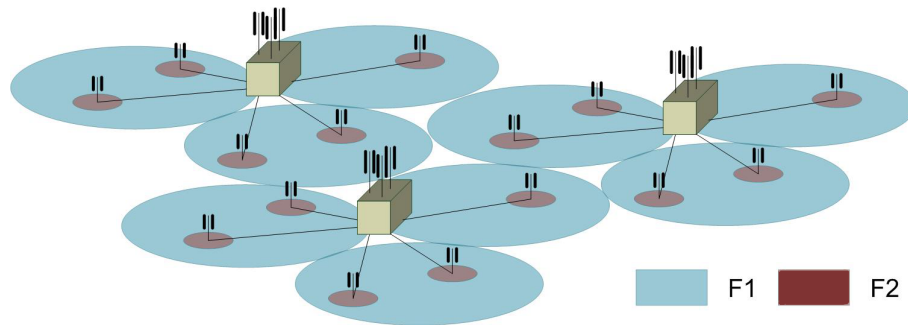


Figure 11. Scenario 4 for CA deployment considering Remote Radio Heads.

### 2.1.2 Carrier Aggregation Implementation Issues.

Implementation of CA capabilities involves several challenges in the design of both the UE and ENodeB. Changes in the system physical layer as well as in the Radio Resource Control (RRC) and Medium Access Control (MAC) sublayers are needed. Some of these changes are discussed in (Iwamura et al., 2010) and summarized as follows:

- Physical Layer: Radio transceivers must be designed according to the type of CA implementation (intra-band or inter-band). In the case of intra-band CA, a single

transceiver with sufficient bandwidth (at least 100 MHz) must be used. In the case of inter-band CA, the simultaneous operation of two transceivers working on different frequency is needed.

- Radio Resource Control (RRC): Channel Quality Indicators (CQI) corresponding to additional CCs for aggregation must be processed in order to perform spectrum assignment. Additional signaling information must be exchanged between UE and ENodeB.
- Medium Access Control (MAC): Scheduling of multiple CCs must be possible. The CQI information obtained from the UE must be used in conjunction with the scheduler policies (priority handling) in order to assign CCs to users. Information regarding assigned spectrum resources must be informed to each UE.

Given the experience of the Wireless Communications Group at the CICESE Research Centre in radio resource management and channel modeling (Andrade and Covarrubias, 2003; Lopez et al., 2005), in this thesis we focus in the MAC sublayer of the ENodeB, specifically in scheduler design for CA implementation in the Downlink channel. Signaling information exchanged between UE and ENodeB is not addressed and thus considered as free from errors. This consideration is often found in literature to evaluate the performance of scheduling strategies.

## 2.2 Scheduler Design for Carrier Aggregation

Radio Resource Management (RRM) is a general term used in wireless communication systems that encompasses the operations related to spectrum management, allocation and assignment. As such, RRM operations are directly related to channel assignment and scheduling (Porto Cavalcanti and Andersson, 2009). In this section we review classic RRM strategies used in circuit switched wireless communication systems. We then present the strategies used in the first evolutions to packet switched wireless cellular communication systems in order to understand the major changes in RRM for current

and next generation broadband wireless communication systems. We finish this section with a review of the state of the art of scheduling proposals for CA.

### **2.2.1 Radio Resource Management in Circuit Switched Cellular Networks.**

Wireless cellular communication systems developed for telephony, such as the Global System for Mobile standard (GSM) managed the spectrum available by dividing it into “narrow”<sup>2</sup> band channels (Rappaport, 2002). Depending on the standard, each narrow band channel could support from 1 up to 64 voice calls.

In order to make an efficient use of the spectrum owned by an operator, each base station disposed of a certain number of narrow band channels. Each channel was available to provide service to users. During the first deployments of wireless cellular communication systems, the available bandwidth was divided in channels and then a subset of the total number of channels was assigned to each base station in order to mitigate interference in frequency reuse patterns (Rappaport, 2002). Figure 12 shows the general structure of the narrow band channels available to a base station. The RRM operations related to this structure of the available spectrum is based on circuit switched connections. Therefore, at the moment a user requests a connection to make a phone call, the base station processes the user information (to check for priorities and/or rights) and if available, a channel is assigned. In digital systems such a GSM a channel is a combination of a frequency and a time slot due to the use of Time Division Multiple Access (TDMA). In systems that make use of Code Division Multiple Access (CDMA) a channel is a combination of a frequency and a code (Rappaport, 2002).

With the ever increasing number of users, a hard limit on the number of channels available on each base station was not efficient. Modifications to channel assignment strategies evolved to Dynamic Channel Assignment (DCA) schemes (Martinez et al., 2010). DCA schemes rely on the knowledge of system load and channel usage in the

---

<sup>2</sup>We will refer to narrow band channels as those used in Second Generation (2G) wireless communication systems, regardless of the bandwidth

whole network (not on a single base station). The system is capable of identifying which channels from a base station are not in use and “borrowing” them to base stations where user demand requires them. These types of schemes are more efficient as they allow an operator to distribute channels dynamically as they are required. Improvements in user capacity and blocking probability with DCA are well documented in literature (Martinez et al., 2010). However, it has to be noted that under high user density scenarios (high traffic demands) fixed channel assignment is a better choice.

### 2.2.2 Radio Resource Management in 3G Cellular Systems.

As wireless communication systems evolved to broadband data solutions, the use of circuit switched links did not offer an efficient use of available spectrum. Third Generation (3G) wireless communication systems evolved into packet switched networks for broadband data communications, but relied on a circuit switched link for voice and as a basic channel in data communications (Holma and Toskala, 2010). Once packet switched communications are used, the concept of the radio channel changes. A single “wide”<sup>3</sup> band radio channel is shared by users. A scheduler is now part of the RRM operations and is in charge of scheduling user data transfers in the time domain, all through the same wide band radio channel. Figure 13 shows the general structure of how each wide band radio channel is used in 3G systems, specifically in the Universal

<sup>3</sup>We will refer to wide band radio channels to those used by 3G and Beyond wireless communication systems

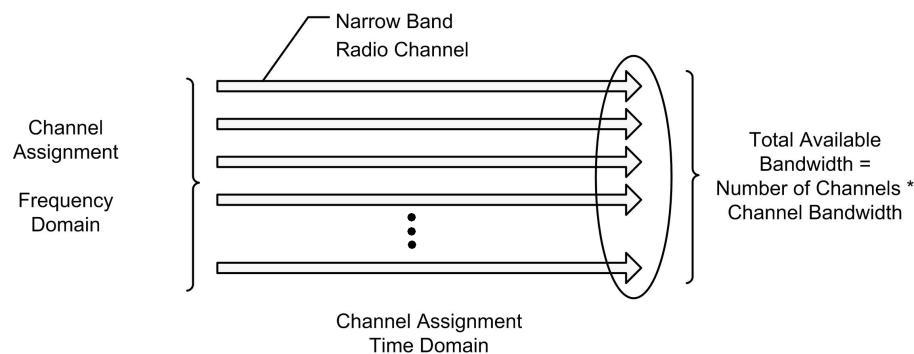


Figure 12. General structure of available spectrum and its use in pre-3G systems.

Mobile Telecommunication System (UMTS).

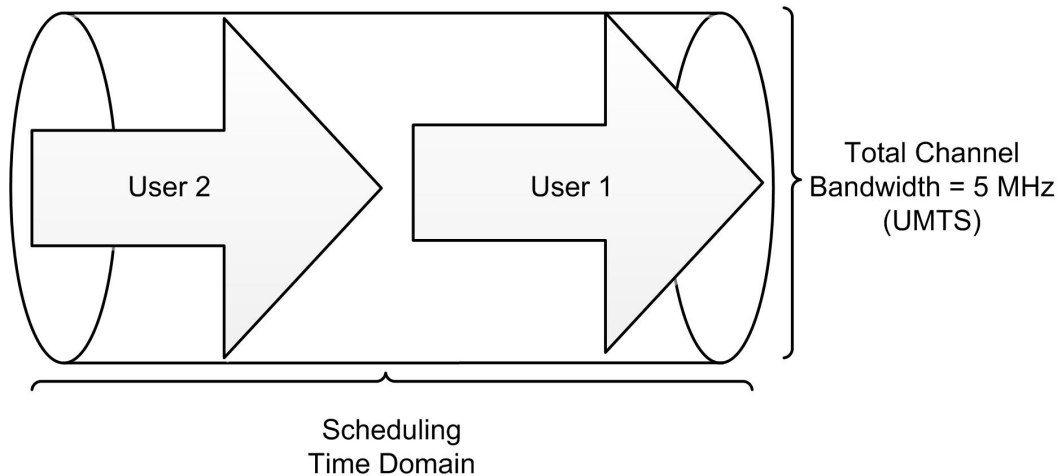


Figure 13. General structure of spectrum usage in 3G systems

Schedulers have been used in wired and wireless data networks. There is a vast theory about scheduler operation and analysis. For an overview of scheduler solutions for wireless communication systems readers are referred to (Gutierrez, 2003). The scheduler becomes particularly important in the performance of a wireless system when the network is highly loaded (Porto Cavalcanti and Andersson, 2009). The basic operation of the scheduler is to determine when each user will make use of the shared spectrum resource. The decisions made by the scheduler to determine when the user can use the channel are based on different factors. These factors include (but are not limited to) channel conditions, type of service requested (voice, multimedia, video, etc.), channel availability, overall network throughput and fairness. Performance will vary depending on the factor that the system uses.

The scheduler has a direct impact in three main aspects of system performance:

- **Fairness:** It is a system performance metric that indicates the tendency of the system to attend all users equally, thus being fair. Fairness can be measured using specific metrics such as Jain's fairness index (Jain et al., 1984). Fairness is measured when the scheduler uses specific metrics to prioritize user requests for data transfers. Fairness can be seen from three different perspectives. Fairness

in resources indicates that the system assigns the same amount of spectrum/time resources to all users. Fairness in throughput indicates that the system balances the available resources in order to assign the same throughput to all users. Fairness in general can be seen as the fact that the scheduler does not perform any kind of prioritization, and thus treats all users in the same manner regardless of their requests or channel conditions (achievable throughput).

- **Throughput:** The overall system throughput depends on the scheduler operation. The scheduler prioritizes user requests for data transfers based on the throughput that each user can achieve. If users with the highest achievable throughput are priority, the overall system throughput can be maximized (Porto Cavalcanti and Andersson, 2009). On the other hand, if users who can achieve the lowest throughput have priority then the overall throughput will not reach the maximum, resulting in an inefficient use of the spectrum resources. Depending on the prioritization policies and metrics used by the scheduler, the maximum throughput achieved by the network will vary.
- **Complexity/Delay:** In order to provide adequate quality of service (QoS) modern wireless communication systems need to respond to user requests in a very short amount of time (1 msec or less, depending on the standard) (Dahlman et al., 2011). The operation of the scheduler may be subject to mathematical operations and optimization processes (Garcia et al., 2012) in order to define the priorities of user assignment. Depending on the implementation of such processes, the complexity and/or the associated delay may become impractical for implementation.

The three aspects described above are well studied in literature in works such as (Gutierrez, 2003), (Han and Lu, 2011), (Kaneko et al., 2006) and (Zhang et al., 2011). In general, there will always be a tradeoff between throughput and fairness. Several scheduler proposals balance the tradeoff between these two objectives by means of optimization. Then, the processes involved in the optimization required maximize both throughput and fairness result in algorithms that may be too complex to implement

with current technology (Porto Cavalcanti and Andersson, 2009). With the evolution of 3G systems and the use of High Speed Packet Access and the corresponding Long Term Evolution (LTE) path followed by the Third Generation Partnership Project (3GPP), the organization of spectrum resources has changed in order to have a flexible use of it. This flexibility allows to use variable channel bandwidths from 1.5 MHz up to 20 MHz (LTE Release 8). This structure allows to attend users efficiently by providing only the required bandwidth for a transmission. The bandwidth required will depend on the service (voice, video, multimedia, etc.), but given the use of Adaptive Modulation and Coding (AMC) the channel conditions are also taken into account. Figure 14 shows the general structure of spectrum usage in LTE Release 8 systems. This new structure brings another level of complexity to scheduler design, as the required amount of spectrum needs to be calculated and its usage optimized. Also, with the use of Orthogonal Frequency Division Multiple Access (OFDMA) the system is considered as Multi-Carrier.

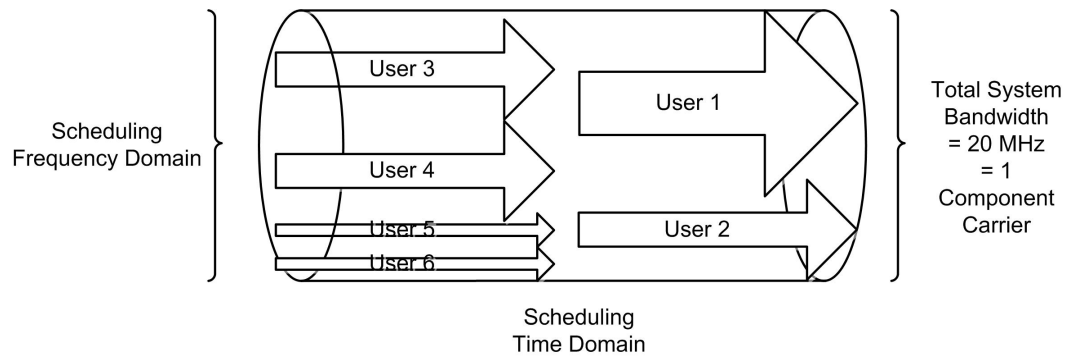


Figure 14. General structure of spectrum usage in LTE Release 8.

Some proposals of schedulers for LTE Release 8 systems can be found in (Porto Cavalcanti and Andersson, 2009) and (Dahlman et al., 2011). Some of the most representative schedulers for LTE Release 8 systems are the following:

- **Round Robin (RR):** This type of scheduler cyclically assigns the channel to users without any priority. It can be seen as a First In First Out (FIFO) type of scheduling, where user requests are buffered and attended sequentially. Since no

priorities are handled, the Round Robin (RR) scheduler is considered to be fair. However, it will not benefit from the channel condition knowledge.

- **Max C/I Ratio:** This scheduler will take advantage of the channel quality observed by each user on the available channel. With the use of AMC schemes, the Max C/I Ratio scheduler will prioritize users with better channel conditions. Users with better channel conditions will be able to make better use of the spectrum, and thus maximize network throughput. However, fairness is not taken into account and users with the lowest channel conditions might suffer from spectrum starvation, even if their condition allows them to be served.
- **Proportional Fair (PF):** This type of scheduler assigns the channel to the user with the best relative channel quality. This relative index is calculated considering a combination of channel quality and the level of fairness desired (Porto Cavalcanti and Andersson, 2009). Depending on the different variations of the PF implementation, the scheduler may take into account past resource allocation, the current level of performance of a user and the instantaneous or average channel quality. The objective of a PF scheduler is to balance the tradeoff between fairness and throughput. If the PF scheduler is implemented at the OFDMA subcarrier level, the scheduler is defined as Multi-Carrier and its complexity is considerably larger than in single carrier implementations. A Multi Carrier PF scheduler is presented in (Han and Lu, 2011).

### 2.2.3 Radio Resource Management in LTE-Advanced Systems

As wireless broadband systems evolve into IMT-Advanced compliant standards, channels of up to 20 MHz are not enough to support the required data rates of 1 Gbps for low mobility users and 100 Mbps for high mobility users. The Release 10 of LTE (LTE-Advanced) uses Carrier Aggregation (CA) in order to increase total channel bandwidth and maintain backward compatibility with User Equipments (UEs) from LTE Release 8. Figure 15 shows the general structure of the available bandwidth. CA allows to

accumulate up to five Component Carriers (CCs) of 20 MHz each<sup>4</sup>. Users with no CA capability or users with no need for bandwidths larger than 20 MHz will make use of CCs without aggregation. However, the possibility of performing CA at the Resource Block (RB) level is present, allowing users with smaller spectrum requirements to still use non-contiguous CA in both intra and inter band cases.

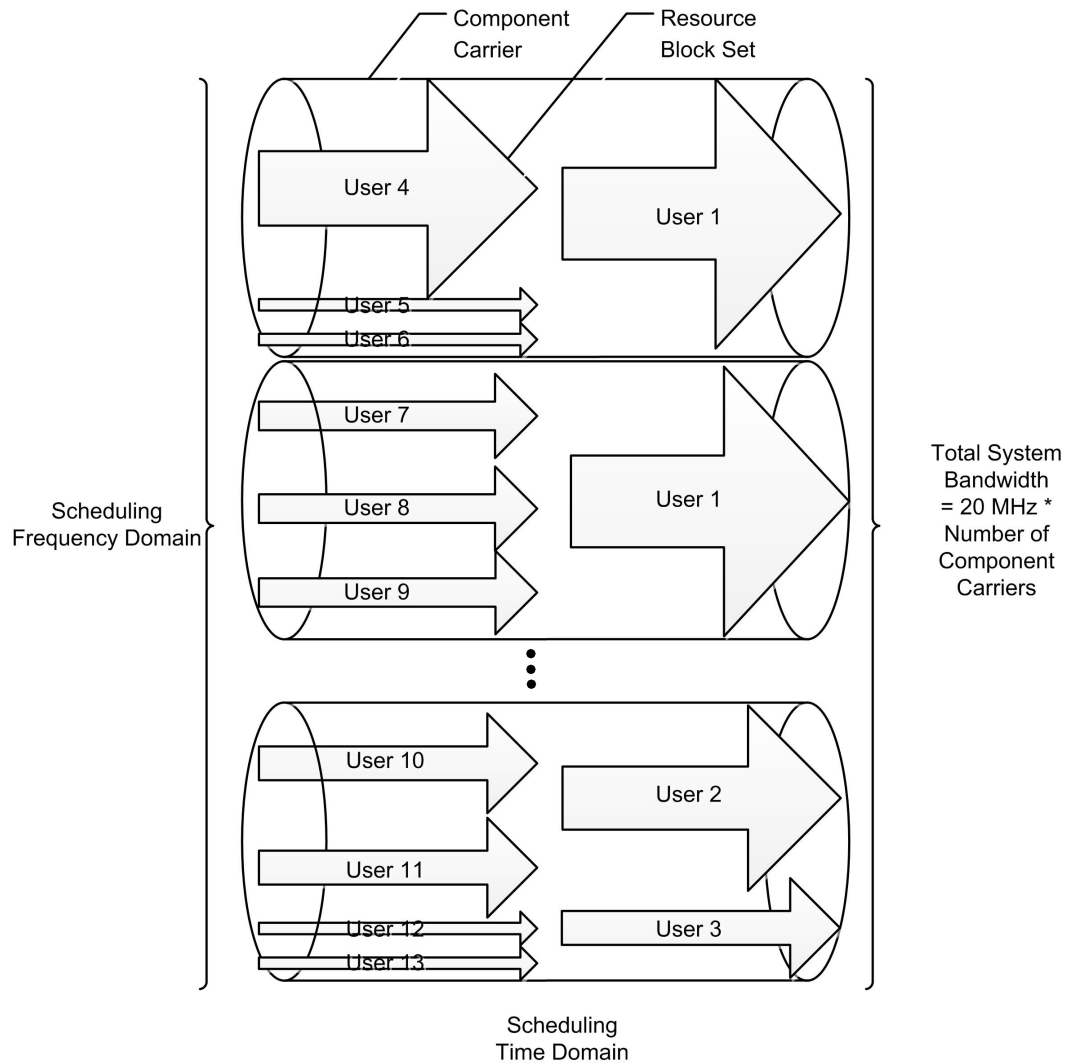


Figure 15. General structure of spectrum usage in LTE Advanced.

In Fig. 15, each flow representing a User corresponds to a set of RBs. In principle, each set will comply with LTE Release 8 standards (Döttling et al., 2009). However,

<sup>4</sup>Release 10 specifies that up to 5 CCs can be aggregated, but only supports aggregation of two for a maximum bandwidth of 40 MHz [TR36.133 2010]

when CA is required (case of User 1), multiple sets of RBs from different CCs are aggregated. By allowing to form a virtual channel with enough bandwidth to achieve the goals of IMT-Advanced, CA plays a vital role in the successful implementation of LTE-Advanced systems. Due to the importance of CA, it has been an important topic of study in the last three years. Each scheduler proposal available in literature is aimed at improving a specific aspect of system performance (fairness, throughput, complexity).

Scheduler proposals for CA found in literature and analyzed for this thesis work vary greatly in operation and performance, as well as in evaluation conditions. In the following, an attempt to categorize the different proposals is presented in order to situate within the state of the art the main contribution of this work.

With regards to scheduler structure, two general structures of scheduler operation are presented in (Chen et al., 2009). These structures correspond to the Disjoint Queue Scheduler (DQS) and the Joint Queue Scheduler (JQS). These two structures are also used by (Lei and Zheng, 2009). Figure 16 shows the structure of the DQS. The main characteristic of DQS is that packets from users are first scheduled to a CC, and then a second scheduler is in charge of assigning RBs from the CC to the corresponding packets. Figure 17 shows the structure of the JQS. In this case, a single scheduler is in charge of assigning resources to user packets directly to RBs within CCs. This strategy considers all available RBs as a single set. Even though in the work of (Meucci et al., 2009) and (Songsong et al., 2009) the structures used are similar in operation, they are regarded as a two stage or a single stage scheduler.

The results obtained from (Chen et al., 2009) show an advantage in terms of throughput and efficiency in spectrum use when JQS is used with different types of schedulers such as PF and RR. The advantage in throughput is due to the fact that since all packets contend for all resources, all of the available RBs are used. This advantage comes with an important tradeoff. Since all the tasks of scheduling are made by a single scheduler, the computational burden is concentrated in one stage. The corresponding delay due to the use of this strategy is not analyzed.

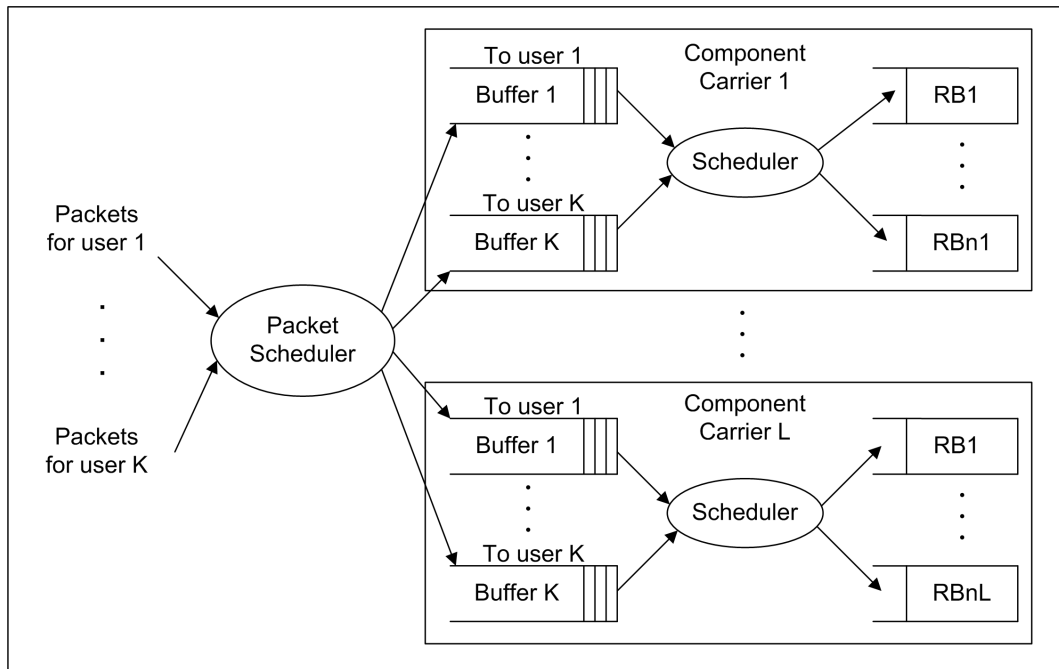


Figure 16. Two stage scheduler structure (Disjoint Queue).

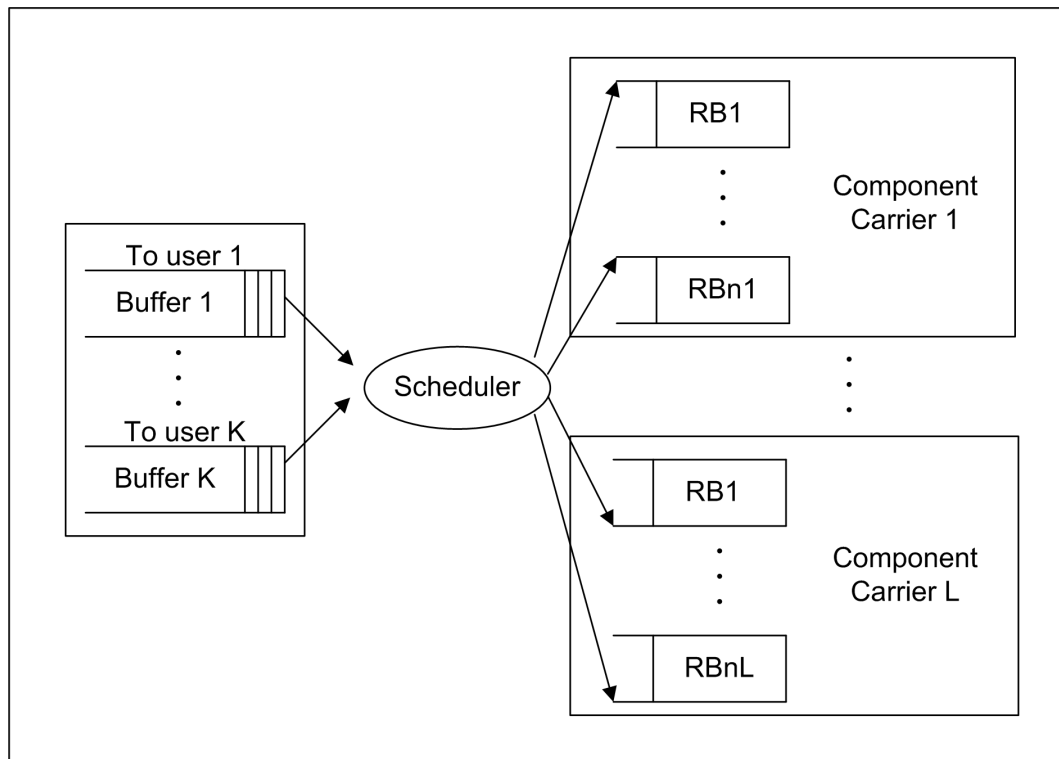


Figure 17. Single stage scheduler structure (Joint Queue).

## 2.2.4 Schedulers for Carrier Aggregation

Scheduler proposals with single and two stages are still presented in recent literature. Examples of two stage proposals can be found in (Ji-hong et al., 2012), (Sivaraj et al., 2012), (Gao et al., 2011), (Zhang et al., 2011). In these works, the first stage is distinguished as the Component Carrier Selection (CCS) or Frequency Domain Scheduler, while the second stage is referred to as the Time Domain Scheduler. Proportional Fair types of schedulers are used at either the Frequency Domain or the Time Domain schedulers. Round Robin schedulers are usually found only in the Time Domain scheduling operation. There are various ways to perform CCS that range from user grouping based on channel conditions (Songsong et al., 2009) to user grouping based on spatially correlated clusters of UEs (Sivaraj et al., 2012).

Given the importance of the Frequency Domain scheduler, the work found in (Liu et al., 2011), (Gao et al., 2011), (Garcia et al., 2012) and (Costa et al., 2012) is focused in the problem of Component Carrier Selection. In these references the application varies from Macrocellular to Femtocellular environments. However, due to the expected increase in LTE-Advanced Femtocells (Garcia et al., 2012) the CCS problem has greater impact in this application due to the probability of interference. A successful implementation of a two stage scheduler relies on proper balancing of load among the available CCs (Garcia et al., 2012).

Another important difference found in literature comes from the spectrum structure. The concept of CA involves the accumulation of complete CCs. Some of the schedulers found in literature make use of a spectrum structure as that in Fig. 13, with the existence of multiple CCs. In those situations, a user is scheduled in one, two or up to five CCs simultaneously depending on its channel conditions and transfer rate required. This strategy can be observed in both single and two stage scheduling structures. The work in (Chung and Tsai, 2010), (Saito et al., 2012b), (Nguyen and Kovacs, 2012), (Gao et al., 2011) and (Wang et al., 2011) make use of full CC assignment. Since the scheduling decisions are made on a small set of resources (the number of available CCs),

the operation of full CC scheduling is considerably fast (Chung and Tsai, 2010). Full CC assignment is useful when user data rates are high and thus require the use of at least a full CC. However, when requested traffic comes from multiple users with low data rate demands, the use of the channel is inefficient (Porto Cavalcanti and Andersson, 2009). This is due to the fact that instead of serving multiple users with low data rate requirements, users are attended individually as only one user per CC can be assigned at a particular time slot.

In order to overcome this limitation, references such as (Songsong et al., 2009), (Chen et al., 2009), (Zhang et al., 2011), (Ji-hong et al., 2012) and (Sivaraj et al., 2012) deal with the assignment of individual RBs. Assignment of individual RBs allows the system to make a more efficient use of spectrum resources, as each RB is individually assigned to the user who maximizes the specific scheduling metric (PF, Max C/I, etc). The cost of handling RBs individually is an increased computational load, with its corresponding delay. Thus, two stage scheduler structures are preferred for individual RB assignment in order to distribute the computational burden.

The evaluation of system performance with the use of a specific type of scheduler is very similar in all studied references. A single cell with users distributed randomly within the ENodeB coverage area is the main evaluation scenario. Mobility and static conditions are considered. The most important aspect for system performance evaluation with the use of a scheduler is the traffic model. Two types of traffic are mainly used. Full buffer traffic with a finite number of users is the main choice when schedulers used are of PF type such as in (Ji-hong et al., 2012), (Saito et al., 2012b), (Sivaraj et al., 2012), (Liu et al., 2011) and (Vivier et al., 2011). For comparison purposes, authors also make use of bursty traffic with finite buffers. In (Sivaraj et al., 2012), heterogeneous traffic is considered as Guaranteed Bit Rate (GBR) services. However, when fairness is evaluated it is mostly done with homogeneous traffic conditions (full buffer type of traffic). This is due to the fact that there is no standardized metric to evaluate fairness when heterogeneous traffic is present.

In all proposals, either direct or modified versions of well known schedulers are used.

Proportional Fair scheduling is one of the main schedulers used due to the possibility to balance system throughput and fairness (Porto Cavalcanti and Andersson, 2009). PF implementations for CA are aimed at providing the same data rate to all users under homogeneous traffic conditions. Due to the requirement of IMT-Advanced systems to support services that range from short messages to real time video conference in high definition (Dahlman et al., 2011), homogeneous traffic is not expected to be present. Therefore, variations of PF schedulers or new proposals are needed to provide the balance between fairness and throughput in LTE-Advanced systems with CA. One of this variations is presented in (Sivaraj et al., 2012). A two stage scheduler with spatial correlation scheduling in the frequency domain and PF type scheduling in the time domain is presented. Depending on the data rate required by the user, data can be scheduled in two available bands, achieving inter-band scheduling. Although the work in (Sivaraj et al., 2012) is focused on the uplink, it can easily be adapted to the downlink.

## 2.2.5 Chapter Summary

In this thesis, a modified single stage scheduler structure is developed. Using the JSQ concept with blind CC selection, we propose the grouping of available RBs in sets prior to their assignment by the scheduler. This proposal aims at emulating the advantages of full CC assignment of simplicity and reduced delay, with the efficiency of individual RB handling reflected in the assignment of only the required spectrum by the user. We focus on the downlink of the system. In order to evaluate the performance of the proposed scheduler, we use bursty traffic with finite buffer with heterogeneous requests. In Chapter 4, the development of the proposed scheduling strategy is presented.

## Chapter 3

# Channel Models for the Evaluation of LTE-Advanced Systems

Given the use of Adaptive Modulation and Coding (AMC) in LTE-Advanced Systems, the use of a given Resource Block (RB) depends on the channel conditions that a user observes on such RB. Under the best channel conditions (Dahlman et al., 2011), the highest order modulation with the least redundancy will be selected by the system. The average channel condition is reported by the User Equipment (UE) to the Enhanced Node B (ENodeB) using a Channel State Indicator Message (CSI). Within the CSI, a quantitative representation of the channel quality is reported using the Channel Quality Indicator (CQI). The CQI reports the average Signal to Interference Noise Ratio (SINR) observed by the UE on a specific channel or RB. Using this information, the ENodeB is able to determine the possible modulation and coding scheme to use in order to achieve a Block Error Rate (BLER) of at most 10% (Döttling et al., 2009).

The achievable bit rate per RB depends directly on the modulation scheme. For the characteristics of the RB structure given in Chapter 2, the use of a QPSK modulation would yield a peak bit rate of 336 kbps. QPSK is the smallest modulation scheme and is selected when the channel conditions are such that the SINR is below 7 dB (Mehlführer et al., 2009). For higher SINR values, modulation schemes such as 16 QAM and 64 QAM are available. Under the best channel conditions (SINR above 20 dB) the 64 QAM modulation scheme is used and a peak data rate of 1.008 Mbps per RB is possible. These peak data rates do not consider the use of a Multiple Input Multiple Output (MIMO) scheme. Considering the impact of the AMC scheme in the achievable bit rate per RB, the scheduler determines the amount of spectrum needed based on the data rate required by the user for a given service and the CQI reported. Using the

CQI information on the available spectrum resources, the scheduler can determine the amount of spectrum required.

Basically, the CQI represents the averaged SINR observed by the UE on the different spectrum resources (Mehlführer et al., 2009). In order to determine the CQI, a channel model is needed to represent the propagation characteristics of a signal at different frequencies. The channel model provides a mean to determine the signal quality and SINR observed by a UE.

### **3.1 The Multi Cluster Gaussian Scatterer Distribution Channel Model**

Current channel model proposals for macrocellular environments consider the existence of multiple scatterer and reflector clusters, specially in bad urban and hilly terrains. Each cluster corresponds to a set of small scatterers or large scattering points such as large buildings, roof edges, building corners, mountain edges, or street apertures (Arias and Manderson, 2006). However, in order to reduce computational complexity, the proposed models limit the number of scatterers in each cluster. This reduced number of scatterers considers only those that account for the strongest multi-path signals. As a small number (lower than 20) of multi-path components is used for each cluster, it is difficult to fit a probability density function that represents their statistical behavior. This situation results in a loss of precision while trying to model real world conditions, where a large (infinite) number of multi-path signals are generated.

In order to evaluate the performance of antenna arrays used in conjunction with proposed IMT-Advanced technologies such as CA, MIMO and Cooperative Multipoint Transmission and Reception (CoMP) in macrocellular environments, there is a need for a spatio-temporal channel model with enough flexibility to serve as a basis that provides enough information as approximate as possible to real operation conditions. For the purpose of evaluation, the basic information needed from the channel model

corresponds to the first order joint and marginal statistics of Time of Arrival (ToA) and Angle of Arrival (AoA). Also, a way to obtain second order statistics such as Angle Spread (AS) and Root-Mean-Square Delay Spread (RMS-DS) is desired. Based on these requirements the Multi-Cluster Gaussian Scatterer Distribution channel model (MC-GSDM) is considered as an attractive alternative.

The MC-GSDM is a single bounce two dimensional geometric channel model that considers the existence of a cluster of scatterers with a Gaussian distribution around the mobile station or user equipment. This cluster is referred to as the primary cluster. Other clusters exist in different positions of the base station coverage area. These clusters are referred to as secondary clusters. Each cluster is characterized by a Scattering Region Width (SRW), Scatterer Density (Cluster Weight) and position. The MC-GSDM represents a channel model that allows to evaluate the time and space diversity characteristics of a vast number of environments by modifying the number of clusters and their individual parameters.

Based on the assumption that multi-path signals generated by scatterer clusters can be modeled as having a Gaussian distribution, the MC-GSDM becomes a good option to evaluate system performance of space-time characteristics. In this chapter, it is shown that based on the analytical expressions that give rise to the statistical behavior of the MC-GSDM, appropriate channel values such as Angular Spread and RMS Delay Spread can be estimated without the need of heavy numerical simulation. Also, since the model considers the existence of an infinite number of multi-path components, the statistics from the analytical expressions better fit the behavior of real world conditions.

This chapter also presents how the information obtained from the MC-GSDM can be used in the context of the Cost 259 proposal as described in (Steinbauer and Molisch, 2001), where in the case of a macrocellular environment clusters are distributed uniformly in space based on a known number of clusters within the base station range. Also, it is possible to use the MC-GSDM within the framework of channel coefficient generation procedure specified in Winner II channel models as presented in (Döttling et al., 2009).

As it can be seen in (Wong et al., 2010), single cluster geometrical channel models do not properly fit some measurement campaign results. However, it is possible to fit a MC-GSDM to almost any measured result. Based on the assumption of multiple clusters of scatterers/reflectors and using analytical expression results instead of heavy numerical simulation the instantaneous channel conditions for the downlink and the uplink will be evaluated.

### 3.1.1 Related work

The results presented in (Ertel et al., 1998), (Ertel and Reed, 1999) and (Petrus et al., 2002) are some references that present different geometric channel models for different types of environments. It has been recently shown in (Wong et al., 2010) that no single channel model is useful for all environments.

Channel models used to evaluate the characteristics of time and space diversity include geometric channel models such as the elliptical and the circular model, as well as the more often used Gaussian model (Le, 2009). In (Andrade and Covarrubias, 2003) and (Janaswamy, 2002) a single cluster Gaussian Scatterer Distribution channel model is thoroughly analyzed. These references take into account the existence of a single cluster of scatterers surrounding the User Equipment (UE). Depending on the SRW of this cluster, the environment behaves as in a microcellular (large SRW) or macrocellular (small SRW).

In (Fuhl et al., 1998) the authors present a unified channel model for future communication systems. This radio channel model considers the existence of multiple clusters affecting the time and spatial characteristics of the channel. Each cluster is composed of a small number of scatterer/reflectors as these are considered the main sources of multipath components. The use of a small number of scatterers (up to 10) in each cluster is helpful to reduce computational burden of simulation, however it becomes difficult to obtain statistical behavior with a small amount of multipath components and no expression for the corresponding first order Probability Density Function (pdf)

is given. Also in (Fuhl et al., 1998) it is shown that a multi-cluster channel model better represents the behavior of most macro-cellular environments. This is one of the reasons why multi-cluster models were selected in the Cost 259 proposal and as part of the WINNER II project (Steinbauer and Molisch, 2001), (Kyosti et al., 2007). Recent publications such as (Chong et al., 2009) and present candidate channel models for future mobile communication systems. In (Chong et al., 2009) two MIMO channel models were taken from the 3G and B3G models in order to determine which one adjusts better to the requirements established for IMT-Advanced systems. These models are discussed in detail in order to understand their mathematical foundations and their simulation procedure. The models are then evaluated with respect to the gains of MIMO schemes proposed for IMT-Advanced systems.

MIMO scheme evaluation can take into account cluster positions and weight (scatterer density) in order to increase diversity gain. In (Chen and Dubey, 2003) the authors consider cluster positions and weight and the gain in MIMO schemes considering a limited number of beams directed at clusters with larger weight is obtained. This work only considers cluster weight as a mean to determine beam directions, no statistical analysis of the channel model is performed. In (Ahmadi-Shokouh, 2005) the expressions for the first order statistics are derived, but they are not evaluated or analyzed. In (Ertel et al., 1998) the authors present the MC-GSDM channel model. However, they only analyze and evaluate first order moments.

A channel model evaluation and simulation approach to determine the effect of multiple clusters in first and second order statistics is presented in this chapter. The approach is based in the use of a large number of scatterers in each cluster in order to achieve a proper statistical fit between simulated data and analytical expression evaluation. This consideration serves as validation of the analytical expressions presented in (Ahmadi-Shokouh, 2005) which enables their use to determine the channel behavior. This chapter also presents the calculation of second order moments corresponding to Angle Spread and RMS Delay Spread, which are important metrics to complement the channel characterization. Using the information provided from the analytical expres-

sions that represent the statistical behavior of the MC-GSDM, a signal level simulation can be performed using a Tapped Delay Line (TDL) model (Jeruchim et al., 2000). The signal level simulation can serve as a basis to determine the CQI to AMC scheme mapping based on the Block Error Rate (BLER) performance.

### 3.1.2 Multi Cluster Gaussian Scatterer Distribution Model

A general multi-cluster Gaussian scatterer distribution model (MC-GSDM) is shown in Fig. 18. Each cluster consists of a set of  $N_i$  scatterers, each one with its own position in an X-Y plane. Scatterers have a two dimensional Gaussian distribution around the center position of their corresponding cluster. The primary cluster is centered around the User Equipment (UE). For simplicity reasons, the axis formed between the base station (BS) and the UE is considered as the reference axis, therefore the angle between the UE and BS is zero degrees.  $D_0$  represents the distance between UE and BS.

The primary cluster is characterized by a SRW denoted with  $\sigma_0$ . The SRW corresponds to the standard deviation of the scatterer's distribution inside the cluster and is a measure of scatterer dispersion (cluster size). The secondary clusters are also characterized by a SRW, denoted by  $\sigma_i$  for the  $i$ -th cluster. The distance between the center of each secondary cluster to the BS is denoted by  $D_d^{(i)}$  while the distance to the UE is denoted by  $D_u^{(i)}$ . The angle between each secondary cluster and the BS is denoted by  $\phi_d^{(i)}$  while the angle between them and the UE is denoted by  $\phi_u^{(i)}$ . To complete the model parameters, the power coming from each cluster is taken into account. This is done using a weight measure assigned to each cluster in the model. From the uplink point of view the weight is considered as the ratio of the power from all the multipaths from a specific cluster with the total power received by the BS from all the multipath components from all clusters. In the simulation model the weight measure for each cluster was numerically calculated, dividing the number of scatterers in a specific cluster by the sum of scatterers of all the clusters in the model. The weight of each cluster is denoted by  $\omega_i$ . This method of measuring a cluster weight is valid in the sense that

scatterers are considered as perfect reflectors and in order to obtain the AoA and ToA probability distribution functions the received power is not taken into account. Using this approach for a higher number of scatterers in a cluster, a higher number of multi path components can be accounted for such cluster and thus a higher power from it is received at the BS. It has to be noted that this way of measuring a cluster weight does not take into account the path loss.

Considering scatterers as perfect reflectors and not considering the path loss to determine the AoA and ToA statistics is a method used to determine first order statistics of the spatial and temporal characteristics of a channel model. For that purpose, only the number of signals arriving from a certain direction with a certain delay is taken into account, but not the power of each component. This approach is widely used in literature and can be seen in references like (Ertel et al., 1998), (Ertel and Reed, 1999), (Petrus et al., 2002) and (Andrade and Covarrubias, 2003). However, as it will be shown in Section 3.5, a path loss model can be considered after the ToA statistic is obtained in order to obtain a Power Delay Profile. The estimation of signal power from the ToA pdf can be used in the joint ToA-AoA pdf in order to obtain an Angular Power Spectrum Distribution as the path loss is dependant of distance and not angle.

The general model makes the following assumptions:

- The model is two-dimensional - Only angle (azimuth) and time of arrival are considered.
- Only single bounce trajectories are considered.
- Path loss is not taken into account to calculate pdf's.
- Low or no mobility is considered (channel is stationary).
- Scatterers are considered as perfect reflectors.
- Each cluster has a large amount of scatterers for statistical purposes.

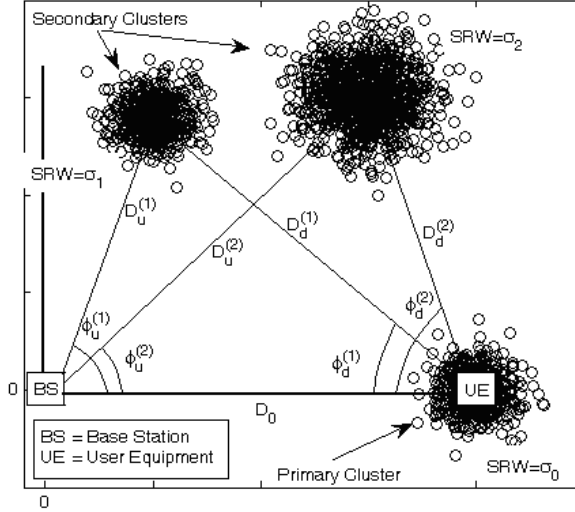


Figure 18. Evaluation Geometry for the MC-GSDM model

### 3.1.3 Uplink modeling and analysis

As presented in (Ahmadi-Shokouh, 2005) the expressions that define the joint ToA-AoA pdf for the uplink as well as their marginal pdf are used. The joint ToA-AoA pdf is expressed by:

$$f_{\tau, \theta_u}(\tau, \theta_u) = \frac{r_u A_u}{\sqrt{2\pi}} \sum_{i=0}^N \frac{w_i}{\sigma_i} \left[ e^{\left( -\frac{\beta_u}{2\sigma_i^2} \right)} \right], \quad (1)$$

where the term  $\beta_u$  corresponds to

$$\beta_u = r_u^2 + (D_u^{(i)})^2 - 2r_u D_u^{(i)} \cos(\theta_u - \phi_u^{(i)}),$$

$r_u$  is the distance between the base station and a specific scatterer located inside the  $i$ -th cluster, and  $r_d$  is the distance between the mobile station and the same scatterer. The total distance traveled by the transmitted signal is the sum of  $r_u + r_d$ , thus the time it takes to each reflected component to arrive to the base station can be measured by:

$$\tau = \frac{r_u + r_d}{c} = \frac{r_u + \sqrt{D_0^2 + r_u^2 - 2r_u D_0 \cos \theta_u}}{c}, \quad (2)$$

from the above,  $r_u$  can be obtained resulting in:

$$r_u = \frac{D_0}{2} \frac{1 - \left(\frac{\tau c}{D_0}\right)^2}{\cos \theta_u - \frac{\tau c}{D_0}}, \quad (3)$$

This term results from the transformation of distance to time of the model using Jacobian transformation of the joint distribution function, where the term  $A_u$  is obtained using:

$$A_u = \frac{1 + \left(\frac{\tau c}{D_0}\right)^2 - 2\frac{\tau c}{D_0} \cos \theta_u}{2\left(\frac{\tau c}{D_0} - \cos \theta_u\right)^2}. \quad (4)$$

In Fig. 19, we can observe the behavior of the joint ToA-AoA pdf (1) for the multi-cluster Gaussian scatterer channel model. For this figure, we considered three clusters (one primary and two secondaries) and the channel parameters shown in Table 1. This behavior is dependent on the model parameters regarding number of clusters, cluster weight, SRW and position. In Fig. 19 the three clusters that are simulated are visible. The primary cluster accounts for the multipath components arriving at 0 degrees of AoA with maximum probability. Given that the multipath trajectories from the primary cluster follow a shorter path, their ToA dispersal is low, up to 4  $\mu$ seconds. The effect of the two secondary clusters is identified at the -45 and 45 degree directions, with higher probability density from the cluster at 45 degrees due to the higher weight. The time dispersal from the multipath components from the secondary clusters is higher, reaching a maximum of 7  $\mu$ seconds.

In order to prove the validity of the presented expressions, numerical simulation of the channel conditions for Table 1 was performed. Figure 20 shows the corresponding simulation scenario. Numerical simulation was performed placing scatterers in an X-Y

**Table 1. Evaluation channel parameters**

i	$\sigma_i$ (m)	$D_i$ (m)	$\phi_i$ (Deg)	$\omega_i$
0	100	1000	0	0.25
1	100	989.95	45	0.25
2	100	989.95	-45	0.5

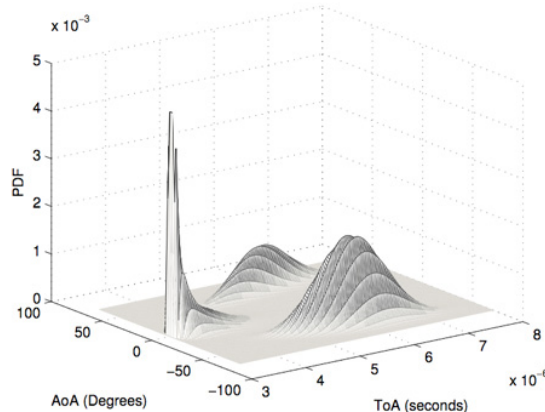


Figure 19. Joint ToA-AoA pdf for a three cluster MC-GSDM channel model.

plane based on the SRW parameters and cluster positions from Table 1. Each scatterer was placed using a two dimensional Gaussian random number generator in order to generate its coordinates. The mean value for each scatterer represents the center position of each cluster. After placing all the scatterers in the scenario, the AoA was calculated using basic geometry. To calculate the ToA values signals are assumed to propagate at the speed of light.

Each scatterer placed in Fig. 20 is then characterized by an AoA and a ToA, forming a ToA-AoA pair. Fig. 21 shows a scatterplot of the ToA-AoA pairs. For evaluation, we empirically considered a total of 20,000 scatterers in the system. From experience in evaluations, this amount of scatterers is known to be sufficient to obtain adequate statistics. The primary cluster had 5000 scatterers, while secondary clusters were considered with 5000 and 10000 scatterers respectively. Using the scatterer density ratio as a weight measure, the primary cluster had a weight of 0.25, while the secondary clusters weighed 0.25 and 0.5 correspondingly.

To obtain the Marginal AoA pdf, the joint ToA-AoA pdf can be integrated with

respect to  $\Theta_u$ , thus the Marginal AoA pdf is given by:

$$\begin{aligned}
 f_{\theta_u}(\theta_u) = & \sum_{i=0}^N \left[ \frac{\sigma_i \omega_i}{\sqrt{2\pi}} e^{-\frac{(D_u^{(i)})^2}{2\sigma_i^2}} + \frac{D_u^{(i)} \omega_i \cos(\theta_u - \phi_u^{(i)})}{2} \right. \\
 & \times e^{-\frac{(D_u^{(i)})^2 \sin^2 \theta_u - \phi_u^{(i)}}{2\sigma_i^2}} \\
 & \left. \times \text{erfc}\left(-\frac{D_u^{(i)} \cos(\theta_u - \phi_u^{(i)})}{\sqrt{2}\sigma_i}\right) \right]. \quad (5)
 \end{aligned}$$

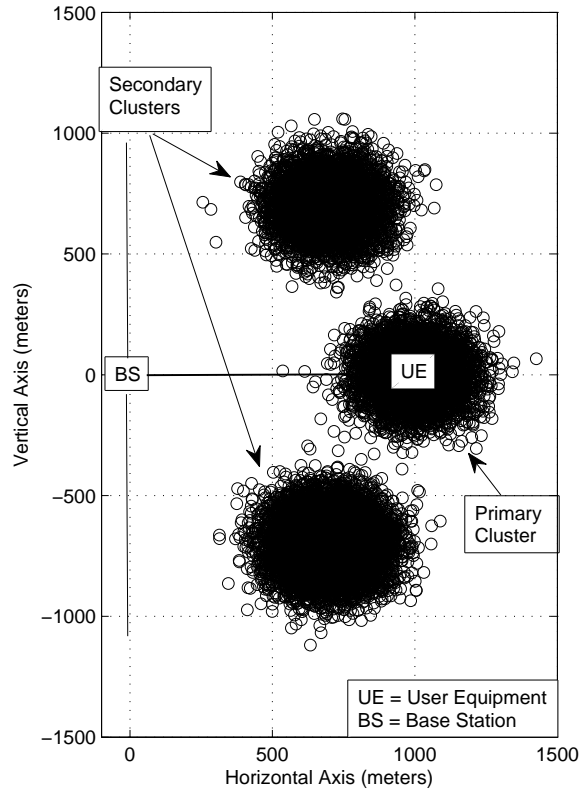


Figure 20. Simulation scenario used for validation.

Figure 22 shows the marginal AoA pdf for the channel parameters shown in Table I. Using the AoA, it is possible to distinguish the three different clusters considered for the evaluation. The marginal AoA pdf varies according to weight, SRW and distance to the base station. In Fig. 22 both secondary clusters are located at the same distance

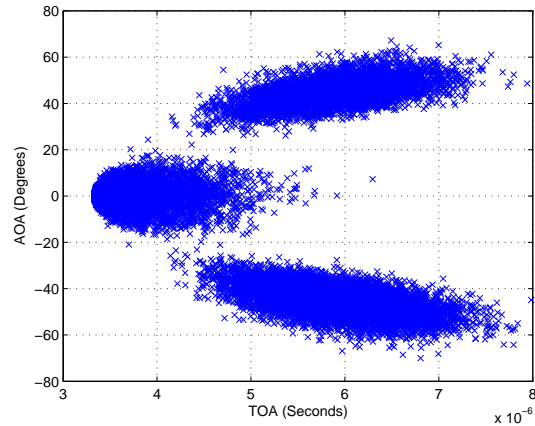


Figure 21. Scatterplot of simulated data showing ToA-AoA pairs for a three cluster MC-GSDM channel model

and have the same SRW, but since their weight is different, the cluster with the largest weight represents a larger amount of components, and thus a larger density. The weight of each cluster has a direct relationship with the probability of signals arriving with a given AoA and ToA. In general, the larger is the weight of a cluster, the higher is the probability to receive multipath signals generated from it. The histogram in Fig. 22 shows a good fit between Eq. 5 the simulated model, this confirms that for the considerations made, the weight measure calculated using the scatterer ratio is adequate.

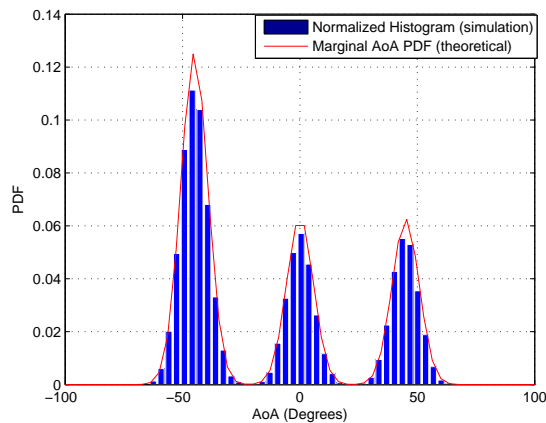


Figure 22. Marginal AoA pdf for the example three cluster MC-GSDM.

Using the same approach, the marginal ToA pdf can be given by:

$$f_{\tau}(\tau) = \int_{-\pi}^{\pi} f_{\tau, \theta_u}(\tau, \theta_u) d\theta_u, \quad (6)$$

$$f_{\tau}(\tau) = \int_{-\pi}^{\pi} \frac{r_u A_u}{\sqrt{2\pi}} \sum_{i=0}^N \left[ \frac{\omega_i}{\sigma_i} e^{-\frac{\beta_u}{2\sigma_i^2}} \right] d\theta_u. \quad (7)$$

The above expression has no direct closed form. In (Andrade and Covarrubias, 2003), an approximation to a close form expression for the marginal ToA pdf of a single cluster scenario is obtained, namely the Gaussian scatterer channel model, however it can not be directly applied to a multiple cluster environment. Figure 23 shows the behavior of the marginal ToA pdf of a multi-cluster environment.

The evaluation of equations 1, 5, and 6 that describe the statistical behavior of the MC-GSDM show results that properly fit with the statistics obtained using numerical simulation. In Fig. 22 and 23, it can be observed that cluster weight has a direct effect in the first order statistics. Those clusters with higher weight account for a higher probability density in the corresponding AoA and ToA. This is easy to observe in the marginal AoA uplink statistic, where the component arriving from -45 degrees shows a higher probability of occurrence due to the larger cluster weight, while the two other clusters show an equal probability of occurrence. This situation is also visible in the ToA uplink statistic, however, since both secondary clusters lie at the same distance from the BS, their ToA components add to increase the probability of signals arriving with an average delay equal of 5.8 microseconds.

In terms of the AoA uplink statistic, the farther a secondary cluster is from the base station the probability of signals arriving from the cluster's mean AoA (cluster center) increases, but the standard deviation is reduced. This is due to the fact that as the distance of a cluster is increased, it is seen as a single source with higher probability. This effect is independent of cluster weight. Far clusters behave as single sources rather than groups of components. This behavior is expected, the presented results show that the model behaves adequately when its parameters are changed. The presented

plots only reflect the behavior of a single case, but exhaustive simulation and analytical expression comparisons were made, all resulting in proper fit.

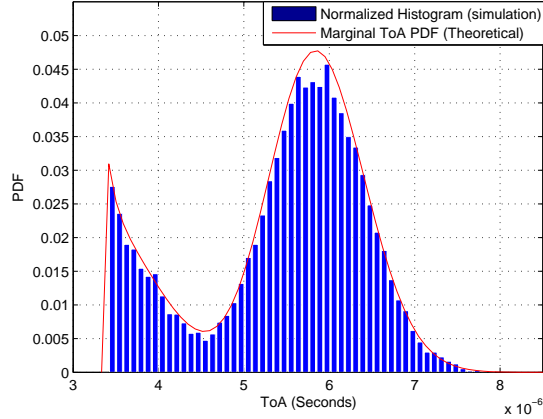


Figure 23. Marginal ToA pdf for a three cluster MC-GSDM.

### 3.1.4 Downlink modeling and analysis

Using the same approach as in the uplink, the downlink can be analyzed and the pdf functions for the joint ToA-AoA and marginal AoA can be obtained. The marginal ToA is not necessary to derive as it behaves in the same way as in the uplink. For the downlink the geometry of the model is maintained, with the difference of the direction of the multipath components, the UE is surrounded by incoming signals, which show a uniform distribution due to the existence of the primary cluster. The reference position for the evaluation scenario is now the UE, and the effects of each cluster are now taken with respect to it. This adjustment of relative positions, allows for a direct use of the expressions derived for the uplink with minor changes. The expressions derived in (Ahmadi-Shokouh, 2005) for the joint ToA-AoA pdf for the downlink, are presented here for fast reference:

$$f_{\tau, \theta_d}(\tau, \theta_d) = \frac{r_d A_d}{\sqrt{2\pi}} \sum_{i=0}^N \frac{\omega_i}{\sigma_i} e^{-\frac{\beta_d}{2\sigma_i^2}}, \quad (8)$$

with  $\beta_d$  as

$$\beta_d = r_d^2 + (D_d^{(i)})^2 - 2r_d D_d^{(i)} \cos(\theta_d - \phi_d^{(i)}), \quad (9)$$

and  $A_d$  as

$$A_d = \frac{1 + \left(\frac{\tau c}{D_0}\right)^2 - 2\frac{\tau c}{D_0} \cos \theta_d}{2 \left(\frac{\tau c}{D_0} - \cos \theta_d\right)^2}, \quad (10)$$

the rest of the terms are obtained from the following equations:

$$r_d = \frac{D_0}{2} \frac{1 - \left(\frac{\tau c}{D_0}\right)^2}{\cos \theta_d - \frac{\tau c}{D_0}}, \quad (11)$$

$$D_d^{(i)} = \sqrt{D_0^2 + (D_u^{(i)})^2 - 2D_0 D_u^{(i)} \cos \phi_u^{(i)}}, \quad (12)$$

$$\phi_d^{(i)} = \arcsin\left(\frac{D_u^{(i)} \sin \phi_u^{(i)}}{D_d^{(i)}}\right). \quad (13)$$

The evaluation of the Joint ToA-AoA pdf for the downlink can be observed in Fig. 24 using the parameters given in Table 1. The downlink presents a change regarding the AoA behavior. To show this behavior, a scatterplot of the ToA-AoA pairs for the downlink is presented in Fig. 25. The primary cluster surrounding the UE produces an AoA component for the 360 degrees. The effect of the primary cluster in the AoA is further analyzed with the marginal AoA pdf. The marginal distribution of the AoA for

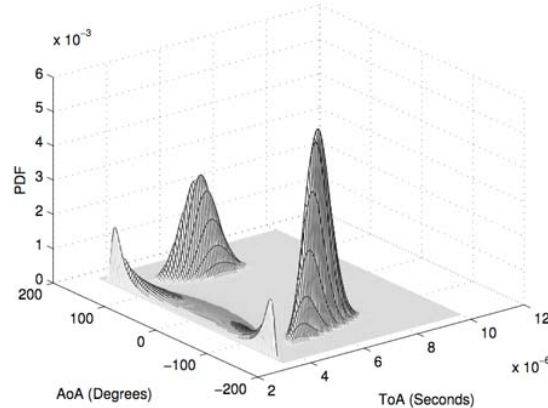


Figure 24. Joint ToA-AoA pdf for the downlink in a three cluster MC-GSDM.

the downlink is expressed by:

$$\begin{aligned}
 f_{\theta_d}(\theta_d) = & \frac{\omega_0}{2\pi} + \sum_{i=1}^N \left[ \frac{\sigma_i \omega_i}{\sqrt{2\pi}} e^{-\frac{(D_d^{(i)})^2}{2\sigma_i^2}} + \frac{D_d^{(i)} \omega_i \cos(\theta_d - \phi_d^{(i)})}{2} \right. \\
 & \frac{(D_d^{(i)})^2 \sin^2(\theta_d - \phi_d^{(i)})}{2\sigma_i^2} \\
 & \left. \times e^{-\frac{(D_d^{(i)})^2 \sin^2(\theta_d - \phi_d^{(i)})}{2\sigma_i^2}} \right. \\
 & \left. \operatorname{erfc} \left( -\frac{D_d^{(i)} \cos(\theta_d - \phi_d^{(i)})}{\sqrt{2}\sigma_i} \right) \right]. \quad (14)
 \end{aligned}$$

In the above expression, the term  $\frac{\omega_0}{2\pi}$  corresponds to the uniform distribution of the angle of arrival of signals coming from the scatterers in the primary cluster. The secondary clusters account for signals with a mean AoA corresponding to the relative position of each secondary cluster with respect to the UE. Fig. 26 shows the behavior of the marginal AoA pdf for the Downlink, together with the histogram for simulated data.

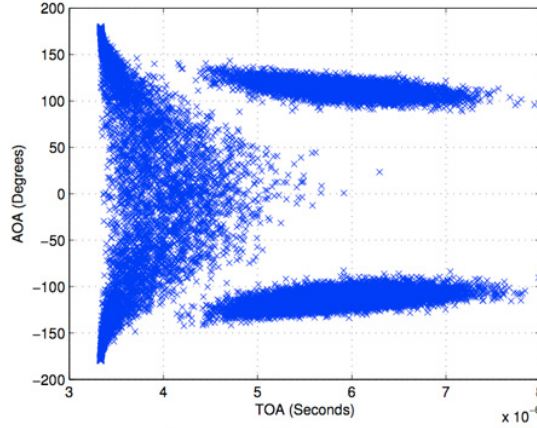


Figure 25. Scatterplot of the ToA-AoA pairs for the downlink of a three cluster MC-GSDM

It can be observed that the multipath components arrive to the mobile unit from every direction. As in the uplink, the effect of the secondary cluster as well as the impact of cluster weight can be observed in Fig. 26. Due to the change of reference in the geometry of the model, the mean AoA of the secondary clusters is now -120 degrees and 120 degrees respectively, with the highest probability density arriving at -120 degrees. As mentioned before, there is no need to evaluate the ToA statistic for

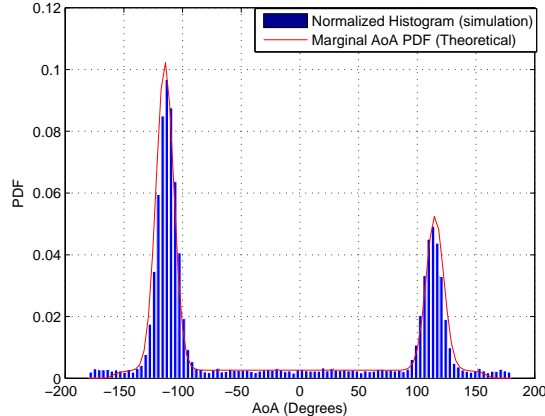


Figure 26. Marginal AoA pdf for the downlink in a three cluster MC-GSDM.

the downlink as it is the same as the uplink.

### 3.1.5 Second order moment analysis of the MC-GSDM

In this section it is analyzed the second order moments corresponding to Angle Spread (AS) and RMS Delay Spread (RMS-DS). These metrics are required to fully model the channel. With the information provided by the AS and RMS-DS, it is possible to represent the model using a TDL in order to perform signal level simulations.

#### Angle Spread

As shown in (Liberti and Rappaport, 1999), the AS of a channel model can be obtained directly from its AoA marginal distribution. Basically, the AS of a channel model is equal to the square root of the variance of the AoA, as follows:

$$AS = \sqrt{\sigma_{\theta_u}^2}. \quad (15)$$

This approach for obtaining the AS of a channel model does not take into account signal power, as such consideration would yield the Angular Power Spectrum Distribution which is not presented in this work. The method used here for calculating AS from the AoA distribution provides a measure of the spatial diversity properties of a

channel.

In a multi-cluster channel model, the AoA statistic can be used to determine the AS directly from the above equation. Another form is to take the AoA of the individual clusters and apply the following expression:

$$AS_{Total} = \sqrt{\sum_i \omega_i \sigma_{\theta_u}^2}, \quad (16)$$

Using Eq. 16, the closed form expression presented in (Andrade and Covarrubias, 2003) can be applied to each cluster. This procedure is only valid for the uplink given that the multipath components of a given secondary cluster are statistically independent from those of the other secondary clusters in the channel model. The expression in (Andrade and Covarrubias, 2003) for the AS of a single cluster model is given by:

$$AS = \sqrt{\frac{\pi^2}{3} + \frac{4\pi D_0 e^{-\frac{(D_0)^2}{4\sigma_0^2}}}{2\sigma_0 \sqrt{2\pi}} \sum_{n=1}^{\infty} \left[ \frac{(-1)^n}{n^2} \cdot k_0 \right]}, \quad (17)$$

where the term  $k_0$  corresponds to:

$$k_0 = I_{\frac{n+1}{2}} \left( \frac{D_0^2}{4\sigma_0^2} \right) + I_{\frac{n-1}{2}} \left( \frac{D_0^2}{4\sigma_0^2} \right), \quad (18)$$

using the above expressions and the independence property among the Gaussian random variables, the total AS of the model can be obtained as:

$$AS_{Total} = \sqrt{\sum_i \omega_i \left[ \frac{\pi^2}{3} + \frac{\alpha_u^{(i)}}{2\sigma_i \sqrt{2\pi}} \sum_{n=1}^{\infty} \left[ \frac{(-1)^n}{n^2} \cdot k_0^{(i)} \right] \right]}, \quad (19)$$

with the terms  $\alpha_u^{(i)}$  and  $k_0^{(i)}$  calculated as follows:

$$\alpha_u^{(i)} = 4\pi D_u^{(i)} e^{-\frac{(D_u^{(i)})^2}{4\sigma_i^2}}, \quad (20)$$

$$k_0^{(i)} = I_{\frac{n+1}{2}} \left( \frac{(D_u^{(i)})^2}{4\sigma_i^2} \right) + I_{\frac{n-1}{2}} \left( \frac{(D_u^{(i)})^2}{4\sigma_i^2} \right). \quad (21)$$

Equation 21 considers the sum of the AoA variances of each cluster taking their weight into account. The total angle spread is the square root of such sum.

As an example of how to use this expression to evaluate the effect of model parameters in the models AS, a simulation using the parameters in Table 2 was performed. Fig. 27 shows the behavior of the total AS while varying the position of a secondary cluster in a two cluster model. Both distance and angular position are varied with respect to the base station. The primary cluster's SRW and distance are kept constant.

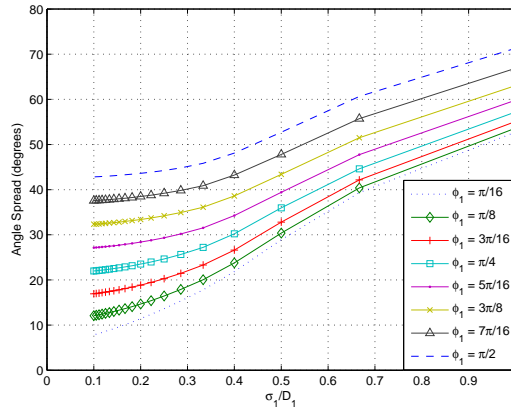


Figure 27. Angle Spread behavior for different secondary cluster position in the example two cluster MC-GSDM.

The angle spread is an important measure of a channel's space diversity. Fig. 27 shows an example evaluation of the expression in 16 for Angle Spread calculation in a MC-GSDM. It can be observed that the typical AS for urban and hilly terrain (20 to 30 degrees) can occur in a Multiple Cluster scenario. This situation reinforces the fact that it is possible to observe statistical behavior similar to that of a single cluster

Table 2. Channel parameters for AS and RMS Delay Spread evaluation

i	$\sigma_i$ (m)	$D_i$ (m)	$\phi_i$ (Deg)	$\omega_i$
0	100	1000	0	0.5
1	Sweep (100-1000)	1000	Sweep (11.25 - 90)	0.5

space-time channel in a multiple clusters scenario. In any case, the results obtained are consistent with the expected behavior of the channel model when the relative position of the secondary cluster is separated from the primary cluster and also its SRW is increased.

### **RMS Delay Spread calculation using a Walfish-Ikegami Cost 231 path loss model**

The RMS Delay spread (RMS-DS) is a time dispersion figure of merit used to evaluate the conditions of a wireless channel. In order to determine the RMS-DS it is necessary to estimate the Power Delay Profile (PDP) of the channel. The PDP is obtained by taking the first detectable signal arriving at the receiver as a reference of time  $\tau_0 = 0$ . Every signal arriving afterwards, is identified with its corresponding power and delay relative to that first arriving signal. The strongest component is considered as power reference with 0dB. Denoting  $a$  as the normalized amplitude and  $P$  as the normalized power of each multipath component and  $\tau$  as its delay, the RMS Delay Spread corresponds to (Rappaport, 2002):

$$\sigma_\tau = \sqrt{\overline{\tau^2} - (\overline{\tau})^2}, \quad (22)$$

with

$$\overline{\tau} = \frac{\sum_k a_k^2 \tau_k}{\sum_k a_k^2} = \frac{\sum_k P(\tau_k) \tau_k}{\sum_k P(\tau_k)}, \quad (23)$$

and

$$\overline{\tau^2} = \frac{\sum_k a_k^2 \tau_k^2}{\sum_k a_k^2} = \frac{\sum_k P(\tau_k) \tau_k^2}{\sum_k P(\tau_k)}. \quad (24)$$

For determining the RMS-DS taking into account the statistical properties of the MC-GSDM, the next procedure was followed:

1. Determine the normalized power from the marginal ToA pdf. This was performed taking directly the ToA statistic, and considering that the larger the probability, the larger the power coming from such multipath component. Fig. 28 shows

the result of this step for the same parameters in Table 1. The normalized power is obtained by normalizing the ToA statistic and representing it in logarithmic scale.

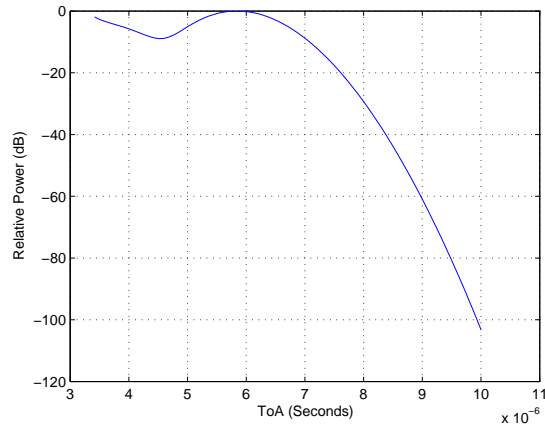


Figure 28. Relative power delay using marginal ToA pdf without path loss consideration.

- Determine the PDP using an appropriate path loss model. The marginal ToA statistic considers scatterers as perfect reflectors, and does not take into account the channel path loss. A simple yet useful way of determining the PDP, is to take the normalized power obtained in the previous step, and apply a channel path loss model to it. For this example the Walfish-Ikegami Cost 231 Path Loss Model was considered. The PDP obtained is shown in Fig. 29

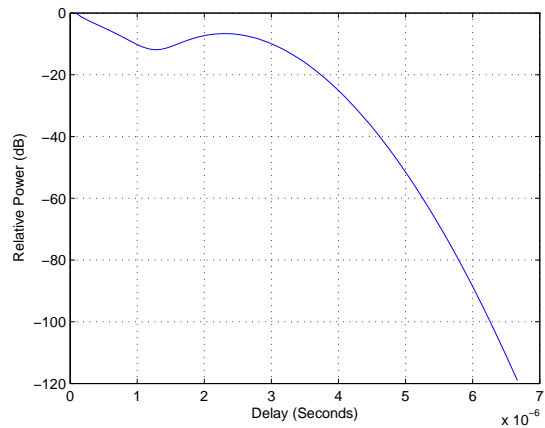


Figure 29. Power Delay Profile using Walfish Ikegami Path Loss Model and the relative power delay.

3. It is possible to compute the RMS-DS using the PDP and equation (22).

This approach is valid due to the assumptions that the scatterers are perfect reflectors and the fact that the path loss is not taken into account to calculate the ToA statistics. Considering scatterers as perfect reflectors implies that each signal arriving at the receiver contains the same power. The total received power is the sum of power of each received signal. With these conditions, if power is taken as the measure to determine the ToA statistic, the pdf could be calculated by dividing the power received at delay time  $\tau_x$  by the total power received. This calculation should provide the same result as counting the number of signals arriving at delay time  $\tau_x$  and dividing by the total number of arriving signals. As such, it should yield the same result as the evaluation of the analytical expressions for ToA. Therefore the ToA pdf can be considered as representing power in a linear scale, allowing to apply the proposed procedure.

Fig. 30 shows the RMS-DS results for different positions of a secondary cluster. The evaluation was performed considering the procedure described and the simulation parameters in Table 2.

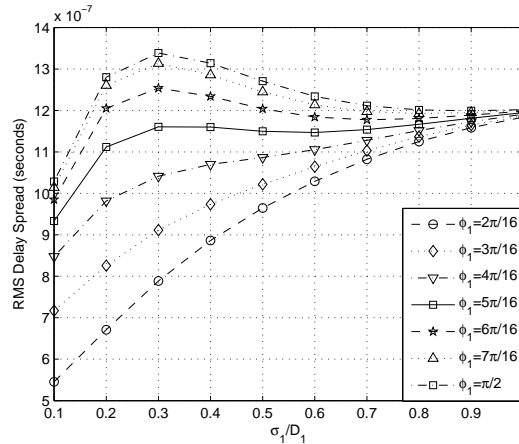


Figure 30. RMS-DS behavior using a two cluster MC-GSDM and parameters of Table 2.

In terms of the RMS-DS for the set of parameters of Table 2, it can be observed that as the secondary cluster angular position is increased with respect to the mobile station ( $\phi_1$  increase) the RMS delay spread also increases. This is due to the higher number of ToA components. However, this increment occurs when the  $\sigma_1/D_1$  ratio is

below 0.5. As this ratio increases to values above 0.7 the RMS delay spread stabilizes. This behavior occurs because the RMS delay spread depends mainly on the secondary cluster once its SRW is twice as large as the SRW of the primary cluster.

## **3.2 The use of the MC-GSDM in the design of future generation wireless systems**

Future wireless communication systems including 4G mobile proposals, such as LTE-Advanced (Parkvall and Astely, 2009), foresee the combined use of different technologies in order to achieve specific data rate and efficiency goals. These technologies include the Carrier Aggregation, Enhanced Multi-Antenna Transmission, Coordinated Multiple Transmission Reception and Relaying. Based on published evaluation methodologies, system design and evaluation using these technologies can benefit from the use of the MC-GSDM as discussed in the following subsections.

### **3.2.1 Cost 259 Directional Channel Modeling**

In (Steinbauer and Molisch, 2001) the Cost 259 modeling framework for directional channel models is presented. In macrocellular environments, a set of random local parameters (number of clusters, number of multipath components per cluster, position, etc.) is used in order to evaluate the performance of systems under a wide range of propagation conditions. Each one of the defined radio environments specifies a minimum number of clusters and a mean number of additional clusters. The procedure to evaluate system performance taking into account a directional channel model involves the generation of several sets of parameters. Each set of parameters considers the placement of clusters using a uniform distribution at a specified maximum distance from the base station. In order to reduce computational burden when simulating these environments, the number of multi-path components for each radio environment is kept low (about 20). This consideration does not reflect the operation under real world

conditions in the sense that an infinite number of multi-path components are generated in a macrocellular environment. Within the Cost 259 framework the MC-GSDM can be used in order to provide the statistical behavior of the multi-cluster scenario. The computational burden of calculating each ray is substituted by the evaluation of the analytical expressions that give rise to the AoA and ToA statistics of the channel model. The information provided by the analytical expressions provides a powerful tool to define the local parameters of each set and perform system evaluation based on the information obtained with the MC-GSDM channel model.

### **3.2.2 WINNER II Channel Modeling**

The WINNER II project Channel Models are presented in (Döttling et al., 2009). A procedure for Channel Coefficient Generation is presented. The general parameters that define the channel coefficients are related to propagation condition, path loss and large scale parameters such as Delay Spread and Angle Spread. The WINNER II proposed framework for the bad urban scenario establishes the placement of five far scatterers in a hexagonal cell. We propose that in order to determine the channel parameters the MC-GSDM can be used. Using the MC-GSDM provides the statistics needed to determine Delay Spread and Angle Spread, as well as a way of generating arrival and departure angles. Using the information provided by the MC-GSDM system evaluation will reflect higher precision than using a small number of scatterers. As well as with the Cost 259 channel modeling, computational burden will not be affected as the behavior of the MC-GSDM can be obtained from the analytical expressions.

## **3.3 Channel Quality Indicator Estimation.**

The Channel Quality Indicator (CQI) is a representation of the average Signal to Interference and Noise Ratio (SINR) observed by the UE on the available radio channels. The information provided by the CQI is used to determine the Adaptive Modulation

and Coding (AMC) scheme to be used. The AMC determines the achievable spectrum efficiency without exceeding a predefined Block Error Rate (BLER). The goal of a CQI estimation from a specific channel model is to define a mapping between the CQI and the AMC. An optimum mapping will be one that for a given CQI uses the maximum modulation index with the minimum coding rate without exceeding the target BLER. If the BLER is considerably below the target for a given CQI, the system is underestimating the CQI which results in the inefficient use of the spectrum. On the other hand, if the BLER is higher than the target, the CQI is overestimated and excessive retransmissions will be required to complete a data transfer due to a higher number of transmission errors.

In order to define a CQI mapping table for a channel model, it is necessary to perform extensive signal level simulations in order to find the SINR levels at which the different modulation and coding combinations achieve the target BLER. For LTE-Advanced systems, a target BLER of 10% is defined (Dahlman et al., 2011). The procedure to find this mapping for a MC-GSDM is as follows:

1. Define a set of parameters for a MC-GSDM: Number of clusters, cluster positions, SWR and weight.
2. Calculate first and second order statistics.
3. Calculate Power Delay Profile (PDP).
4. Represent the channel with a Tapped Delay Line (Jeruchim et al., 2000).
5. Perform signal level simulations considering the specifications of LTE-Advanced (Orthogonal Frequency Division Multiplexing, QPSK up to 64 QAM Modulation, Turbo Coding, etc.) (Mehlführer et al., 2009).
6. Determine a CQI-AMC mapping table.

Since each set of parameters of the MC-GSDM represents a completely different channel, the procedure to find a CQI-AMC mapping has to be performed for each set.

This involves an infinite number of possibilities considering the four degrees of freedom of the MC-GSDM (number of clusters, position, SRW and weight). If the procedure is performed on a single set of parameters of the MC-GSDM, the resulting mapping table will only be valid for that channel. This defines an opportunity to define mapping tables corresponding to averages of different sets of parameters under certain limits (a maximum number of clusters, a maximum SRW, etc.). However, finding such mapping tables involves a huge simulation effort considering a complete simulation model of an LTE-Advanced system. Such work is beyond the scope of this thesis, but can be addressed as a future research project.

Since the parameter required by the base station to handle UE requests is the SINR, represented by a CQI level, in this thesis project a simple model considering Path Loss and Noise is used to perform the evaluations. This model is widely used in literature for scheduler evaluation, since only the mapping table of the CQI-AMC is required. The mapping table used for the evaluation of our scheduler proposals is presented in (Mehlführer et al., 2009) and (Meucci et al., 2009).

### 3.4 Chapter Summary

This chapter presented a complete characterization of the MC-GSDM in terms of its ToA-AoA statistics as well as the second order statistics corresponding to Angle Spread and RMS Delay Spread. It was shown that the analytical expressions that model the statistical behavior of the MC-GSDM properly fit simulated data. A procedure to determine the Power Delay Profile from the marginal ToA pdf statistic, is proposed and used in conjunction with a Walfish-Ikegami Cost 231 path loss model, to calculate the RMS Delay Spread of a specific set of parameters for the channel model. This procedure is valid based on the initial assumptions of the channel model. The applicability of the MC-GSDM to 4G system design and evaluation is discussed. Although standard channel models exist for 3G and B3G systems that are applicable to 4G proposals, the MC-GSDM can be used as an alternative to represent multi-path signal behavior with

higher precision.

From the AS evaluation of a MC-GSDM it was shown that it is possible to obtain AS values typical of single cluster environments. Thus it is important to be able to determine when multiple clusters are present in order to get the most out of them. For characterization of a specific environment, it is easier to distinguish the presence of multiple clusters from the AoA statistic. From the ToA statistics it may become difficult to distinguish between a single cluster scenario or a multiple cluster one.

The presence of multiple clusters may provide several advantages. It is possible to use the information concerning these clusters and take it into account for a more efficient system design. As resources such as power and spectrum usage take more importance in wireless communication system design, proper channel modeling becomes a key component to achieve optimum performance. As it can be determined from the results of different channel measurement campaigns, existing geometrical channel models do not properly fit some measured data. However, most measured environments can be fitted to a MC-GSDM channel model with specific parameters such as number of clusters, position and SRW. The use of the MC-GSDM for evaluation of system performance is considered as future work due to the extensive simulation effort required that is beyond the scope of this thesis work. In the following chapter, we propose a scheduling strategy for Carrier Aggregation that allows to reduce the delay of resource assignment. In order to evaluate the performance of the proposed scheduling strategy, we make use of a direct mapping of the CQI-AMC as defined in (Meucci et al., 2009). The SINR to CQI mapping used corresponds to (Mehlführer et al., 2009).

# Chapter 4

## Scheduling Algorithms for Carrier Aggregation.

Scheduler operation for Carrier Aggregation (CA) involves the capacity of the scheduler to assign multiple spectrum resources, even if these are fragmented or in different frequency bands. Depending on the operation of the scheduler, three types can be implemented: contiguous CA, non-contiguous intra-band CA, and inter-band CA. It has been shown in (Chen et al., 2009) that an inter-band CA scheduler has the capacity to increase throughput in comparison to contiguous CA and non-contiguous intra-band CA. In this chapter, we develop a scheduler for contiguous CA implementation and compare it to a scheduler for inter-band CA.

### 4.1 Introduction

In this chapter we present a scheduling strategy based on the assignment of pre-organized RB sets. We will refer to this strategy as Set Scheduling. The main idea behind Set Scheduling corresponds to reducing the delay in resource assignment by organizing RBs in sets prior to their assignment by the scheduler, in comparison to an individual RB assignment strategy. This idea was presented in (Galaviz et al., 2011). In this chapter, Set Scheduling is further analyzed and evaluated in a macro-cellular environment in order to fully understand its potential in reducing delay due to resource assignment when compared to Block by Block Scheduling. In order to present Set Scheduling, two different algorithms for organizing RBs in sets are evaluated. Results obtained through the evaluation in a macrocellular environment show that Set Scheduling achieves a 4-fold scheduling delay reduction and 5% user capacity improvement when compared to a Block by Block Scheduling strategy. We will also discuss how

it provides a more efficient use of available resources as compared to what is achieved in (Chung and Tsai, 2010). Considering that packet delay involves the scheduling process, packet fragmentation and reconstruction (when using CA), signaling and physical layer processes, an improvement in the delay caused by any of these processes will eventually impact on packet delay. Therefore, depending on the delay contribution of each process, the achieved reduction in scheduling delay using our proposal may have an important impact on packet delay.

## 4.2 Evaluation Scenario and Simulation Parameters

### 4.2.1 Evaluation Scenario

For evaluation, we consider a single cell scenario in a macrocellular urban environment. Figure 31 shows this scenario. Users are uniformly distributed within the base station's (eNodeB) coverage area. Although a uniform user distribution does not fit the general case in practical environments, for a densely populated macrocellular urban scenario it is widely used in literature, see for instance (Shirakabe et al., 2011). A uniform user distribution is adequate for algorithm evaluation in this type of scenario when a uniform user density is used.

At each scheduling slot, user requests are received with a Poisson distribution with mean  $\lambda_u$ . Each request specifies a data rate  $R_{b_{u_i}}$  and a file size  $S_{b_{u_i}}$  for the  $i$ -th user. Each request is also associated with a channel quality indicator (CQI) report. The CQI will determine the achievable data rate and the amount of data that can be transported on a RB. Therefore the requested data rate will eventually define the bandwidth required by the user (number of required RBs), while the file size will define the number of packets needed to be transmitted (time slots) for a given CQI value.

We consider that the available bandwidth is organized in component carriers (CC) (Yuan et al., 2010). For evaluation we considered the characteristics of the long term evolution system (LTE) as presented in (Mehlführer et al., 2009). There are a total of  $L$  CC's.

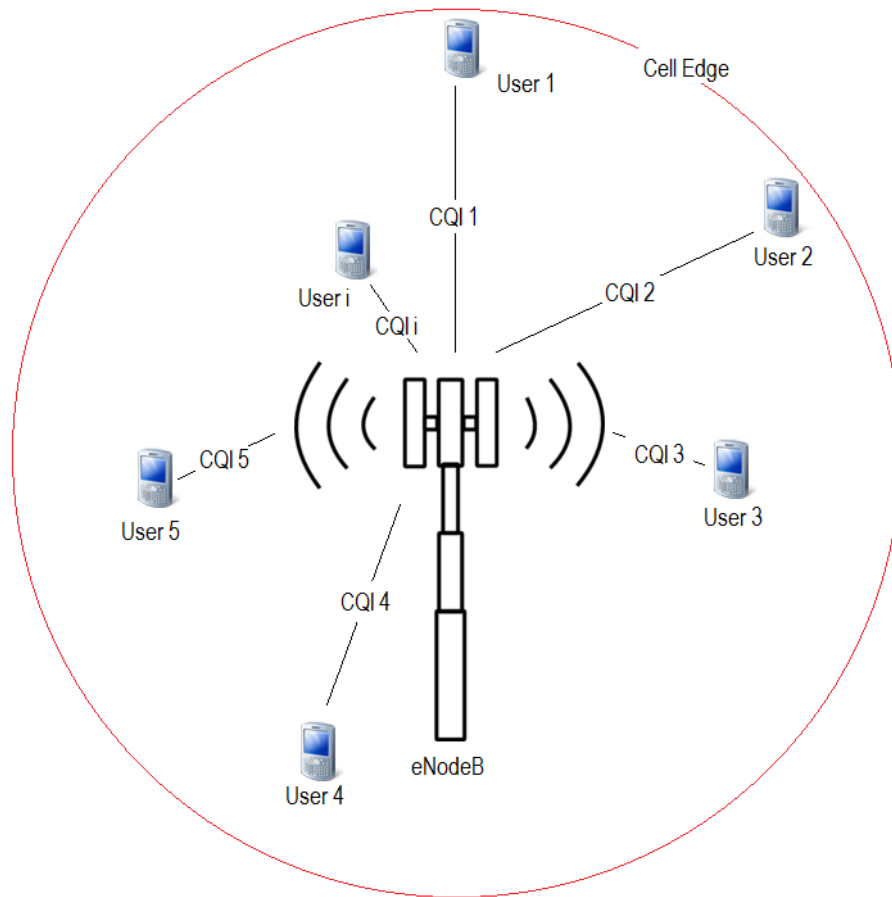


Figure 31. Single cell evaluation scenario.

The  $l$ -th CC, where  $l \in 1 \dots L$ , is composed of an integer number of RBs, where one RB is the minimum assignable resource to a user. Each RB is by itself a set of OFDM subcarriers. For our evaluation, RBs are represented as binary vectors for each of the frequency bands used. The position within the vector specifies the center frequency of the RB, a value of “1” indicates that the RB is available while a value of “0” indicates that the RB is not available.

The achievable data rate per RB is variable, and depends on the CQI of user  $i$  on CC  $l$ . In order to obtain the CQI, the signal to noise ratio (SNR) to CQI mapping presented in (Mehlführer et al., 2009) was used. This mapping is represented by Equation (25), valid for macrocellular scenarios for the 700 MHz, 2.3 GHz, 3.4 GHz frequency bands.

$$\text{CQI} = 0.5250 * \text{SNR dB} + 4.5. \quad (25)$$

where SNR dB is the user signal to noise ration (in dB) per user. As presented in (Mehlführer et al., 2009), this mapping guarantees decodability of the transmitted information with a block error rate (BLER) of at most 10%. A Block is considered as a Transport Block formed by the packed data, Cyclic Redundancy Check (CRC) code, Forward Error Correction (FEC) code and pilot symbols (Dahlman et al., 2011). A 10% BLER indicates that at most 1 out of every 10 blocks transmitted may have an error, detected by the CRC. Our evaluation considers that requests are from slow moving or fixed users, therefore the CQI is maintained until the transmission of data is completed. For illustration purposes our simulations are based on a single cell multi-user scenario. Interference on the system is not taken into account.

An SNR estimation is required to calculate the CQI. In order to obtain the SNR for each user, we considered the path loss (PL) and thermal noise. The PL was obtained using the ITU-R macrocellular urban NLOS scenario defined in (ITU-R, 2009) shown in Equation (26).

$$\begin{aligned} \text{PL(dB)} = & 161.04 - 7.1 * \log_{10}(W) + 7.5 * \log_{10}(h) \\ & - (24.37 - 3.7 * ((h/hbs)^2)) * \log_{10}(hbs) \\ & + (43.42 - 3.1 * \log_{10}(hbs)) * (\log_{10}(d) - 3) \\ & + 20 * \log_{10}(fc) \\ & - (3.2 * (\log_{10}(11.75 * hut))^2 - 4.97). \end{aligned} \quad (26)$$

The parameters for Equation (26) are taken from (ITU-R, 2009) and are as follows:  $W$  is the street width (20 m),  $h$  is the average building height (20 m),  $hbs$  is the base station height (25 m),  $hut$  is the user terminal height (1.5 m),  $d$  is the distance between user terminal and base station (variable with user position) and  $fc$  is the operating

frequency in GHz (2.3 and 3.4 GHz).

A thermal noise power spectral density of  $-174$  dBm/Hz was considered in order to calculate the SNR per user. The 2.3 GHz and 3.4 GHz frequency bands were used with equal transmission power. The transmission power of eNodeB was adjusted in order to have a minimum CQI of 5 at the cell edge in the 2.3 GHz frequency band. Since both bands transmit at the same power, a lower CQI is expected in the 3.4 GHz band for a given user.

The data rates associated to CQI values presented in Table 3 are taken from (Meucci et al., 2009). In Table 3,  $S(\text{CQI})$  represents the transport block size, which defines the amount of data that can be transmitted per RB given a CQI value.  $R(\text{CQI})$  represents the achievable bit rate for a specific CQI value.

Table 3. CQI to  $S(\text{CQI})$  and  $R(\text{CQI})$  mapping.

CQI	Modulation	$S(\text{CQI})$ [bits]	$R(\text{CQI})$ [kbps]
CQI 5	QPSK	377	188.5
CQI 8	QPSK	792	396.0
CQI 15	QPSK	3319	1659.5
CQI 22	16-QAM	7168	3584.0

The total number of RBs  $N_i$ , required by user  $i$  is such that:

$$\sum_{j=1+k_{i-1}}^{N_i+k_{i-1}} R(\text{CQI})_j \geq R_{b_{u_i}}. \quad (27)$$

where the term  $k_{i-1}$  represents the index of the last RB assigned to the previous user.

The restriction in Equation (27) guarantees that the sum rate of the assigned RBs is at least equal to the data rate required by a user. For a given user  $i$ ,  $N_i$  is upper bounded by

$$Nb_i^u = \frac{R_{b_{u_i}}}{R(\text{CQI})_{Lo}}. \quad (28)$$

where  $Nb_i^u$  is the upper bound on the number of RBs required by user  $i$  when all assigned RBs have an equal and the lowest achievable CQI, termed  $R(\text{CQI})_{Lo}$ . In the

same way, the lower bound on  $N_i$  can be represented as:

$$Nb_i^l = \frac{R_{b_{u_i}}}{R(\text{CQI})_{H_i}}. \quad (29)$$

where  $Nb_i^l$  is the lower bound on the number of RBs required by user  $i$  when all assigned RBs have an equal and the highest achievable CQI, termed  $R(\text{CQI})_{H_i}$ . Any possible value of  $N_i$  will fall within these two limits and depends specifically on the user channel conditions on the available carriers.

## 4.2.2 Simulation Parameters

Table 4 shows the simulation parameters used in all of the evaluations performed, and their corresponding values.

Table 4. Simulation parameters and values

Parameter	Value
Site layout	Single cell, omnidirectional antenna
Path loss	ITU-R urban macrocellular NLOS (ITU-R, 2009)
User location	Uniformly dropped within cell
Operation frequency	2.3 and 3.4 GHz
Thermal noise PSD	-174 dBm/Hz
Minimum CQI at cell edge	5 @ 2.3 GHz
Available resource blocks	20 @ 2.3 GHz, 160 @ 3.4 GHz
Requests per slot $\lambda_u$	25, Poisson distributed
Requested data rate $R_{b_{u_i}}$	Uniformly distributed (1 kbps to $R_{b,\text{max}}$ )
Requested file size $S_{b_{u_i}}$	Uniformly distributed (100 bits to $S_{b,\text{max}}$ )
Simulated slots	500

## 4.3 Set Scheduling and resource block organization algorithm

### 4.3.1 Set Scheduling

In order to understand the difference between the proposed Set Scheduling strategy and Block by Block Scheduling, let us first explain the operation of the latter. Figure 32 shows the general structure of the Block by Block Scheduling strategy presented in (Lei and Zheng, 2009), (Songsong et al., 2009) and (Chen et al., 2009).

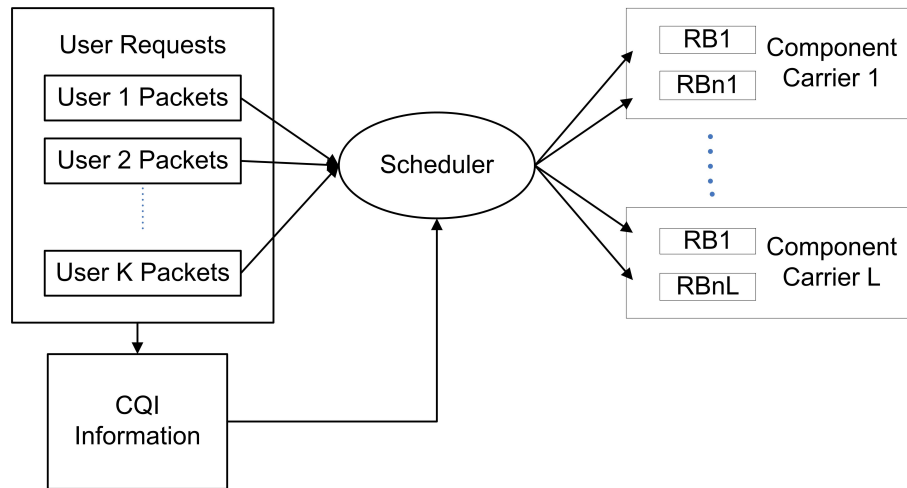


Figure 32. General Block by Block Scheduling.

In Block by Block Scheduling each available RB is handled individually. Depending on the scheduler used (i.e., Proportional Fair, Processor Sharing), the scheduling metrics are evaluated for each RB. The user who maximizes the specific scheduling metric obtains the RB assignment. This process is repeated until all RBs are assigned, time at which some users will complete all of their  $N_i$  RBs (with  $N_i$  subject to the constraint in Equation (27)).

We consider that there is a drawback in a block by block scheduling strategy. For a user  $i$  who requires  $N_i$  RBs, the time required to assign all of them is of at least  $N_i$  times of that required to assign a single RB. This time can grow even more if the RBs assigned are not contiguous. There is also the possibility that after all the available

RBs are assigned, some users will not complete the total number of required RBs. This may result in inefficient use of the available resources.

As a solution to the potentially excessive delay in block by block scheduling, we propose the use of a Set Scheduling strategy as shown in Figure 33. By using Set Scheduling, available RBs are first organized in sets prior to assignment by the scheduler. Each set as a whole is available to the scheduler. For a user who requires a total of  $N_i$  RBs, if a set of size  $N_i$  or larger is available, it is assigned to that user in a single operation.

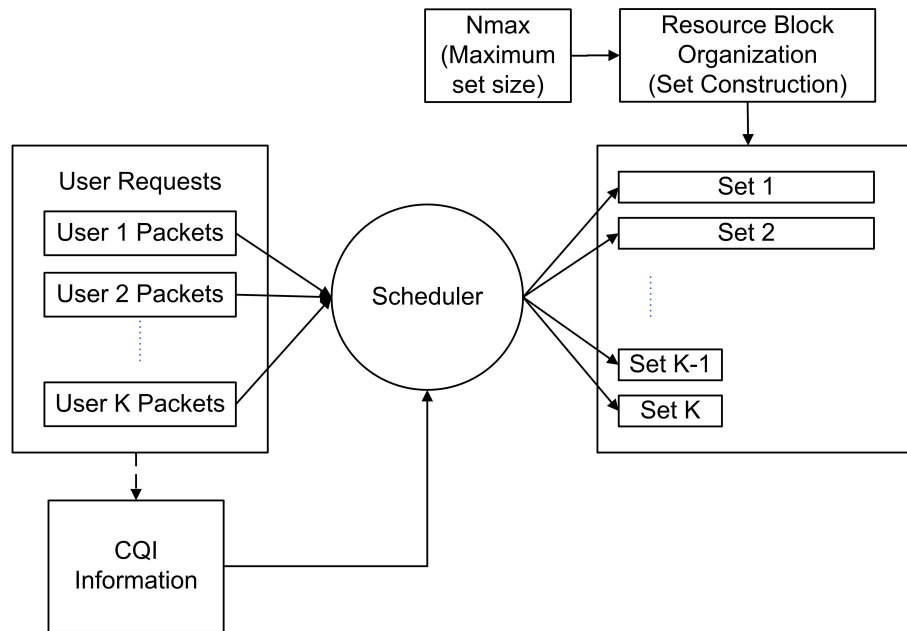


Figure 33. Set Scheduling strategy.

There is one main drawback in the proposed Set Scheduling strategy. Additional complexity at the scheduler is required due to the RB organization algorithm. However, depending on the algorithm itself, this complexity can be low compared to the rest of the scheduler components.

### 4.3.2 Resource block organization algorithm

The operation of the Set Scheduling strategy is subject to the use of a resource block organization algorithm. Figure 34 shows a block diagram of one of the proposed resource

block organization algorithms as presented in (Galaviz et al., 2011). The algorithm in Figure 34 will be referred to as Algorithm 1. The operation of Algorithm 1 is based on the search of consecutive available RBs. In this regard, Algorithm 1 finds the first available RB from the vector containing RB availability information, and then checks for the contiguous RB for availability. This process is continued until the contiguous RB checked is not available, or until a total of  $N_{max}$  contiguous RBs are found.  $N_{max}$  specifies the maximum size of a set. The index (position) of each RB found available is stored in a row of a Set Matrix. The last column of the row contains the size of the corresponding set. After a set has been formed, a new set is started by finding the next available RB, starting the search at the index position where the previous set was finished. The Set Matrix is ready when no more RBs are available to form a set. This process is executed at each scheduling slot, before the assignment of resources.

A different RB Organization algorithm is shown in Figure 35, and will be referred to as Algorithm 2. In Algorithm 2, the output is the same as in Algorithm 1 and corresponds to the Set Matrix. However, each organization algorithm operates differently. At the beginning, Algorithm 2 must find the first available RB to form a set. The index corresponding to this RB is considered as the first in the set. Then, Algorithm 2 finds the first non-available RB starting the search at the index of the RB of the previous step. This process can be thought of as a search of the beginning and end of a set. The size of the set is verified, and if it is greater than  $N_{max}$  then the set found is truncated and a new set is formed immediately with the remaining RBs.

Note that the presented algorithms perform Contiguous CA. This simplifies the organization algorithm operation, but lacks the capacity to form sets from non-contiguous RBs. It has to be remarked that the organization operation is based solely on RB availability.

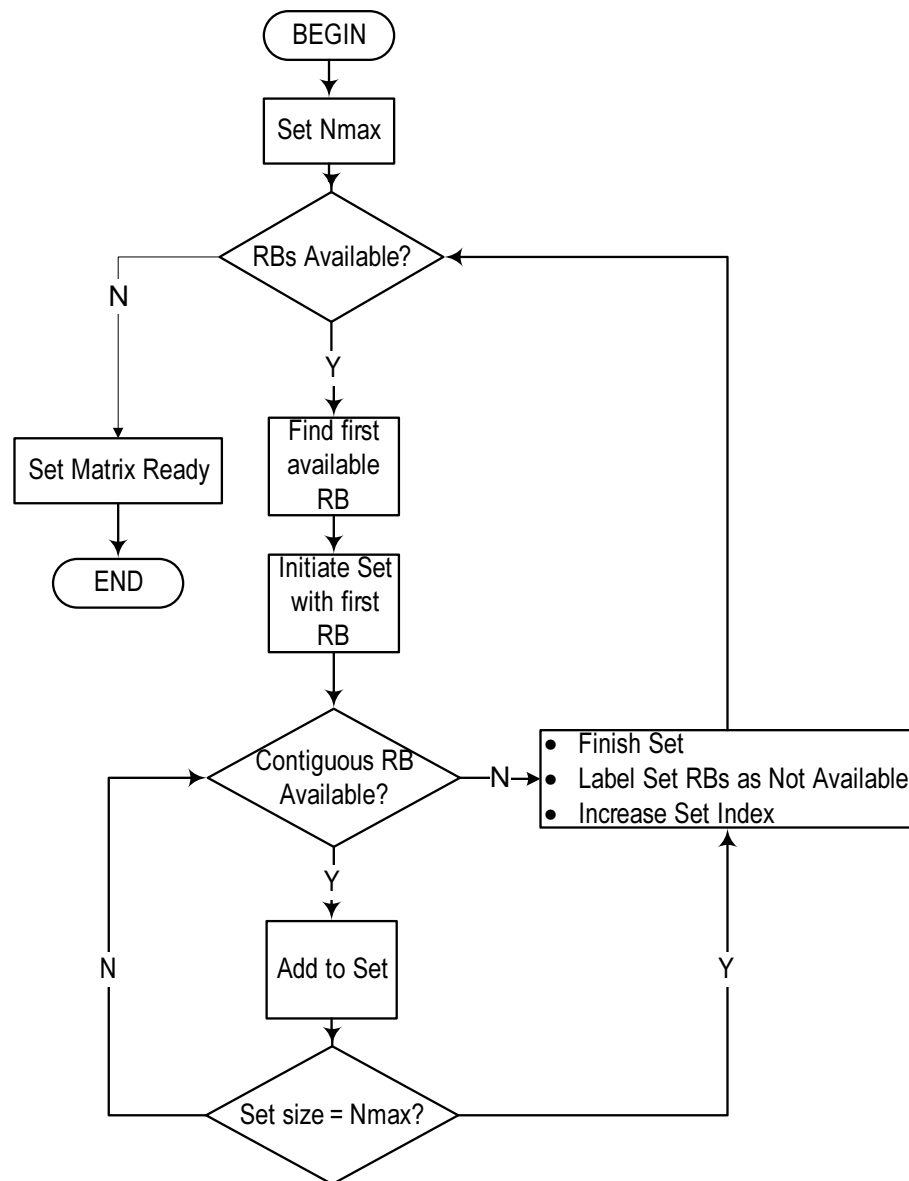


Figure 34. Resource block organization algorithm—Algorithm 1

### 4.3.3 Operation of Set Scheduling

Algorithms 1 and 2 were used for set construction in the Set Scheduler structure presented in Figure 33. At each scheduling slot, sets are formed using all the available RBs. The scheduler then assigns each available set to users according to the scheduling rules. Due to the dynamic nature of the resource use, each set can have a different number of RBs with a minimum of one, and a maximum of Nmax.

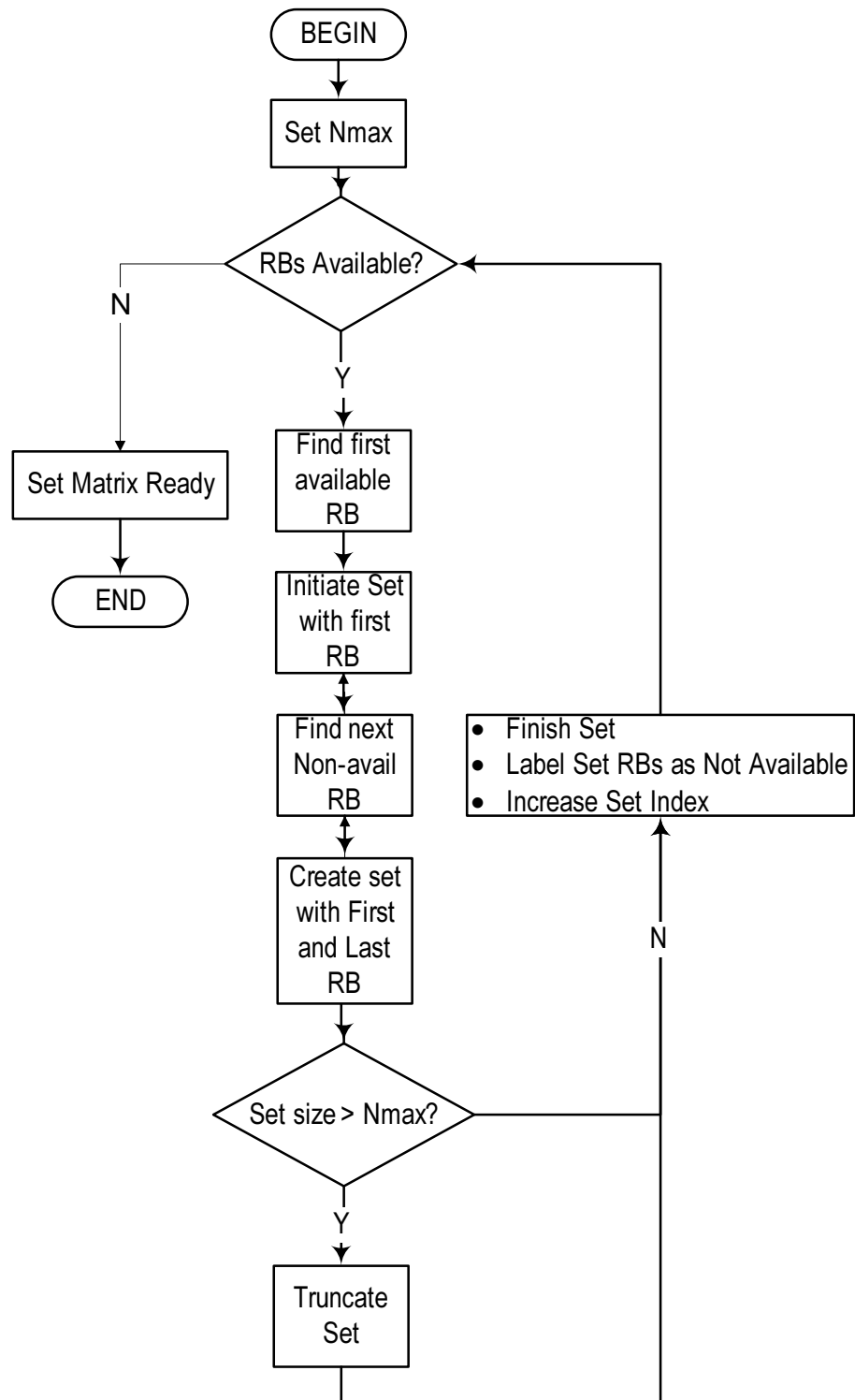


Figure 35. Resource block organization algorithm—Algorithm 2

Once the Set Matrix is ready, the scheduler proceeds to the resource assignment operation. An important restriction of our Set Scheduling evaluation is that sets are assigned to a user if and only if the user has the same CQI for all the RBs in the set. This yields a disadvantage in terms of resource assignment, but it reduces the delay involved in evaluating the constraint of Equation (27). It also guarantees decodability considering that the CQI is adequate for all the RBs in the set. In order to understand the impact of this restriction, consider a user that has different CQI levels in contiguous frequencies that span an available set. For such user, service would be denied until a set that falls within a range of frequencies that have the same CQI level is available. In the best case this restriction results in delayed attention, and in the worst case it would result in an unattended user request. Although this restriction seems to severely affect QoS, in our evaluations with no interference the probability that a user shows different CQI levels within a frequency band (2.3 or 3.4 GHz) is less than 3%. In real world applications, the use of adequate interference control mechanisms reduces the probability that a user experiences different CQI levels within a frequency band. This situation does not occur with Block by Block Scheduling since each RB is handled individually.

In our implementation, during the assignment process the scheduler first looks for a set that matches the number of required RBs for a given user. If such set is not available, the scheduler is able to assign a set with a larger number of RBs. Only the required RBs will be assigned. The unused RBs from that set will be used to form a new set. The scheduling slot ends when all sets are assigned or all user requests are attended. Non attended users are queued for the next scheduling slot.

When compared to the scheduling presented in (Chung and Tsai, 2010), there is an important advantage of using Set Scheduling. In (Chung and Tsai, 2010) resources are assigned also as sets, but each set corresponds to a complete CC. This means that if a CC is composed of 100 RBs and a user requires 101 RBs, a total of 200 RBs will be assigned, corresponding to two CCs. Set Scheduling will only assign as many RBs as required, allowing to use unassigned RBs at a next scheduling slot. Still, it is not

possible to directly compare our proposal with that in (Chung and Tsai, 2010) since we do not perform an evaluation with fixed set size.

## 4.4 Evaluation results and analysis

Using the parameters from Table 4, numerical evaluations were performed to assess the performance of Set Scheduling and Block by Block Scheduling. The scheduling strategy shown in Figure 32 was implemented with non-contiguous inter-band CA subject to the restriction in Equation 27. The scheduling strategy in Figure 33 was implemented as described in Section 3. For evaluation, a Round Robin scheduler was used. Although the evaluation scenario is simple, it allows to focus in the assessment of the capabilities of Set Scheduling.

The value of  $N_{\max}$  was evaluated at 15, 18, 20 and 22 RBs. The value of  $R_{b\max}$  was evaluated between 2,200 and 7,000 kbps and for a given CQI value it determines the average number of RBs that will be required per user. The value of  $S_{b\max}$  was evaluated at 2000, 3000, 4000 and 5000 bits, and for a given CQI value it determines the average number of time slots required to complete a user request transmission.

### 4.4.1 Delay analysis

The expected delay due to resource assignment in block by block scheduling can be estimated using Equation 30.

$$E[\text{Delay}] = E[N] \cdot \tau_s. \quad (30)$$

where  $E[\text{Delay}]$  is the expected delay to assign all the required RBs to a given user,  $E[N]$  is the expected number of RBs per user and  $\tau_s$  is the time required to assign one single RB.

To calculate  $E[N]$  we will use the conditional expectation method. Thus, note that

for a given CQI value,  $N$  can be calculated as:

$$N = \frac{R_{b_u}}{R(\text{CQI})}$$

$$\forall R(\text{CQI}) > 0 \quad (31)$$

where  $R_{b_u}$  is a random variable and  $R(\text{CQI})$  is assumed to be constant and non-zero. Therefore we can obtain

$$E[N] = E\left[\frac{R_{b_u}}{R(\text{CQI})}\right] = \frac{1}{R(\text{CQI})}E[R_{b_u}]$$

$$\forall R(\text{CQI}) > 0, \quad (32)$$

Now, in order to obtain  $E[N]$ , we use

$$E[N] = E[E[N|R(\text{CQI})]] = E\left[\frac{1}{R(\text{CQI})}E[R_{b_u}]\right]$$

$$\forall R(\text{CQI}) > 0, \quad (33)$$

Given the restriction of  $R(\text{CQI}) > 0$  and the statistical independence between  $R(\text{CQI})$  and  $R_{b_u}$ , we can now write

$$E[N] = E\left[\frac{1}{R(\text{CQI})}|R(\text{CQI}) > 0\right]E[R_{b_u}]. \quad (34)$$

where  $R(\text{CQI})$  is assumed to be a discrete random variable with values indicated in Table 3, the term  $E\left[\frac{1}{R(\text{CQI})}|R(\text{CQI}) > 0\right]$  can be obtained as follows

$$E\left[\frac{1}{R(\text{CQI})}|R(\text{CQI}) > 0\right] = \sum \frac{1}{R(\text{CQI})}p(R(\text{CQI})|R(\text{CQI}) > 0). \quad (35)$$

Note that  $R(\text{CQI})$  depends directly on the CQI value. A numerical analysis of the CQI for the evaluation scenario and parameters of Section 2, showed that the CQI behaves as a random process with exponential probability density function (pdf). This behavior was verified using  $Q-Q$  plots showing a perfect fit. Considering this and the

discretization of  $R(\text{CQI})$  due to the mapping in Table 1, it is possible to obtain specific values for the term  $E\left[\frac{1}{R(\text{CQI})} | R(\text{CQI}) > 0\right]$ . Numerical evaluation found that for the 2.3 GHz band there is an  $E[\text{CQI}] = 8.85$ , while for the 3.4 GHz band  $E[\text{CQI}] = 7.12$ . For the 2.3 GHz frequency band,

$$E\left[\frac{1}{R(\text{CQI})} | R(\text{CQI}) > 0\right] = 0.00251 = \frac{1}{399 \text{ kbps}}. \quad (36)$$

Since this value corresponds to a data rate per RB not supported, it is possible to say that the value would be in fact  $\frac{1}{396 \text{ kbps}}$  for the 2.3 GHz frequency band. In the same fashion, it was found that for the 3.4 GHz frequency band

$$E\left[\frac{1}{R(\text{CQI})} | R(\text{CQI}) > 0\right] = 0.00292 = \frac{1}{343 \text{ kbps}}. \quad (37)$$

which given the discretization of  $R(\text{CQI})$  results in a value of  $\frac{1}{188.5 \text{ kbps}}$ .

Given the uniform distribution of the requested data rate, we can assume that  $E[R_{b_u}] = R_b \text{ max} / 2$ . Once the value of  $E[N]$  is obtained using (34), the expected delay for the assignment of resources in Block by Block Scheduling in terms of  $\tau_s$  can be calculated using Equation (30).

The expected delay when using Set Scheduling can be estimated using Equation (38).

$$E[\text{Delay}_{\text{set}}] = E[\tau_o] / \lambda_u + \tau_s. \quad (38)$$

where  $E[\text{Delay}_{\text{set}}]$  represents the expected delay per user due to resource assignment using Set Scheduling;  $E[\tau_o]$  represents the time required by the RB organization algorithm to obtain the Set Matrix;  $\lambda_u$  is the average number of user requests per scheduling slot.

Using numeric evaluation, both RB organization algorithms were evaluated in order to determine the parameter  $E[\tau_o]$  for the evaluation conditions specified in Table 4. Figure 36 shows the evaluation of  $E[\tau_o]$  for the minimum and the maximum values of

$N_{\max}$ , with respect to the percentage of available RBs. For this evaluation, available RBs were randomly distributed. The parameter  $E[\tau_o]$  is expressed in terms of  $\tau_s$ .

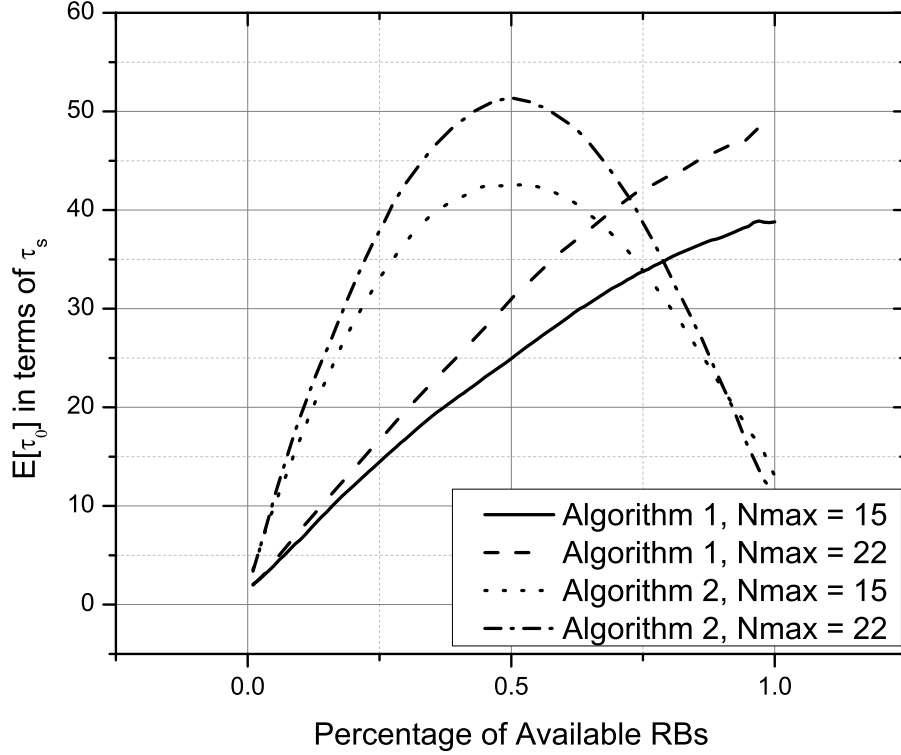


Figure 36. Expected time required to execute the RB organization algorithm.

For Algorithm 1 the maximum value of  $E[\tau_o]$  is obtained when all RBs are available, and in the worst case for a value of  $N_{\max} = 22$ , it corresponds to  $49 \cdot \tau_s$ . Using Equation (38), for the preceded worst case scenario, the expected delay due to resource assignment using Set Scheduling corresponds to  $E[\text{Delay}_{\text{set}}] = 49 \cdot \tau_s / 25 + \tau_s = 2.96 \cdot \tau_s$ . This delay calculation considers only the availability of RBs and the value of  $N_{\max}$ . For this calculation, it is assumed that all user requests are attended.

As it can be observed in Figure 36 there is an important difference in the behavior of the proposed algorithms. Algorithm 1 has a monotonically increasing response with respect to available RBs while algorithm 2 is a parabola which has a maximum value when 50% of RBs are available. When the percentage of RBs is below 70%, Algorithm 1 outperforms Algorithm 2 in terms of  $E[\tau_o]$ . However, when a higher percentage of RBs is available for scheduling Algorithm 2 shows a much lower delay. When resources

are more fragmented, Algorithm 1 will show a lower delay than Algorithm 2. This information is valuable since it makes possible to select an algorithm based on the expected availability of RBs. It is possible to have both algorithms in a system and switch between them depending on the resource availability in order to reduce resource assignment delay.

It is also possible to observe in Figure 36 that the expected delay  $E[\tau_o]$  is also dependant on Nmax. It is shown that the larger the value of  $N_{max}$ , the higher the expected delay  $E[\tau_o]$ . In Algorithm 1, the worst case of delay shows that for Nmax = 22,  $E[\tau_o] = 49$ , while for Nmax = 15,  $E[\tau_o] = 38$ . This is a significative difference that can also be observed for Algorithm 2. Given this behavior, in order to reduce delay as much as possible the lowest possible value of Nmax has to be selected.

Figure 37 shows a comparison between the expected delay of Block by Block Scheduling for the different values of  $E[R_{b_u}]$  (in 2.3 a 3.4 GHz bands), with the expected delay for resource assignment when using Set Scheduling in the worst case of Algorithm 1. For Set Scheduling, delay is not dependent of  $E[R_{b_u}]$ , but rather on the parameters of the RB organization algorithm (Nmax) and RB availability. It is also independent on the frequency band. The delay in block by block scheduling is dependent on both  $E[R_{b_u}]$  and the frequency band, given that the operating frequency determines the number of expected RBs required per user. For the evaluation parameters used, Set Scheduling takes at most the same delay as Block by Block Scheduling for resource assignment. When compared to the 3.4GHz band it can reduce the delay by up to six times.

#### 4.4.2 Complexity description

In order to compare the complexity of Block by Block Scheduling and Set Scheduling we present the general operation of both strategies. Only the general case for each process is described for comparison. The operations not included in each process are the same for each strategy. The operations not considered include frequency band distinction, restrictions such as the maximum value of RBs per user (Nmax), and storage operations

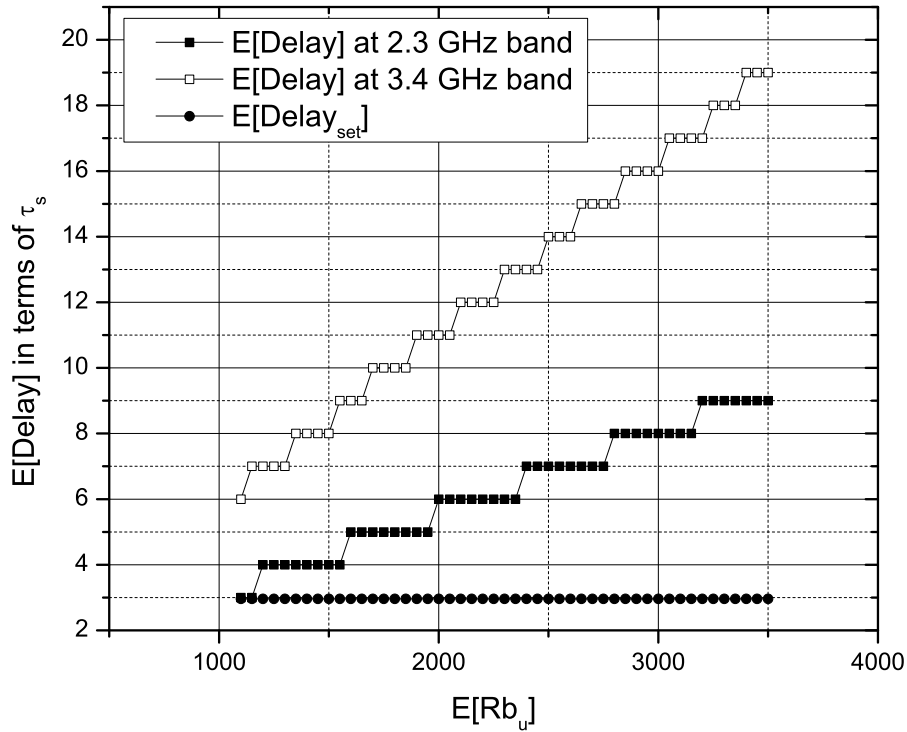


Figure 37. Expected delay due to resource assignment.

of the set matrix.

Algorithm 3 shows the general operation of Block by Block Scheduling. For each user request, this strategy will find and assign as many RBs as required in order to meet the restriction given in Equation 27. Therefore, for a total of  $N_i$  RBs, each user needs a total of  $N_i$  *find* operations, as well as  $N_i$  *assign* and  $N_i$  *update* operations. As previously discussed, the delay due to resource assignment using this strategy will in fact depend on the value of  $N_i$ . Since LTE-Advanced systems allow up to 500 RBs to be assigned to a single user in order to exceed the 1 Gbps requirement for IMT-Advanced systems, the delay of Block by Block Scheduling can become considerably high. However, it has the advantage that each available RB can be optimally used for a given CQI value. The achievable data rate will be considered independently for each assigned RB.

Algorithm 4 shows the general operation of Set Scheduling. In this procedure, each user request within the assignment process requires only one *calculate* operation, one *find* operation and one *assign* operation. Since the number of required RBs is known

---

**Algorithm 3** General Block by Block Scheduling process
 

---

$i$  is the index for the user requests  
 $j$  is the index for the RB vector  
 $R(\text{CQI})_j$  is the achievable data rate for  $\text{RB}_j$   
**for** Each scheduling slot **do**  
   **while** RBs Available **do**  
     **if** User requests in queue **then**  
        $i \leftarrow$  User Index  
       Updated Sum Rate  $\leftarrow$  User  $i$  Requested Data Rate  
       **while** Updated Sum Rate  $> 0$  **do**  
         **find:** Available  $\text{RB}$   
          $j \leftarrow$  Available  $\text{RB}$  index  
         **assign:**  $\text{RB}_j$  to User  $i$   
         **update:** Updated Sum Rate = Updated Sum Rate -  $R(\text{CQI})_j$   
       **end while**  
       **increment:** User Index  
     **else**  
       **break:** No more user requests, process completed  
     **end if**  
   **end while**  
**end for**

---

due to the restriction of equal CQI for the RBs in a set, no *update* operation is required. In Set Scheduling, the main cause of delay is the execution of the resource block organization algorithm at each scheduling slot. However, as it was presented in Section 4.4.1, the organization of available RBs in sets depends mainly on the availability of RBs and the implementation of the organization algorithm. Since the RB organization algorithm is executed once per scheduling slot, the delay due to its execution can be considered as “distributed” among the attended users.

From the algorithms presented in Section 4.4.1, a complexity comparison between both strategies is possible. Consider the construction of one set and its assignment to one user. Table 5 shows a comparison in terms of the number of operations that each strategy performs in order to assign the required RBs to a given user. Each operation is considered as having the same complexity. Although not all the operations are shown, Table 5 does allow for a general comparison. In total,  $3N_i$  operations are required by Block by Block Scheduling in order to assign  $N_i$  RBs to a user. On the other hand,

---

**Algorithm 4** General Set Scheduling process
 

---

```

for Each scheduling slot do
  execute: Resource Block Organization Algorithm (see Fig. 34 and 35)
  while RB Set Available do
    if User requests in queue then
       $i \leftarrow$  User Index
      calculate  $N_i \leftarrow$  Number of required RBs for user  $i$  for the different CQI values
      find: Set with size  $\geq N_i$ 
      assign:  $N_i$  RBs from set to User  $i$ 
      increment: User Index
    else
      break: No more user requests, process completed
    end if
  end while
end for

```

---

Set Scheduling requires a total of  $N_i + 4$  operations when using the RB Organization Algorithm 1, and a total of five operations when using the RB Organization Algorithm 2. Note that when using RB Organization Algorithm 2, the number of operations does not depend on  $N_i$ . We observed that the most time consuming operation within our simulation environment is the *find* operation. The *check* operation corresponds to the verification of contiguous RBs in Algorithm 1 (see Figure 34). Therefore, the main difference between both algorithms is that Algorithm 1 uses one *find* operation and  $N_i$  *check* operations per set, while Algorithm 2 performs two *find* operations per set. For any case, the number of operations performed by Set Scheduling including the RB organization algorithm is lower than for Block by Block Scheduling, with an exception when the number of required RBs is  $N_i = 1$ . The complexity advantage of Set Scheduling increases with  $N_i$ .

#### 4.4.3 User capacity analysis

In order to evaluate the performance of Set Scheduling in terms of user capacity, we derived a metric that represents the percentage of user requests that remain in the scheduler queue after a given number of user drops. The number of user drops used in

Table 5. Comparison of the number of operations required per attended user considering Block by Block Scheduling and Set Scheduling

Operation	Number of operations		
	B by B scheduling	Set Scheduling	RB org. Alg. 1, (Alg. 2)
Find	$N_i$	1	1, (2)
Assign	$N_i$	1	0, (0)
Update	$N_i$	0	0, (0)
Calculate	0	1	0, (0)
Check	0	0	$N_i$ , (0)
Total	$3N_i$		$N_i + 4$ , (5)

our evaluation corresponds to 500 as presented in Table 4. This amount of user drops was obtained through a generate and test algorithm, given that simulating a larger number of user drops does not change the user capacity metric. Equation (39) shows how the metric is calculated

$$PQ = 1 - (U_{att}/U_{rec}). \quad (39)$$

where PQ is the percentage of user requests in queue;  $U_{att}$  represents the number of attended requests;  $U_{rec}$  corresponds to the number of received requests.

Figure 38 shows a comparison of the PQ metric between Block by Block Scheduling and Set Scheduling for  $S_b\max = 2,000$  bit. The lower PQ metric value represents less users in queue. A PQ metric value of 0 indicates all users were attended. Although the different Set Scheduling evaluations vary in performance, there is always one that outperforms the Block by Block Scheduling behavior. For an  $S_b\max = 2,000$  bit the best performance is obtained when  $N_{\max} = 20$ , with a PQ metric up to 5% lower than that of Block by Block scheduling (achieved at  $R_b\max = 5,800$  kbps).

Figure 39 shows the same comparison but with  $S_b\max = 5,000$  bit. As it can be observed, the best performance in terms of the PQ metric is obtained with Set Scheduling for  $N_{\max} = 18$ . It is noticeable that the value of  $N_{\max}$  that minimizes the PQ metric depends on traffic demands. This brings the opportunity to use statistical traffic information in order to select the best value of  $N_{\max}$  at each scheduling slot in

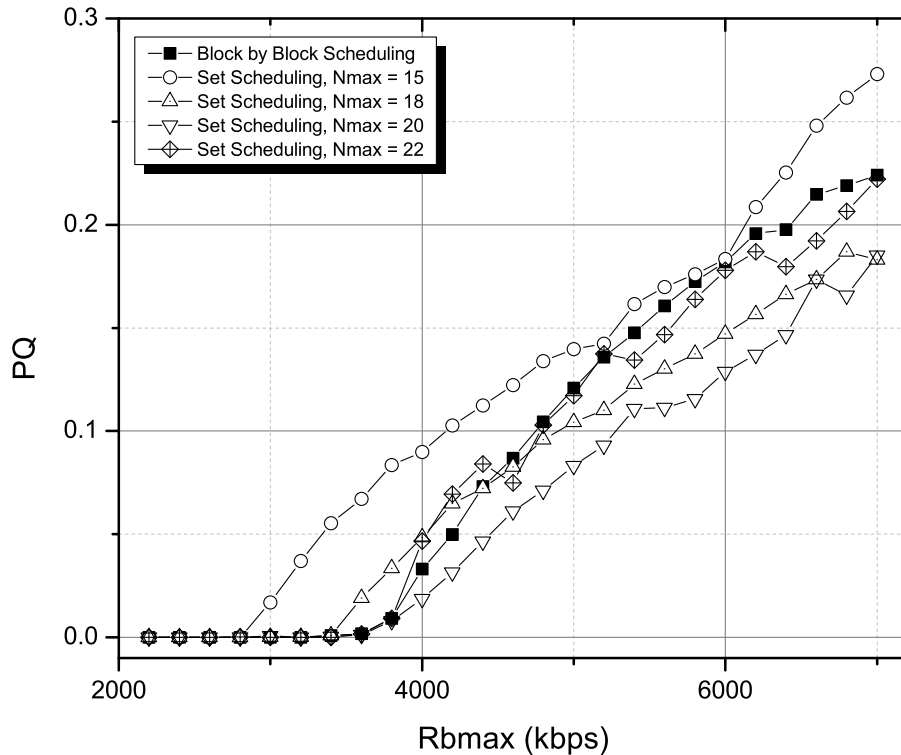


Figure 38. PQ metric of the different scheduling strategies for a maximum file size  $S_b \max = 2,000$  bits.

an adaptive fashion.

From figures 38 and 39 it is also possible to bring the information provided by the Set Scheduling delay analysis. Using either one of the proposed algorithms for set construction, the lowest possible delay is achieved with the lowest value of  $N_{\max}$ . Therefore, from the PQ analysis, when two or more performance curves overlap the best selection of  $N_{\max}$  will correspond to the lowest value. As such, in Figure 38 a value of  $N_{\max} = 15$  will be preferred for values of  $R_b \max$  lower than 3,000 kbps, while for values of  $R_b \max$  between 3,000 and 3,500 kbps a value of  $N_{\max} = 18$  is preferred. For  $R_b \max$  greater than 4,000 kbps a value of  $N_{\max} = 20$  performs the best.

In Fig. 40 the best performing results for the different values of  $S_b \max$  are shown. It is important to note that, for the evaluated conditions, the larger the file size, the smaller value of  $N_{\max}$  must be selected to achieve a better performance (lowest value of the PQ metric). As expected, at higher  $S_b \max$  the PQ metric is increased. In all

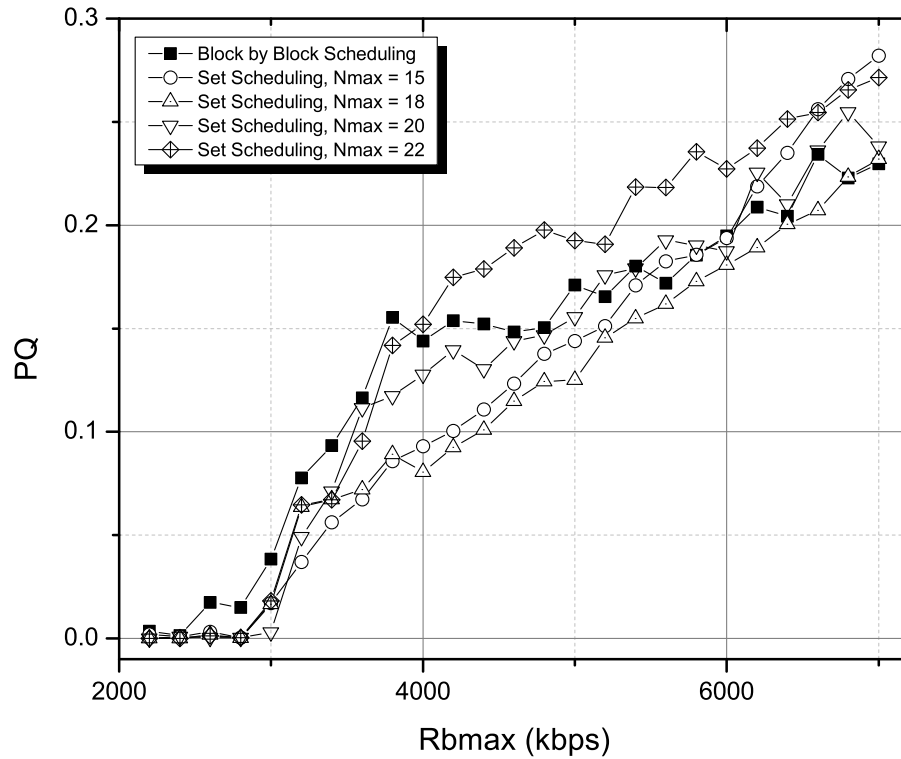


Figure 39. PQ metric of the different scheduling strategies for a maximum file size  $S_b \max = 5,000$  bits.

of the evaluations, Block by Block Scheduling was outperformed by at least one of the Set Scheduling configurations.

Once the average requested data rate increases to a point where it is not possible to attend all requests at every scheduling slot, the PQ metric starts to increase indicating a reduction in system capacity. Also, it can be observed that the average data rate at which the system cannot attend all requests is lower as the average user file size increases. This is particularly visible in Figure 40, where all curves show a very similar slope that starts to increase at a lower value of parameter  $R_b \max$  as  $S_b \max$  increases. This behavior implies that as  $S_b \max$  increases, less RBs are available at each scheduling slot. As this happens, the point of system resource depletion occurs at a lower value of average user requested data rate.

The lower PQ metric means that the cell capacity is increased. Statistically, overall throughput can be calculated by multiplying the PQ metric times the mean data rate

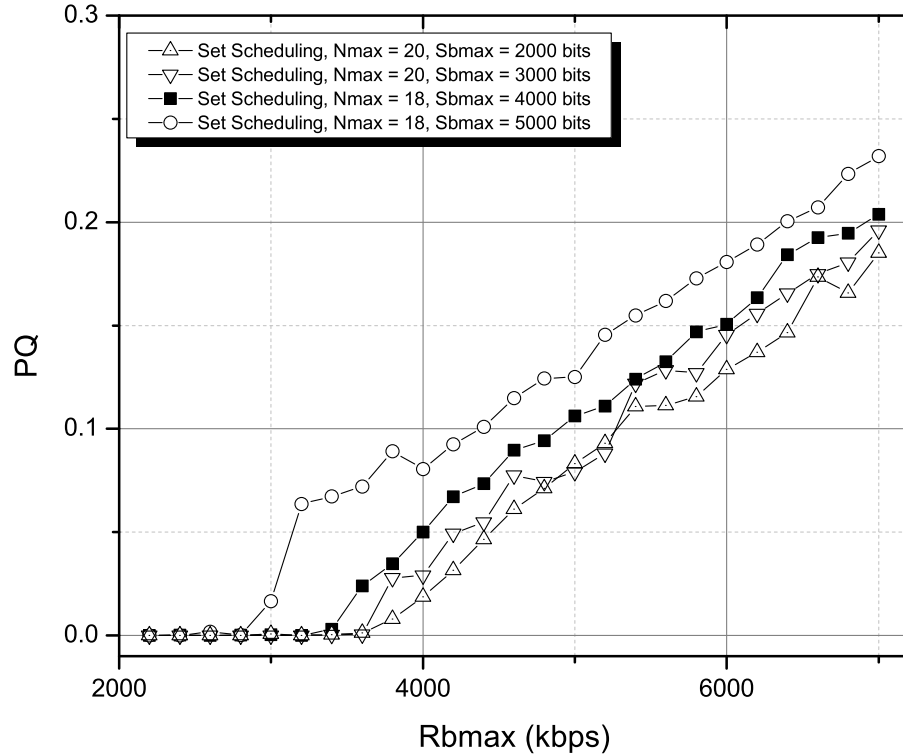


Figure 40. PQ metric for the different maximum file size  $S_b \max$  of the best performing scheduling strategies.

requested and the average number of users. Once the PQ metric is greater than zero, all of the available RBs are used at each scheduling slot, indicating that the throughput is at a maximum for the scheduling and traffic conditions.

#### 4.4.4 Throughput evaluation

Since the PQ metric is not commonly used in literature to evaluate user capacity, in this section we provide an evaluation of the throughput behavior for the proposed Set Scheduling strategy. The simulation parameters used to evaluate throughput are shown in Table 4. The maximum requested bit rate  $R_b \max$  was evaluated from 2,000 to 10,000 kbps in 2,000 kbps increments.  $S_b \max$  was evaluated for 2,000 and 6,000 bits. For Set Scheduling, a value of  $N_{\max} = 20$  was used.

Figure 41 shows the throughput percentage calculated using Equation 40.

Throughput percentage = Total assigned throughput / Total requested throughput.

(40)

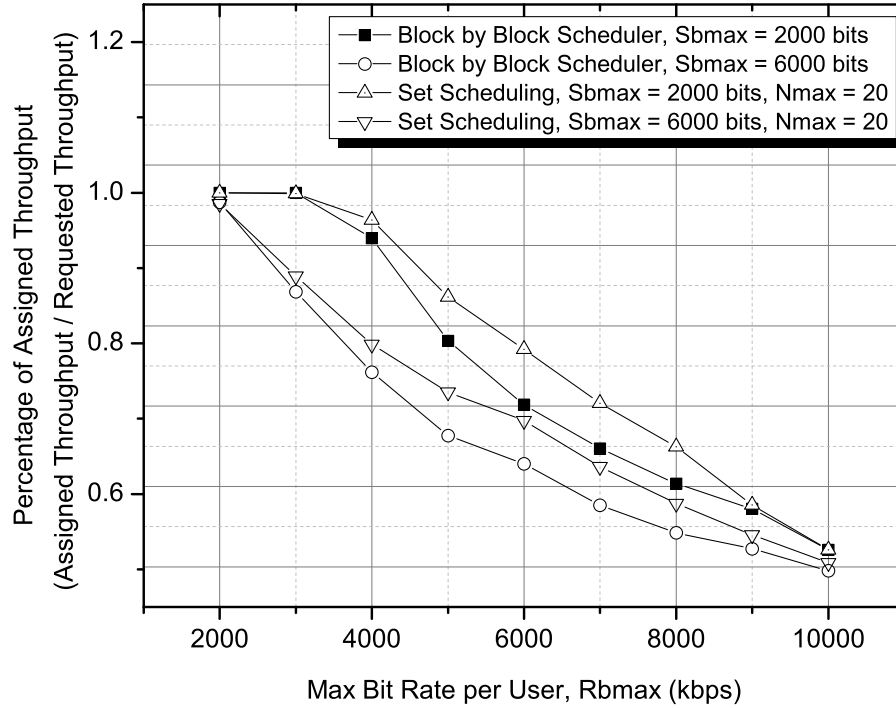


Figure 41. Throughput percentage (assigned throughput/requested throughput) for Block by Block Scheduling and Set Scheduling.

Equation 40 allows to compare Block by Block Scheduling and Set Scheduling fairly. From Figure 41 it is possible to observe that for both scheduling strategies, for a larger value of  $S_{bmax}$  the Throughput Percentage decays. This is due to the fact that as the file size increases, the number of time slots required by the user to complete a transfer also increases, thus reducing the number of available RBs at each scheduling slot. It is also possible to observe that in each case of  $S_{bmax}$ , Set Scheduling outperforms Block by Block Scheduling by up to 8 percent observed at a value of  $R_{bmax} = 6,000$  kbps. However, this advantage is reduced as  $R_{bmax}$  increases. This is due to the fact that at some point the maximum throughput that can be handled by the system is reached by both scheduling strategies. This point is reached when  $R_{bmax}$  is 10,000 kbps for a

value of  $S_b \text{ max} = 2,000$  bits.

Figure 42 shows the average user throughput assigned by the schedulers. It is possible to observe the saturation of system resources as  $R_b \text{ max}$  increases. For a given value of  $S_b \text{ max}$ , Set Scheduling outperforms Block by Block Scheduling until the maximum throughput that the system can handle is reached. This behavior is consistent with that in Figure 41.

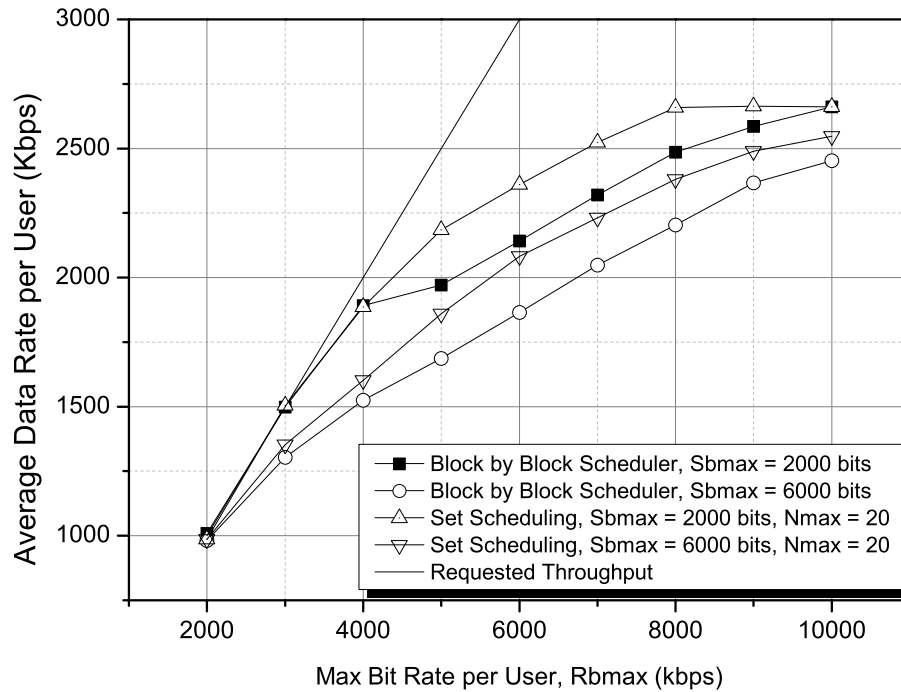


Figure 42. Average assigned throughput per user for Block by Block Scheduling and Set Scheduling.

## 4.5 Chapter Summary

A scheduling strategy for CA using pre-organized RB sets was presented and evaluated. We presented an analytical evaluation framework to determine the expected number of RBs required by users, based on a mapping of CQI values to data rates per RB and the statistical behavior of the CQI. This framework allowed us to evaluate a macro-cellular environment in order to determine the potential delay advantage of using Set Scheduling.

Two different RB Organization Algorithms were implemented. It was possible to observe a marked difference in the delay behavior of the evaluated algorithms in terms of the percentage of available RBs. A dependance to the percentage of available RBs as well as to the value of  $N_{max}$  were observed. This opens the possibility of designing a different RB organization algorithm with improved behavior and lower delay when compared to the algorithms presented. The capacity of reducing delay due to resource assignment using Set Scheduling depends directly on the performance of the RB Organization Algorithm.

Although the RB organization algorithm used provided only contiguous CA functionality, it still outperformed a block by block scheduler that used non-contiguous inter-band CA. Some of the improvements that can be made to the scheduling strategy presented in this chapter include the possibility of aggregating sets. Set aggregation can improve throughput. Also, it is possible to design a different type of scheduler whose metrics are calculated for a whole set. Another improvement is the possibility of implementing an adaptive RB organization algorithm, that takes into account the statistical behavior of user requests.

In general, we were able to show that Set Scheduling has the capacity of reducing the delay due to resource assignment when compared to Block by Block Scheduling without affecting user capacity.

# Chapter 5

## Set Scheduling with Fairness Considerations

In this chapter, a Multi Carrier Proportional Fair (MCPF) algorithm as presented in (Kim and Han, 2010) is implemented and evaluated. The capacity to balance traffic loads of MCPF is only useful when traffic is homogeneous (same service) and all users have the same requirements. Moreover, MCPF becomes useful only when equal amounts of spectrum can be assigned to each user. In order to evaluate fairness under heterogeneous traffic conditions (different services) we develop a metric based on the a-posteriori probability of attention to users. Using the Cumulative Distribution Function (CDF) of the probability of attention with respect to the required data rate, a numerical value of fairness can be obtained. With the proposed metric it is possible to evaluate fairness of set scheduling. It is found that fairness can be controlled with the adaptation of the maximum number of RBs per set,  $N_{\max}$ .

### 5.1 Introduction

As presented in Chapter 4, the main task of a scheduler within the Radio Resource Management operation is to determine how the available bandwidth has to be shared between competing users in order to meet an objective (Stanczak et al., 2009). The scheduler can be designed to maximize a specific objective. One such objective is to allocate resources to users that maximize the total network throughput, subject to individual channel conditions. However, this strategy may be unfair since some users may be denied service due to their specific channel conditions. As an example, a user at the cell edge may be able to be attended, but a user close to the ENodeB will be preferred due to better channel conditions. For this reason, any scheduler must address

the issue of fairness (Stanczak et al., 2009).

The concept of fairness is well known in network engineering. In terms of resource management, fairness usually refers to the possibility of the system to distribute resources equally to all the users in a network, either wired or wireless. The system resources that are to be distributed among users are typically bandwidth or time. This depends on the type of system (Frequency Division Multiplexing or Time Division Multiplexing). In general, the system resource assigned to a user in a data network will have an impact on the users throughput. Therefore, another fairness concept is regarded as the possibility of allowing all users to achieve equal throughput. These two perspectives of fairness derive in two different fairness objectives. One of them is to distribute resources evenly between competing users and another one is to allow all users to achieve the same throughput. In wired networks it is considered that all users have the same channel capacity due to a good Signal to Noise Ratio (SNR) (Massoulié and Roberts, 2002). Therefore, in wired networks the concept of fairness is typically based on equally distributed resources. Given that all users have the same channel conditions, for a same share of resource users will also achieve the same throughput.

This situation changes completely for wireless networks. Due to the various conditions that users may have (position, speed, shadowing, etc.) the SNR for each user is different, therefore each user has a different channel capacity. Since the channel capacity varies as a function of SNR, assigning equal resources (i.e. bandwidth) will yield different throughput to each user. Because of this situation, fairness based on throughput is the choice for wireless networks (Porto Cavalcanti and Andersson, 2009).

One of the most popular concepts of fairness is Max-Min Fairness. In its definition, Max-Min Fairness states that a feasible set of flows (user transfers) is defined to be max-min fair if any individual flow cannot be increased without decreasing another flow (Stanczak et al., 2009). The concept of Max-Min Fairness is to treat all users as fairly as possible by making all data rates as large as possible. If an individual user data rate is increased, the data rate for another user will be decreased (Massoulié and Roberts, 2002). The main drawback of Max-Min Fairness is that the achieved

fairness is usually at the expense of a considerable drop in efficiency in terms of total throughput (Stanczak et al., 2009). Given the tradeoff between throughput and fairness as described in Chapter 4, Max-Min Fairness would represent the opposite extreme of a Max C/I scheduling strategy.

In order to evaluate fairness in a wireless network, different metrics are used in literature. The most popular corresponds to Jain's fairness metric (Jain et al., 1984) and is obtained with eq. 41

$$F = \frac{\left(\sum_{k=1}^n \bar{r}_k\right)^2}{n\left(\sum_{k=1}^n \bar{r}_k^2\right)}. \quad (41)$$

where  $F$  is Jain's fairness index;  $\bar{r}_k$  is the  $k$ -th user's throughput and  $n$  represents the number of system users (Jain et al., 1984).

Jain's fairness index raises to a maximum value of 1 when all rates  $\bar{r}_k > 0$  are equal and a minimum value of  $\frac{1}{n}$  when one user is assigned all of the available throughput and the rest of the users are not assigned with resources (and thus no throughput). Jain's fairness index is applicable to wireless networks since it measures fairness from a throughput perspective. The maximum fairness achieved when all users have the same throughput is not necessarily a favorable condition, since given the different values of user SNR, more resources (bandwidth) will be required by users with poor channel conditions.

## 5.2 Schedulers with Fairness

In order to balance the tradeoff between throughput and fairness, several schedulers have been proposed in literature in works such as (Han and Lu, 2011), (Kim and Han, 2010), (Chung and Tsai, 2010) and (Mehrjoo et al., 2010). Although there are significant differences among these published works, the use of a Proportional Fair (PF) type of scheduler is maintained. A general Multi Carrier PF (MCPF) scheduler solves

the objective function in eq. 42 (Kim and Han, 2010):

$$\begin{aligned}
& \max \sum_j \sum_i \frac{\phi_{ij}^n x_{ij}^n}{R_i^{n-1}} \\
& \text{s.t. } \sum_j \phi_{ij}^n \leq 1, \forall j \\
& \phi_{ij}^n \in \{0, 1\}.
\end{aligned} \tag{42}$$

where  $i$  is the user index,  $j$  is the carrier index and  $n$  is the time slot index;  $\phi_{ij}^n$  is an index which takes the value of 1 if carrier  $j$  is assigned to user  $i$  at time slot  $n$ ;  $x_{ij}^n$  is the achievable data rate of user  $i$  on carrier  $j$  at time slot  $n$ ;  $R_i^{n-1}$  is the average data rate of user  $i$  at time slot  $n - 1$  (average data rate taken at the previous time epoch)(Kim and Han, 2010).

The definition of MCPF used in (Kim and Han, 2010) is general, and corresponds to maximizing the overall PF metric. The PF metric is basically the ratio of the achievable data rate of user  $i$  on carrier  $j$  with respect to the average data rate previously achieved by user  $i$ . This policy implies that, for users with the same achievable data rate, a user with a historical average data rate lower than other users, will have a higher PF metric, while if the historical data rate for a user is higher, its PF metric will be lower. The objective function tries to find a set of carrier assignments that maximize the PF metric over all users competing for service. Therefore, in order to find the optimum solution to this function, all competing users must be evaluated in all available carriers. This is a known Non Polynomial Hard (NP-Hard) problem (Stanczak et al., 2009) when multiple carriers are considered (as in OFDMA systems). Figure 43 represents the carrier assignment problem of MCPF. Each user will be assigned a set of carriers such that the PF metric over all users is maximized. Therefore, an optimum solution to this problem needs all carriers to be evaluated on all users in order to find the set of carriers assigned to each user that will maximize the objective function in eq. 42.

The solution space for the MCPF in (Kim and Han, 2010) can be reduced if Set Scheduling as presented in Chapter 4 is used. Using Set Scheduling, users will compete

User / Carrier	Carrier 1	Carrier 2	Carrier 3	Carrier 4	Carrier 5	Carrier 6	...	Carrier j
User 1	1	1	0	0	0	1		0
User 2	0	0	1	0	0	0		1
User i	0	0	0	1	1	0		0

Figure 43. Representation of the MCPF problem.

Usr / Set	Set 1	Set 2	Set 3	Set 4	Set 5	Set 6	...	Set j
User 1	1	0	0	0	0	0		0
User 2	0	0	1	0	0	0		0
User i	0	0	0	1	0	0		0

Figure 44. Representation of the PF with Set Scheduling problem.

for sets of carriers, instead of individual carriers. Figure 44 represents the problem associated with PF with Set Scheduling, with the restriction that only one set per user can be assigned. In this thesis, we analyzed PF with set scheduling by means of computer simulation. The objective function in eq. 42 was first adapted to the set scheduling problem. In order to do this, the index  $j$  refers to a set. The restriction of a single set per user was also implemented.

For our evaluation, a full buffer traffic model with 60 users was considered. Users were uniformly distributed within a single ENodeB coverage area. In order to solve the optimization problem, an evolutive algorithm was implemented (Han and Lu, 2011). A population of one (single solution) was evolved for a total of 300 iterations, always keeping the best solution (elitism). Each evolution consisted on a random solution to the assignment problem. In order to evaluate the benefits of MCPF, two cases were considered. The first case assumes equal sized sets of resources, while the second considers randomly sized sets of resources. This was done in order to evaluate the performance of MCPF when the available spectrum resources vary in bandwidth, as in LTE-Advanced systems (Dahlman et al., 2011).

Figure 45 shows the performance of MCPF with uniformly sized spectrum resources

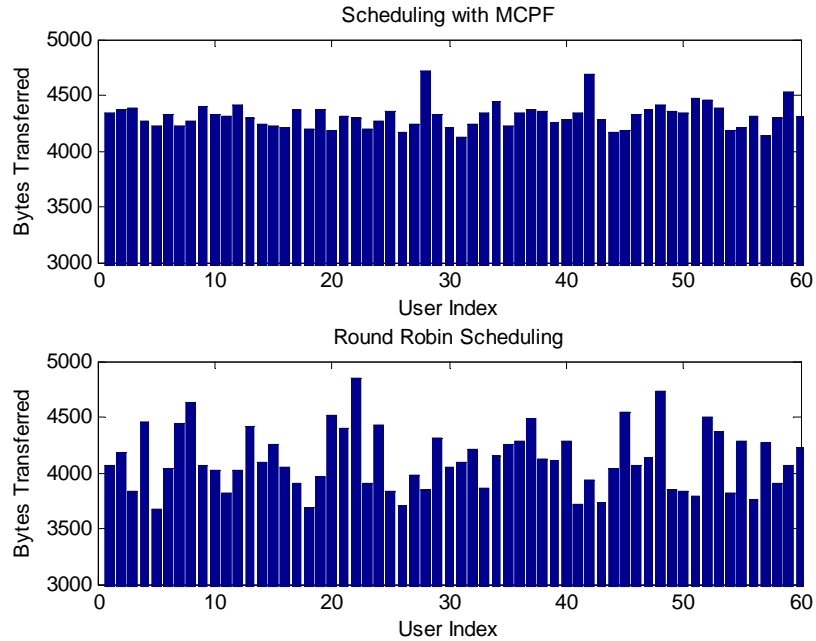


Figure 45. Throughput per user considering uniform set sizes and homogeneous traffic.

of 1 MHz with 60 users compared to a Round Robin (RR) scheduler. Figure 46 shows the performance of MCPF with non-uniformly sized spectrum resources. The size of each available resource was random, with a uniform distribution between 100 kHz and 1 MHz and 60 users, compared with a RR scheduler.

In order to analyze the performance of MCPF, in Table 6 we show a comparison of the statistics of user throughput.

Table 6. Comparison of MCPF and RR schedulers with uniformly and non-uniformly sized spectrum resources.

Scheduler Type	$\sigma$ (kbps)	$\mu$ (kbps)	Cell Throughput (kbps)	Fairness
RR Uniform	277.3	4114.0	246,840	0.9956
RR Non-Uniform	334.4	4662.3	279,740	0.9950
MCPF Uniform	112.9	4312.6	258,760	0.9993
MCPF Non-Uniform	236.4	4674.2	280,450	0.9975

From Table 6, it can be observed that MCPF performs better than a RR scheduler when uniform resources are distributed among users. Compared to a RR scheduler, the use of MCPF with uniformly sized resources reduced the standard deviation ( $\sigma$ ) of user throughput by 60%. Also, average user throughput and cell throughput were

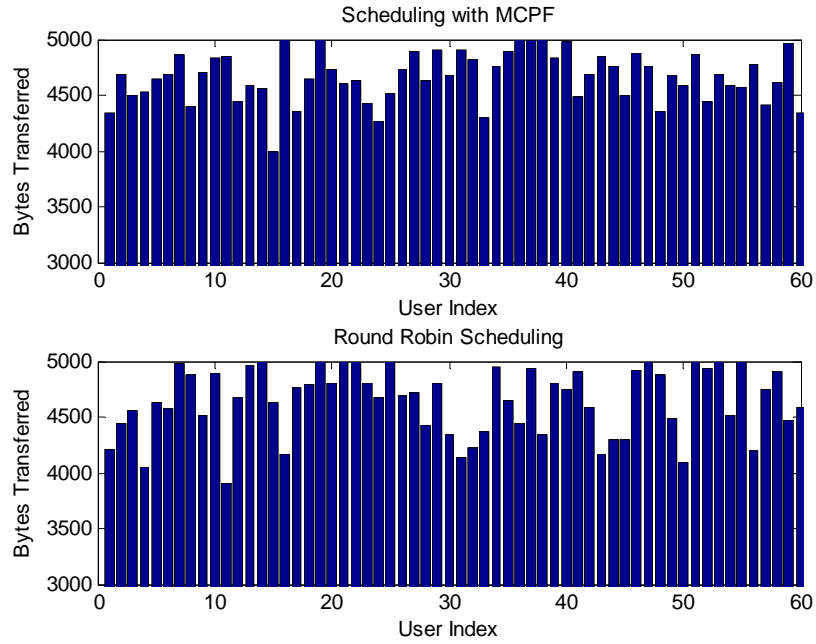


Figure 46. Throughput per user considering non-uniform set sizes and homogeneous traffic.

increased by 5%. This reduction of the standard deviation reflects the capacity of MCPF to share system resources fairly in order to maintain the same user throughput to all users. MCPF achieves this task without affecting cell throughput and average user throughput, that were in fact increased. The fairness index reflects the capacity of MCPF to improve fairness to users. However, since RR is a fair scheduling policy, the improvement in Jain's fairness index is not significant.

In the case of non-uniformly sized resources, MCPF is also capable of improving the evaluated metrics. However, the improvement is not as significant as in the case of uniformly sized resources. For example, the reduction in standard deviation is of only 30%. This is visible in Fig. 46, where the variations in user throughput are not evidently improved between MCPF and RR schedulers. Also, the improvement in average user throughput and cell throughput was of only 0.2%. Although Jain's fairness index is still close to the maximum achievable, the use of MCPF in non-uniformly sized resources does not provide of significant gains in terms of throughput and fairness in comparison to a RR scheduler. This result is important since it shows that MCPF

is not an adequate option in systems that make use of non-uniformly sized spectrum resources as those used in Set Scheduling.

### 5.3 Fairness under Heterogeneous Traffic Conditions

From the traditional perspective, fairness is focused on providing the same amount of resources or throughput to all users. Metrics to evaluate system fairness are aimed at numerically identify the degree of fairness from this perspective. For example, Jain's fairness index is maximum when all users achieve equal throughput (Jain et al., 1984). One of the main components of IMT-Advanced (Dahlman et al., 2011) is to support a wide range of services. These services go from short messaging services with data rate requirements of 5 kbps to real time high definition video conference with data requirements of 100 Mbps. Under these conditions where traffic is heterogeneous, the traditional concept of fairness loses its application. Under different data rate requirements based on the type of service requested, a fairness policy that attempts to provide the same throughput to all users is not useful. Therefore, the concept of fairness has to change in wireless systems with heterogeneous traffic, as a result of supporting a wide range of services.

In order to deal with fairness under heterogeneous traffic conditions, we derive a generalized concept of fairness based on the probability of the system to attend a user request:

*A scheduler that attends service requests from users with different requirements will be fair if all user requests have the same probability of being attended.*

This concept of fairness is valid in the sense that, if all user requests have the same probability of being attended regardless of channel conditions or requirements, then the system is not biased and has no priorities in how each request is handled. Thus, it is said to be fair.

Although this concept of fairness is present in literature as part of the general idea of fairness (Porto Cavalcanti and Andersson, 2009), it is not useful when system resources

or throughput are to be evenly distributed among users. However, the generalized concept of fairness presented here is appropriate to evaluate systems with heterogeneous traffic conditions.

In order to measure fairness based on probability of attention, we derive a fairness metric based on the Gini coefficient (Dianati et al., 2005). The Gini coefficient measures the inequality among values of different distribution. One of its main applications is to measure the inequality within a population's income. In order to obtain the Gini coefficient, a reference of equal distribution is considered. Based on the Cumulative Distribution Function (CDF) of a random variable with equal (uniform) distribution, the variable under study is compared to it and the difference is quantified to obtain a value for the so called Gini coefficient.

Given the relationship between data rate and bandwidth due to the use of Adaptive Modulation and Coding, we base our measurement of fairness in the data rate required by users. For our definition, we consider as a reference the CDF of a uniformly distributed set of data rates (all data rates equally probable). This represents our fairness reference. A plot of the CDF of the data rates of attended users is considered for measurement. Figure 47 shows an example of two CDFs. Reference data corresponds to a uniformly distributed normalized data rate. Based on the Gini coefficient, we first quantify the difference between the reference CDF and the evaluated data CDF. This is done by calculating the area between both curves. Once this area is calculated, the result is divided by the area under the reference curve in order to calculate a percentage. This calculation will yield a value of 1 when the difference between both CDFs is maximum (i.e. CDF of data is zero for all data rate values) and a value of 0 when both CDFs are the same. In order for our proposed metric to be consistent with Jain's index, we subtract the resulting percentage to a value of 1.

Let  $F_X(x)$  be the reference CDF for uniformly distributed data rate  $X$  and  $F_Y(y)$  the CDF of the data rates of attended users. Then, the fairness index based on the Gini coefficient  $F_G$  is calculated using Eq. 43.

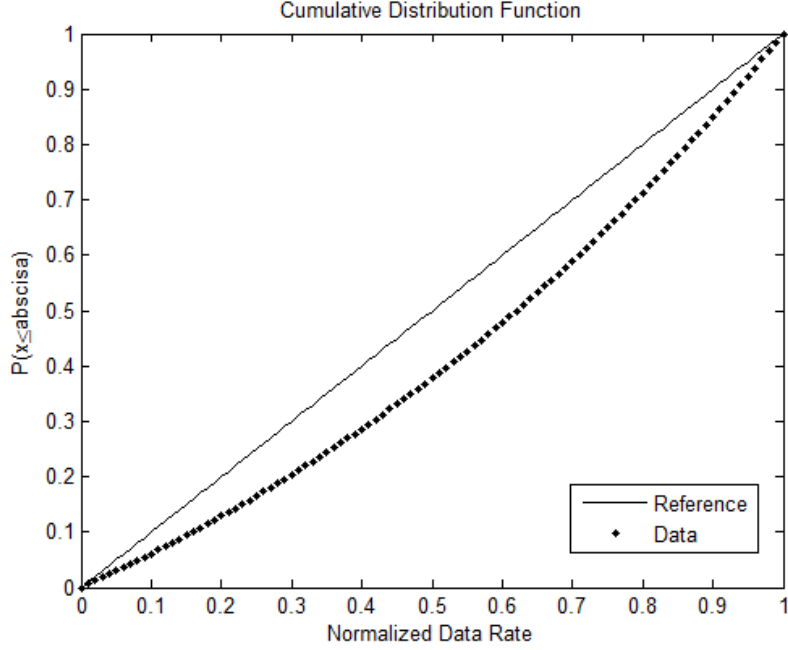


Figure 47. CDF plots for the reference data set and the evaluated data set.

$$F_G = 1 - \frac{\left| \int_0^1 F_X(x) - \int_0^1 F_Y(y) \right|}{\int_0^1 F_X(x)}. \quad (43)$$

Using the proposed metric, fairness can be evaluated under heterogeneous traffic conditions. Moreover, the reference CDF used to calculate  $F_G$  does not necessarily corresponds to a uniform distribution. In fact, the reference CDF needs to match that of the user requests. For a given probability distribution of user requests, the system will be fair if it attends requests with the same probability as they are generated. For instance, if only two types of services with data rates A and B are requested by users, and 30% of those requests correspond to traffic type A and 70% correspond to traffic type B, the system will be fair if it attends type A requests with probability of 0.3 and type B requests with a probability of 0.7. The corresponding reference CDF would be that of a discrete variable with two possible values and the fairness metric is to be calculated with it. However, depending on the reference CDF, negative fairness values

may occur.

## 5.4 Evaluation of Fairness with Set Scheduling

The proposed fairness metric was used to evaluate Set Scheduling. Using the scenario and parameters described in Chapter 4, we evaluate the process of user requests and resource scheduling. Heterogeneous traffic conditions were evaluated, considering uniformly distributed requested data rates from 1 kbps to  $R_{\max}$  and uniformly distributed packet sizes ranging from 100 bits to  $S_{\max}$ . Evaluations were performed for different  $R_{\max}$  and  $S_{\max}$  values. In our implementation, we base the fairness metric on the CDF of a user request being attended in terms of the requested data rate. The obtained CDF corresponds to the probability of a user request of less than or equal to a certain data rate being successfully attended. In order to obtain such CDF, the statistics of attended users are kept unchanged. The memory requirement for this operation is not more than that of a Proportional Fair scheduler that keeps track of the average data rate achieved by each user.

Figure 48 shows the CDF of attended users for  $N_{\max} = 21$  and a maximum data rate  $R_{\max} = 7000$  kbps. Different values of  $S_{\max}$  were evaluated. As it can be observed, the CDF has very slight changes with respect to  $S_{\max}$ . This behavior was observed with all the evaluations for different values of  $R_{\max}$  and  $N_{\max}$ . In order to confirm that  $S_{\max}$  does not have an important impact in Fairness for a given value of  $R_{\max}$  and  $N_{\max}$ , the fairness index  $F_G$  was calculated and is shown in Fig. 49 in terms of  $R_{\max}$  for different values of  $S_{\max}$ . The results shown in Fig. 49 confirm that for our evaluation of  $F_G$  in terms of  $R_{\max}$ , the effect of changes in  $S_{\max}$  can be neglected.

Figure 50 shows the CDF of attended users for  $N_{\max} = 21$  and different values of  $R_{\max}$ . Since it has been determined that variations in  $S_{\max}$  have a very small effect on the evaluated CDF and Fairness, the CDFs presented correspond to a single value of  $S_{\max} = 2000$  bits. For  $N_{\max} = 21$ , it can be observed that as the maximum data

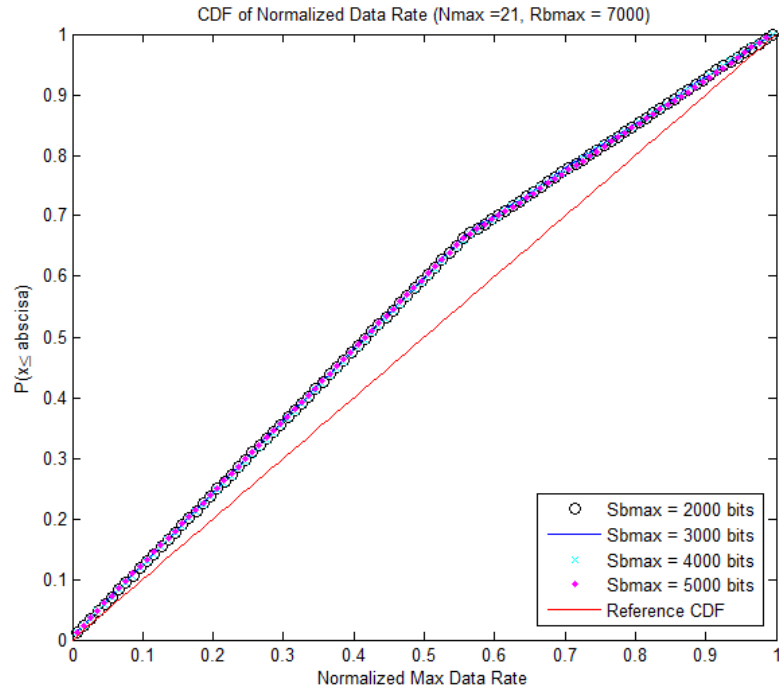


Figure 48. CDF plots of Normalized Max Data Rate for  $N_{\max} = 21$  and  $R_{\max} = 7000$  kbps.

rate is increased, the separation between the evaluated CDF and the reference CDF is increased, thus a decreased value of  $F_G$  is expected as  $R_{\max}$  increases.

In order to determine the impact of  $N_{\max}$  on the fairness index  $F_G$ , evaluations with different values of  $N_{\max}$  were performed. Figure 51 shows the evaluation of  $F_G$  for different values of  $N_{\max}$  ranging from 21 to 29 and a fixed value of  $S_{\max} = 5000$  bits. The parameter  $R_{\max}$  was varied from 4000 kbps to 7000 kbps. As it can be observed in Fig. 51, an increase in  $N_{\max}$  has a direct impact in fairness. As maximum data rates increase, fairness starts to decrease in every curve. For a maximum evaluated size of  $N_{\max} = 29$ , the corresponding fairness metric shows the highest (best) behavior. As  $N_{\max}$  is increased the variation in fairness between evaluations starts to decrease. Further evaluations with larger values of  $N_{\max}$  were performed finding that for the evaluated conditions fairness did not improve significantly. It is important to note that as  $N_{\max}$  increases fairness is never reduced.

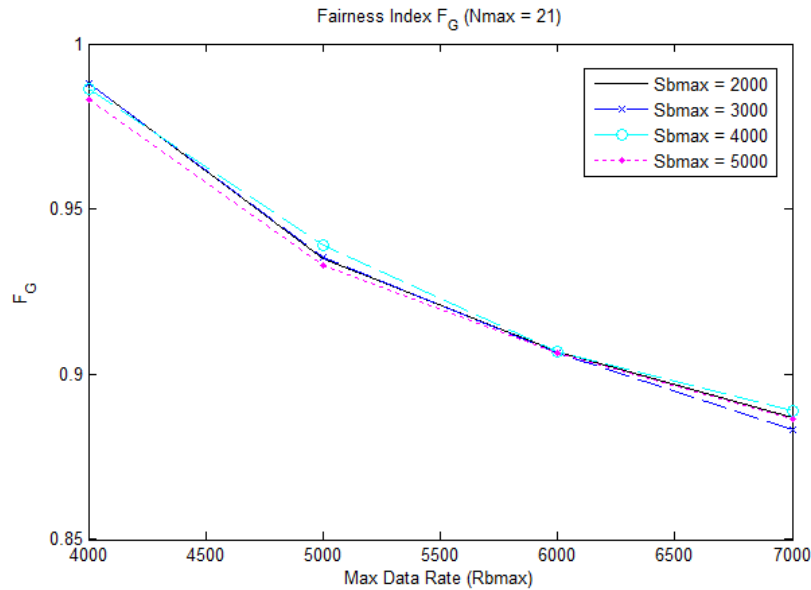


Figure 49. Fairness Index  $F_G$  for  $N_{\max} = 21$

## 5.5 Chapter Summary

In this chapter we discuss the issue of fairness in systems with heterogeneous traffic conditions. We show that one of the most popular schedulers, namely the MCPF scheduler, is not suitable for non-uniformly sized spectrum resources. Moreover, in the presence of heterogeneous traffic, the PF metric will benefit users with lower data rate requirements.

In order to analyze fairness in systems with heterogeneous traffic conditions, we derived a fairness metric based on the Gini coefficient. This metric is adequate to quantify fairness when users have different data rate requirements that depend on the service requested. The Gini coefficient has been used in (Dianati et al., 2005) and more recently in (Mehrjoo et al., 2010). Our implementation of a fairness index based on the Gini coefficient is however not found in literature and is therefore a contribution of this work. Our fairness index calculation  $F_G$  can be adapted to any reference CDF depending on the traffic behavior, it only has to be noted that once the reference CDF is not that of a uniformly distributed random variable, the fairness index can have negative values. However, the maximum value of 1 will in every case represent the total

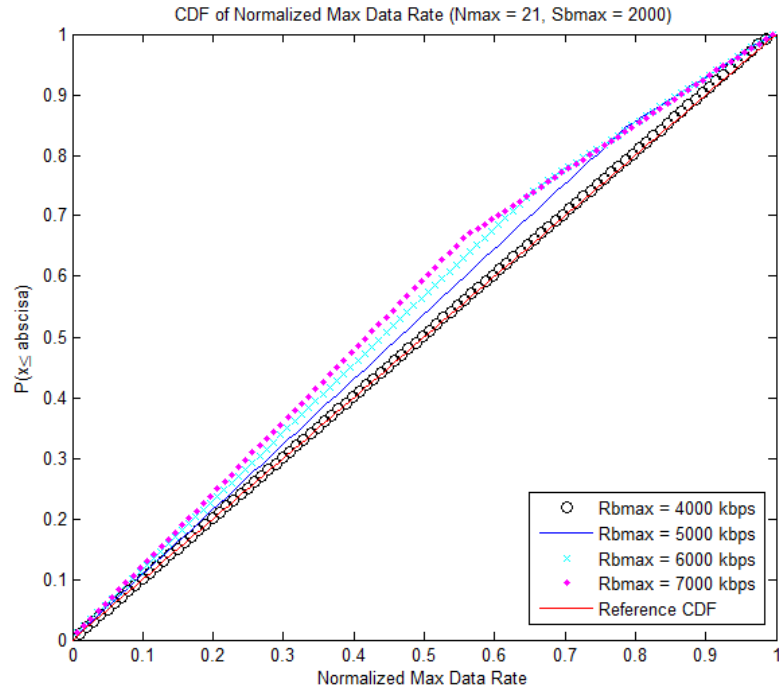


Figure 50. CDF plots of normalized Max Data Rate for  $N_{\max} = 21$  and  $S_{b\max} = 2000$  bits fairness case.

An evaluation of fairness for set scheduling was performed using the proposed metric. Since the main resource for a wireless communication system is spectrum, we based our fairness evaluation on the probability of a user with data rate requirement  $R_b$  being attended. Using this information as a probability density function, the CDF for evaluation of the fairness metric can be obtained. Two major findings are important. First, for fairness based on data rate, the packet size does not affect the corresponding fairness metric. Second, in set scheduling fairness is directly affected by the maximum set size  $N_{\max}$ . For the evaluated conditions, fairness index is increased as  $N_{\max}$  increases. However, combining the findings in Chapter 4 with the results in this chapter, we determined that the behavior observed in the CDFs in Fig. 50, for  $N_{\max}=21$  the system serves users with lower data rates with higher probability than users with higher data rates. This is due to the fact that as the system operates, less sets with large number of Resource Blocks (RBs) are available, thus users with high data rate requirements

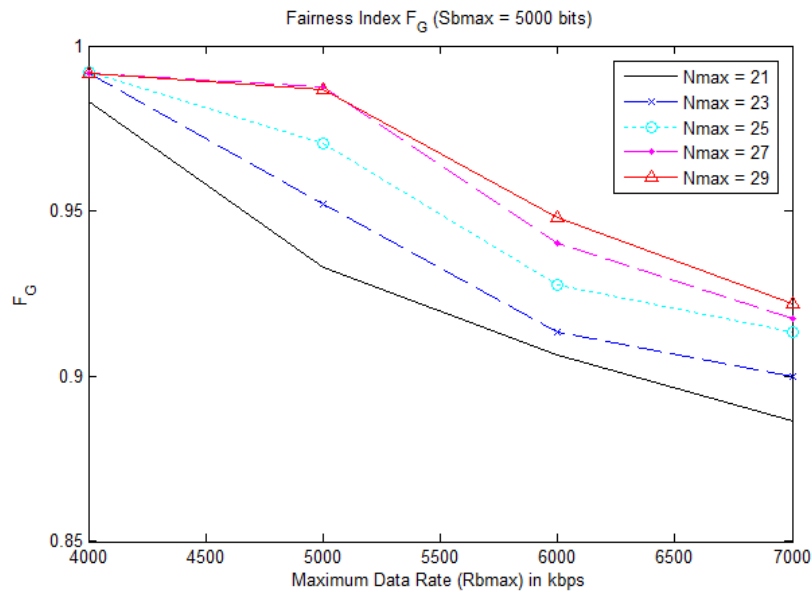


Figure 51. Fairness Index  $F_G$  for Sbmax = 5000 bits

spend more time in queue. However, as  $N_{max}$  increases, the system assigns and releases sets with large number of RBs making them available. This balances the probability of users being attended. However, as described in Chapter 4, this increases the percentage of users in queue and reduces throughput.

The results obtained in Chapter 4 and this chapter provide the necessary information for the design of an adaptive scheduler that can balance between three objectives, which are percentage of users in queue, throughput, and fairness. As it has been shown, for the scenario and evaluation parameters, the performance of the system can be controlled with a single scheduler parameter:  $N_{max}$ .

# Chapter 6

## Conclusions and Future Work.

This chapter provides a summary of this thesis, highlighting the overall research achievements and contributions. It also provides recommendations for future research directions.

### 6.1 Summary of Research Results.

#### 6.1.1 Channel Modeling Results Summary.

This work focused on scheduler design for Carrier Aggregation (CA) for LTE-Advanced systems. LTE-Advanced systems as well as other broadband wireless communication systems such as Wireless Man Advanced make use of Adaptive Modulation and Coding (AMC) schemes to improve spectrum efficiency. The adaptability of the modulation index as well as the coding rate depend directly on channel conditions. Therefore, in order for a scheduler to take advantage of the benefits of AMC in terms of efficient use of the radio channel, the scheduler needs the information corresponding to the channel quality observed by the user on every available spectrum resource to be scheduled.

Given the aforementioned relationship between channel conditions and scheduler operation, this thesis project was divided in two main parts. The first part was to study a channel model that represents the propagation characteristics of a bad urban macrocellular scenario. We proposed the Multi Cluster Gaussian Scatterer (MCGS) channel model in this work. The model has four degrees of freedom that determine channel response: number of clusters, position of clusters, Scattering Region Width (SRW) of each cluster and the amount of scatterers per cluster (weight). Depending on these parameters, the MCGS channel model can represent a microcellular environment

as well as a highly dispersive macrocellular environment. This makes the MCGS model very flexible, as it can be used to represent a wide range of scenarios. As a result of our study of this model, we developed a method to obtain the second order statistics of the channel model directly from the first order statistics. Using the mathematical expressions that represent the first order statistics corresponding to Angle of Arrival (AoA) and Time of Arrival (ToA), our method allows to obtain a Power Delay Profile (PDP) and Angle Spread (AS). Using numerical simulation we showed that the mathematical expressions for first and second order statistics properly fit simulated data.

The contribution of this method is that it allows to evaluate a highly dispersive channel model without heavy numerical computation. Instead of considering multiple rays (ray tracing) which is known to be computationally heavy (Steinbauer and Molisch, 2001), our method allows to represent the channel using the mathematical model directly. In order to do this, once the PDP is obtained it is possible to implement a Tapped Delay Line (TDL) that represents its behavior for signal level simulation. Using the TDL, it is possible to determine the behavior of a signal traveling through the analyzed environment.

Even though the MCGS channel model allows for simulation of a wide range of environments, there are two main reasons why it was not further used in the evaluation of schedulers for CA. First, every set of parameters of the MCGS channel model represents a different environment. An infinite number of combinations of number of clusters, position, SRW and weight can exist. A methodology to deal with this situation presented in (Döttling et al., 2009) establishes that these parameters can be randomly generated between specified limits in order to obtain a set of evaluations to present a statistical result. This would have represented an extensive amount of simulation and analysis only to determine channel behavior, which is beyond the scope of this work.

Second, the figure of merit needed to evaluate the performance of a system with a scheduler is the Signal to Interference and Noise Ratio (SINR). AMC schemes are directly related to the SINR via the report of the Channel Quality Indicator (CQI) from the User Equipment (UE). Therefore, regardless of how a value of SINR is achieved in

simulation, the performance of a system with AMC and a CA scheduler will not vary. This means that, if a specific value of SINR is obtained for a given set of parameters of the MCGS channel model and the same value of SINR is obtained using only Path Loss (PL) and thermal noise, both evaluations will result in the same performance when link level simulation is realized. Since link level simulation reduces computational burden and is widely used in literature to determine system performance using a specific scheduler (Shen et al., 2012), (Wang et al., 2012), (Liu et al., 2011) and (Chen et al., 2009), we decided to use this strategy using a single cell scenario with a macrocellular bad urban PL model and thermal noise.

The statistics of CQI behavior for a uniform distribution of users within a single base station scenario without interference (as presented in Chapter 4) were obtained. It was first found that using the ITU-R macrocellular bad urban PL model used, the CQI has an exponentially distributed Probability Density Function (pdf). The mean CQI depends on the frequency band, and within a given frequency band the mean CQI does not show significant changes between Component Carriers (CC). This result has an important impact in CQI reporting granularity. Given that within a band, a specific user will not see a difference in CQI between existing CCs (and thus no difference in AMC scheme), it is only necessary for the UE to transmit a single CQI value per band. This is only valid when no interference is present.

The relationship between the CQI and the corresponding AMC scheme, dictates how each Resource Block (RB) can be used (throughput and packet size). As described in Chapter 2, the throughput and amount of bits that can be handled by each RB depend on the AMC used. Taking this into account, an evaluation on the statistical behavior of the number of RBs required by the users in a system under the scenario presented in Chapter 4 was performed. The main result of this evaluation showed that it is possible to predict, on average, the number of RBs required by each user based on the statistical traffic requirements given data rate ( $R_b$ ) and a packet size ( $S_b$ ) requirements. The required data rate has a direct impact on the number of RBs needed, and the packet size determines the average time slots that each RB remains assigned

to a user to complete a transfer. Using this information, a scheduler can be designed accordingly. Since the traffic requirements of system users may change, keeping track of the statistical data rate and packet size needs can be used to dynamically adjust scheduler operation. The results obtained from the channel modeling section of this thesis project were fundamental for the remaining research.

### 6.1.2 Scheduler Design Results Summary.

The second part of this thesis project deals with scheduler design for CA and is included in Chapters 4 and 5. Set Scheduling presented in Chapter 4 was designed to take advantage of the knowledge of the average number of RBs per user. The scheduler was designed on the basis that, if users require on average a certain number of RBs, resource assignment would be faster if a set of at least that amount of RBs is readily available for scheduling when compared to RB by RB scheduling as presented in (Chen et al., 2009), (Songsong et al., 2009) and (Lei and Zheng, 2009). The analysis and evaluation of the proposed Set Scheduling strategy showed the following advantages when compared to RB by RB assignment:

- Reduction of delay for resource assignment when the average number of RBs per user is more than 3.
- Reduction of percentage of users in queue for specific values of the maximum number of RBs per set,  $N_{max} = 18$  and  $N_{max} = 20$ .
- Increase in cell throughput for values of  $N_{max} = 18$  and  $N_{max} = 20$ .

The implementation of Set Scheduling requires the use of an algorithm to form the sets from the available RBs. Two different set forming algorithms were presented in Chapter 4. It was found that the set formation algorithm has a direct impact on the delay required to organize all available RBs in sets. For the two algorithms presented, it was shown that the lower the value of  $N_{max}$ , the lower the delay to organize RBs in sets. However, the implementation of Set Scheduling limits scheduling

to the use of contiguous CA. Another important restriction is that all RBs in a set must have the same CQI. These restrictions limit the usage of the available resources. The main advantage of RB by RB assignment is that it has the capacity to optimize spectrum usage by handling each RB individually, allowing for non-contiguous intra and inter band CA implementation. The optimization in spectrum usage would involve to evaluate each RB to each competing user, and assigning it to the user that maximizes the evaluation metric (fairness, max C/I, PF, etc.). This process would become time consuming.

The designed scheduler was further evaluated in order to determine its fairness in Chapter 5. A Multi Carrier Proportional Fair was implemented. It was determined that the typical concept of fairness for packet switched systems is not adequate for evaluating a system with heterogeneous traffic conditions. A fairness metric based on the Gini coefficient was developed and used to evaluate fairness of the proposed scheduler under heterogeneous traffic. The development of the fairness metrics is one of the contributions of this project, as no other fairness metric for heterogeneous traffic was identified in literature.

Using the Gini coefficient based fairness metric, it was found that Set Scheduling fairness depends directly on  $N_{max}$ . For small values of  $N_{max}$ , the system will provide sets that benefit users with lower bandwidth requirements. Thus, it is possible to attend more users with low requirements and increment cell throughput. As  $N_{max}$  increases, fairness also increases but users with higher bandwidth requirements are served with the same probability as users with lower requirements. This causes less overall users to be attended and a reduction in throughput may occur. This behavior shows the typical tradeoff between throughput and fairness.

With the results obtained, general conclusions of this thesis work can be made and future lines of research can be defined.

## 6.2 Summary of Contributions

In this section, we highlight the general conclusions obtained from the realization of this research project.

In terms of channel modeling, the following conclusion can be made:

- As determined by the analysis performed, the CQI statistical behavior depends mainly on the Signal to Noise Ratio (SNR), the number and position of users and the transmission power and the operating frequency.

In terms of scheduler design, the following conclusions can be made:

- The time required by a scheduler to group RBs into sets depends on the amount of RBs available and the maximum number of RBs per set.
- Using a Round Robin Scheduler in conjunction with organized sets of RBs allows for a reduction of the percentage of user requests in queue of up to 10% when compared to individual RB scheduling. It also increases throughput by up to 5%.
- The value of  $N_{max}$  is directly responsible for fairness and throughput in Set Scheduling. It also determines the maximum delay in resource assignment.
- The use of Multi Carrier Proportional Fair does not provide of significant gains in throughput and fairness when resources to be assigned are unequally sized.
- The Gini coefficient based fairness metric  $F_G$  is adequate for quantitatively measuring fairness under heterogeneous traffic conditions.

With regards to the main objective purpose of this research, we conclude that the characteristics to be considered in the design of scheduling algorithms that support Carrier Aggregation (CA) in next generation wireless communication systems are:

- Statistical behavior of CQI to determines the average number of RBs per user. This is essential to design a scheduling strategy that suits the amount of spectrum resource required by users.

- Type of traffic. The type of traffic determines how the system will measure fairness and throughput. Depending on the characteristics of traffic, a scheduler may benefit from the proposed Set Scheduling strategy. Set Scheduling strategy was designed taking in mind heterogeneous traffic requests.
- Fairness/Throughput tradeoff. This will depend on the operator QoS objectives. In Set Scheduling, the Fairness/Throughput tradeoff can be adjusted with a single parameter (Nmax).

### 6.3 Future Research and Recommendations.

The results obtained, together with the conclusions made, have helped to identify various lines of future research work.

In terms of channel modeling, the Multi Cluster Gaussian Scatterer channel model (MCGS) can be evaluated as specified in (Döttling et al., 2009) in order to obtain statistical data that can serve to design a CQI-AMC table or estimation algorithm. This will involve intensive signal level simulation.

A two stage scheduler structure using Set Scheduling can be designed in order to take advantage of frequency and time scheduling. This strategy may allow to match Set Scheduling with non-contiguous intra and inter band CA, improving QoS guarantees. This strategy would involve Set Aggregation.

Evaluate Set Scheduling with different core schedulers. The scheduler used in the evaluations performed in this work is a Round Robin scheduler. A different type of scheduler may be used in order to improve a specific metric, such as throughput or fairness.

The use of the proposed fairness metric based in the Gini coefficient can be further analyzed in order to determine its sensibility to changes in traffic conditions as well as the cases where it can be applied.

Evaluate the performance of Set Scheduling with dynamically adaptive Nmax. Nmax

has a direct impact on throughput and fairness. An algorithm to adaptively adjust  $N_{\max}$  in order to adjust system metrics can be designed. This will involve the optimization of the value of  $N_{\max}$  for a required objective.

# References

- 3GPP (2010). R2-100963: Stage 2 description of carrier aggregation. 3GPP TSG-RAN Meeting 69. Retrieved from: [http://www.3gpp.org/ftp/tsg\\_ran/WG2\\_RL2/TSGR2\\_69/docs/R2-100963.zip](http://www.3gpp.org/ftp/tsg_ran/WG2_RL2/TSGR2_69/docs/R2-100963.zip).
- Abdullah, M. and Yonis, A. (2012). Performance of lte release 8 and release 10 in wireless communications. In *Cyber Security, Cyber Warfare and Digital Forensic (CyberSec), 2012 International Conference on*.
- Ahmadi-Shokouh, J. (2005). Analytically derived uplink/downlink toa/doa distributions with multi-gaussian model of scatterers' spatial distribution. In *Military Communications Conference, 2005. MILCOM 2005. IEEE*.
- Al-Shibly, M., Habaebi, M., and Chebil, J. (2012). Carrier aggregation in long term evolution-advanced. In *Control and System Graduate Research Colloquium (ICSGRC), 2012 IEEE*.
- Analysys Mason (2011). The momentum behind LTE worldwide. GSMA White Paper. Retrieved from: <http://www.gsma.com/spectrum/wp-content/uploads/2012/03/momemtumbehindltewhitepaperjan10.pdf>.
- Andrade, A. and Covarrubias, D. (2003). Radio channel spatial propagation model for mobile 3g in smart antenna systems. *Transactions on Communications, IEICE*, E86-B(1):213–220.
- Arias, M. and Manderson, B. (2006). Clustering approach for geometrically based channel model in urban environments. *Antennas and Wireless Propagation Letters, IEEE*, 5(1):290 –293.
- Cattoni, A., Nguyen, H., Duplicy, J., Tandur, D., Badic, B., Balraj, R., Kaltenberger, F., Latif, I., Bhamri, A., Vivier, G., Kovacs, I., and Horvath, P. (2012). Multi-user mimo and carrier aggregation in 4g systems: The samurai approach. In *Wireless Communications and Networking Conference Workshops (WCNCW), 2012 IEEE*.
- Chen, L., Chen, W., Zhang, X., and Yang, D. (2009). Analysis and simulation for spectrum aggregation in lte-advanced system. In *Vehicular Technology Conference Fall (VTC 2009-Fall), 2009 IEEE 70th*.
- Chen, Y. and Dubey, V. (2003). Effect of weightage of cluster power in multi-cluster mobile radio channels. In *Communications, 2003. APCC 2003. The 9th Asia-Pacific Conference on*.

- Chong, C., Watanabe, F., Kitao, K., Imai, T., and Inamura, H. (2009). Evolution trends of wireless mimo channel modeling towards imt-advanced. *Transactions on Communications, IEICE*, E92-B(9):2773–2788.
- Chung, Y.-L., Jang, L.-J., and Tsai, Z. (2011). An efficient downlink packet scheduling algorithm in lte-advanced systems with carrier aggregation. In *Consumer Communications and Networking Conference (CCNC), 2011 IEEE*.
- Chung, Y.-L. and Tsai, Z. (2010). A quantized water-filling packet scheduling scheme for downlink transmissions in lte-advanced systems with carrier aggregation. In *Software, Telecommunications and Computer Networks (SoftCOM), 2010 International Conference on*.
- Costa, G., Cattoni, A., Kovacs, I., and Mogensen, P. (2012). A fully distributed method for dynamic spectrum sharing in femtocells. In *Wireless Communications and Networking Conference Workshops (WCNCW), 2012 IEEE*.
- Dahlman, E., Parkvall, S., and Sköld, J. (2011). *4G LTE/LTE-Advanced for Mobile Broadband*. Academic Press, Oxford, UK.
- Dianati, M., Shen, X., and Naik, S. (2005). A new fairness index for radio resource allocation in wireless networks. In *Wireless Communications and Networking Conference, 2005 IEEE*.
- Döttling, M., Mohr, W., and Osserain, A. (2009). *Radio Technologies and Concepts for IMT-Advanced*. John Wiley and Sons, Ltd., West Sussex, UK.
- Ertel, R., Cardieri, P., Sowerby, K., Rappaport, T., and Reed, J. (1998). Overview of spatial channel models for antenna array communication systems. *Personal Communications, IEEE*, 5(1):10–22.
- Ertel, R. and Reed, J. (1999). Angle and time of arrival statistics for circular and elliptical scattering models. *Selected Areas in Communications, IEEE Journal on*, 17(11):1829–1840.
- Fuhl, J., Molisch, A., and Bonek, E. (1998). Unified channel model for mobile radio systems with smart antennas. *Radar, Sonar and Navigation, IEE Proceedings -*, 145(1):32–41.
- Galaviz, G., Covarrubias, D., and Andrade, A. (2011). On a spectrum resource organization strategy for scheduling time reduction in carrier aggregated systems. *Communications Letters, IEEE*, 15(11):1202–1204.
- Gao, S., Tian, H., Zhu, J., Chen, L., and She, X. (2011). A throughput-optimized component carrier selection algorithm for lte-advanced systems. In *Communication Technology and Application (ICCTA 2011), IET International Conference on*.

- Garcia, L., Kovacs, I., Pedersen, K., Costa, G., and Mogensen, P. (2012). Autonomous component carrier selection for 4g femtocells - a fresh look at an old problem. *Selected Areas in Communications, IEEE Journal on*, 30(3):525–537.
- Gavrilovska, L. and Talevski, D. (2011). Novel scheduling algorithms for lte downlink transmission. In *Telecommunications Forum (TELFOR), 2011 19th*.
- Gilstrap, D. (2012). Traffic and market report. Ericsson Report. Retrieved from: [http://www.ericsson.com/res/docs/2012/traffic\\_and\\_market\\_report\\_june\\_2012.pdf](http://www.ericsson.com/res/docs/2012/traffic_and_market_report_june_2012.pdf).
- Gutierrez, P. (2003). *Packet scheduling and quality of service in HSDPA*. PhD thesis, Aalborg University, Denmark.
- Han, A. and Lu, I.-T. (2011). Optimizing beyond the carrier by carrier proportional fair scheduler. In *Sarnoff Symposium, 2011 34th IEEE*.
- Holma, H. and Toskala, A., editors (2010). *WCDMA for UMTS: HSPA Evolution and LTE*. John Wiley and Sons, Ltd., West Sussex, UK.
- ITU (2010). Itu world radiocommunication seminar highlights future communication technologies. International Telecommunication Union Press Release. Retrieved from: [http://www.itu.int/net/pressoffice/press\\_releases/2010/48.aspx](http://www.itu.int/net/pressoffice/press_releases/2010/48.aspx).
- ITU-R (2008). Key results of world radiocommunication conference (wrc-07). International Telecommunication Union, Document Number GSC13-GRSC6-12. Retrieved from: [http://www.itu.int/dms\\_pub/itu-t/oth/21/04/T21040000030014PPTE.ppt](http://www.itu.int/dms_pub/itu-t/oth/21/04/T21040000030014PPTE.ppt).
- ITU-R (2009). Guidelines for evaluation of radio interface technologies for imt-advanced. International Telecommunication Union ITU-R Report M.2135-1. Retrieved from: [http://www.itu.int/dms\\_pub/itu-r/opb/rep/R-REP-M.2135-1-2009-PDF-E.pdf](http://www.itu.int/dms_pub/itu-r/opb/rep/R-REP-M.2135-1-2009-PDF-E.pdf).
- Iwamura, M., Etemad, K., Fong, M.-H., Nory, R., and Love, R. (2010). Carrier aggregation framework in 3gpp lte-advanced [wimax/lte update]. *Communications Magazine, IEEE*, 48(8):60–67.
- Jain, R., Chiu, D., and Hawe, W. (1984). A quantitative measure of fairness and discrimination for resource allocation in shared computer system. Eastern Research Lab DEC-TR-301 Report. Retrieved from: <http://www1.cse.wustl.edu/jain/papers/ftp/fairness.pdf>.
- Janaswamy, R. (2002). Angle and time of arrival statistics for the gaussian scatter density model. *Wireless Communications, IEEE Transactions on*, 1(3):488–497.
- Jeruchim, M., Balaban, P., and Shanmugan, K. (2000). *Simulation of Communication Systems: Modeling, Methodology and Techniques (Information Technology: Transmission, Processing and Storage)*. Kluwer Academic/Plenum Publishers, New York, USA.

- Ji-hong, Z., Hui, L., and Hua, Q. (2012). A spf-pf crossing component carrier joint scheduling algorithm. In *Advanced Communication Technology (ICACT), 2012 14th International Conference on*.
- Kakishima, Y., Takeda, K., Kawamura, T., Kishiyama, Y., Taoka, H., and Nakamura, T. (2011). Experimental evaluations on carrier aggregation and multi-user mimo associated with evd-based csi feedback for lte-advanced downlink. In *Wireless Communication Systems (ISWCS), 2011 8th International Symposium on*.
- Kaneko, M., Popovski, P., and Dahl, J. (2006). Proportional fairness in multi-carrier system: upper bound and approximation algorithms. *Communications Letters, IEEE*, 10(6):462–464.
- Kim, H. and Han, S. (2010). A simplification of proportional fair scheduling in multi-carrier transmission systems. *Transactions on Communications, IEICE*, E95-B(9):2469–2472.
- Kyosti, P., Meinila, J., and Hentila, L. (2007). Winner ii channel models: Part i channel models d1.1.2 v1.1. Winner II Project Report IST-4-027756. Retrieved from: <http://projects.celtic-initiative.org/winner+/WINNER2-Deliverables/D1.1.2v1.1.pdf>.
- Lazarus, M. (2010). The great spectrum famine. *Spectrum, IEEE*, 47(10):26–31.
- Le, K. (2009). On angle-of-arrival and time-of-arrival statistics of geometric scattering channels. *Vehicular Technology, IEEE Transactions on*, 58(8):4257–4264.
- Lei, L. and Zheng, K. (2009). Performance evaluation of carrier aggregation for elastic traffic for lte-advanced systems. *Transactions on Communications, IEICE*, E92-B(11):3516–3519.
- Liberti, J. and Rappaport, T. (1999). *Smart Antennas for Wireless Communications: IS-95 and Third Generation CDMA Applications*. Prentice Hall PTR, Upper Saddle River, USA.
- Liebl, G., de Moraes, T., Soysal, A., and Seidel, E. (2012). Fair resource allocation for the relay backhaul link in lte-advanced. In *Wireless Communications and Networking Conference (WCNC), 2012 IEEE*.
- Liu, L., Li, M., Zhou, J., She, X., Chen, L., Sagae, Y., and Iwamura, M. (2011). Component carrier management for carrier aggregation in lte-advanced system. In *Vehicular Technology Conference (VTC Spring), 2011 IEEE 73rd*.
- Lopez, C., Covarrubias, D., Munoz, D., and Panduro, M. (2005). Statistical cellular gaussian scatter density channel model employing a directional antenna for mobile environments. *AEÜ International Journal of Electronics and Communications*, 59(3):195–199.

- Martinez, D., Andrade, A., and Martinez, A. (2010). Interference-aware dynamic channel allocation scheme for cellular networks. In *Performance Evaluation of Computer and Telecommunication Systems (SPECTS), 2010 International Symposium on*.
- Massoulié, L. and Roberts, J. (2002). Bandwidth sharing: objectives and algorithms. *Networking, IEEE/ACM Transactions on*, 10(3):320–328.
- Mehlführer, C., Wrulich, M., Ikuno, J., Bosanska, D., and Rupp, M. (2009). Simulating the long term evolution physical layer. In *European Signal Processing Conference, EUSIPCO 2009, 17th*.
- Mehrjoo, M., Awad, M., Dianati, M., and Shen, X. (2010). Design of fair weights for heterogeneous traffic scheduling in multichannel wireless networks. *Communications, IEEE Transactions on*, 58(10):2892–2902.
- Meucci, F., Cabral, O., Velez, F., Mihovska, A., and Prasad, N. (2009). Spectrum aggregation with multi-band user allocation over two frequency bands. In *Mobile WiMAX Symposium, 2009. MWS '09. IEEE*.
- Nardelli, B. and Knightly, E. (2012). Closed-form throughput expressions for csma networks with collisions and hidden terminals. In *INFOCOM, 2012 Proceedings IEEE*.
- Nguyen, H. T. and Kovacs, I. (2012). Downlink radio resource management for lte-advanced system with combined mu-mimo and carrier aggregation features. In *Vehicular Technology Conference (VTC Spring), 2012 IEEE 75th*.
- Parkvall, S. and Astely, D. (2009). The evolution of lte towards imt-advanced. *Journal of Communications*, 4(3):146–154.
- Parkvall, S., Dahlman, E., Furuskar, A., Jading, Y., Olsson, M., Wanstedt, S., and Zangi, K. (2008). Lte-advanced - evolving lte towards imt-advanced. In *Vehicular Technology Conference, 2008. VTC 2008-Fall. IEEE 68th*.
- Petrus, P., Reed, J., and Rappaport, T. (2002). Geometrical-based statistical macrocell channel model for mobile environments. *Communications, IEEE Transactions on*, 50(3):495–502.
- Porto Cavalcanti, F. and Andersson, S., editors (2009). *Optimizing Wireless Communication Systems*. Springer, New York, USA.
- Rappaport, T. (2002). *Wireless Communications: Principles and Practice*. Prentice Hall PTR, Upper Saddle River, USA, 2nd edition.
- Saito, K., Kakishima, Y., Kawamura, T., Kishiyama, Y., Taoka, H., and Andoh, H. (2012a). Experimental evaluations on 4-by-2 mu-mimo achieving 1 gbps throughput using amc with outer-loop threshold control for lte-advanced downlink. In *Vehicular Technology Conference (VTC Spring), 2012 IEEE 75th*.

- Saito, K., Kakishima, Y., Kawamura, T., Kishiyama, Y., Taoka, H., and Andoh, H. (2012b). Field experiments on throughput performance of carrier aggregation with asymmetric bandwidth in lte-advanced. In *Future Network Mobile Summit (FutureNetw)*, 2012.
- Shayea, I., Ismail, M., and Nordin, R. (2012). Capacity evaluation of carrier aggregation techniques in lte-advanced system. In *Computer and Communication Engineering (ICCCE), 2012 International Conference on*.
- Shen, Z., Papasakellariou, A., Montojo, J., Gerstenberger, D., and Xu, F. (2012). Overview of 3gpp lte-advanced carrier aggregation for 4g wireless communications. *Communications Magazine, IEEE*, 50(2):122–130.
- Shirakabe, M., Morimoto, A., and Miki, N. (2011). Performance evaluation of inter-cell interference coordination and cell range expansion in heterogeneous networks for lte-advanced downlink. In *Wireless Communication Systems (ISWCS), 2011 8th International Symposium on*.
- Sivaraj, R., Pande, A., Zeng, K., Govindan, K., and Mohapatra, P. (2012). Edge-prioritized channel- and traffic-aware uplink carrier aggregation in lte-advanced systems. In *World of Wireless, Mobile and Multimedia Networks (WoWMoM), 2012 IEEE International Symposium on a*.
- Songsong, S., Chunyan, F., and Caili, G. (2009). A resource scheduling algorithm based on user grouping for lte-advanced system with carrier aggregation. In *Computer Network and Multimedia Technology, 2009. CNMT 2009. International Symposium on*.
- Stanczak, S., Wiczanowski, M., and Boche, H. (2009). *Fundamentals of Resource Allocation in Wireless Networks*. Springer, Berlin, GER.
- Steinbauer, M. and Molisch, A. (2001). *Wireless Flexible Personalised Communications*, chapter Directional Channel Modeling, pages 148–171. John Wiley and Sons, Ltd., West Sussex, UK.
- Takeda, K., Sagae, Y., Ohkubo, N., and Ishii, H. (2012). Investigation on rate matching and soft buffer splitting for lte-advanced carrier aggregation. In *Vehicular Technology Conference (VTC Spring), 2012 IEEE 75th*.
- Vivier, G., Badic, B., Cattoni, A., Choi, H.-N., Duplicy, J., Kaltenberger, F., Kovacs, I., Nguyen, H., and Sezginer, S. (2011). Spectrum aggregation: Initial outcomes from samurai project. In *Future Network Mobile Summit (FutureNetw)*, 2011.
- Wang, H., Nguyen, H., Rosa, C., and Pedersen, K. (2012). Uplink multi-cluster scheduling with mu-mimo for lte-advanced with carrier aggregation. In *Wireless Communications and Networking Conference (WCNC), 2012 IEEE*.

- Wang, H., Rosa, C., and Pedersen, K. (2011). Performance analysis of downlink inter-band carrier aggregation in lte-advanced. In *Vehicular Technology Conference (VTC Fall), 2011 IEEE*.
- Wong, K., Wu, Y., and Abdulla, M. (2010). Landmobile radiowave multipaths' doa-distribution: Assessing geometric models by the open literature's empirical datasets. *Antennas and Propagation, IEEE Transactions on*, 58(3):946–958.
- Wu, F., Mao, Y., Huang, X., and Leng, S. (2012). A joint resource allocation scheme for ofdma-based wireless networks with carrier aggregation. In *Wireless Communications and Networking Conference (WCNC), 2012 IEEE*.
- Yuan, G., Zhang, X., Wang, W., and Yang, Y. (2010). Carrier aggregation for lte-advanced mobile communication systems. *Communications Magazine, IEEE*, 48(2):88–93.
- Zhang, L., Zheng, K., Wang, W., and Huang, L. (2011). Performance analysis on carrier scheduling schemes in the long-term evolution-advanced system with carrier aggregation. *Communications, IET*, 5(5):612–619.